Genetic interaction of Tbx1 and *Pitx2* is required for early heart development

Zur Erlangung des akademischen Grades eines

DOKTORS DER NATURWISSENSCHAFTEN
(Dr. rer. nat.)

der Fakultät für Chemie und Biowissenschaften der
Universität Karlsruhe (TH)
vorgelegte

DISSERTATION

von

Dipl.-Biol. Sonja Nowotschin

aus Karlsruhe

Dekan: Prof. Dr. Manfred Kappes
Referent: Prof. Dr. Reinhard Paulsen
Korreferentin: Prof. Dr. Bernice E. Morrow
Tag der mündlichen Prüfung: 16.12.2005

Acknowledgements

First and foremost, I would like to thank both my advisors: Prof. Dr. Paulsen, my advisor in Germany, for his interest in this thesis and his willingness to support an external Ph.D. thesis and Prof. Dr. Bernice Morrow, my advisor at the Albert Einstein College of Medicine, Bronx, NY, for the opportunity to work in her laboratory. She has been an exceptional mentor and I am grateful for her constant support and encouragement, as well as for the opportunity to work independently.

I also want to thank my present and former lab members, Dr. Vimla Aggarwal, Jun Liao, Melanie Babcock, Jelena Arnold, Evan Braunstein, Dr. Mary King, Dr. Joy Neil, Dawn Lee, Dr. Dwight Codero and Dr. Donna Evans Febres for their assistance and helpful discussions especially I would like to thank Jun and Vimla for reading my thesis manuscript, Melanie for wonderful entertainment in the lab and Dawn who helped me maintaining my mouse colony in the beginning.

Special thanks to Dr. Marina Campione for helping me understanding the phenotype of my mice and for introducing me to heart anatomy, her helpful discussions, her encouragement during my years in science and for having me over in your lab in Italy to learn how to do in situs on sections. I appreciate that very much. “Molte grazie”. Also thanks to Mara and Alessandra in Marina’s lab who let me use all their equipment and were wonderful lab companions for one week.

I also would like to thank the Molecular Genetics office Lucy Costello, Donna Lombardi, Vivian Gradus, Heather Nonnon and Karen Roman for excellent administration.

I am very grateful to Dr. Michael Papetti, Dr. Kaichun Wei who had always time for me to discuss technical problems of experiments.
I would like to thank my friends Dr. Radma Mahmood, for her help with embedding embryos and various histological problems, Dr. Melinda Pirity and Rachele Arrigoni for support, discussions and encouragement.

Most of all I would like to thank Uwe for his tremendous support and encouragement in the last 15 years and of course my family for their support and understanding (especially Nadine and Vanessa) that I have spent the last years abroad.

Abstract

Congenital heart disease is the most common birth defect occurring in 1 out of 100 live births. Gene inactivation has shed significant light on the genes that are involved in regulating the proper morphogenesis of the heart. One of them is the T-box transcription factor *TBX1*, which has been implicated in 22q11 deletion syndrome, (22q11.DS; DiGeorge/velo-cardio-facial syndrome). Patients with 22q11DS exhibit multiple congenital malformations including severe cardiovascular defects. One goal is to understand the etiology of the cardiovascular defects in this syndrome. However, though inactivation of *Tbx1* in the mouse results in neonatal lethality due to severe heart defects, the molecular mechanisms of *Tbx1* are still elusive. In this thesis, I show that *Tbx1* is co-expressed with the *bicoid*-like homeobox transcription factor *Pitx2* in cells of the left secondary heart field from E8.0 onwards. *In situ* hybridization studies reveal down-regulation of *Pitx2* in these cells in the *Tbx1*-/- embryos. To investigate a possible genetic interaction of both genes, I crossed *Tbx1*+/- and *Pitx2*+/- mice. The double heterozygous mice showed reduced viability and died perinatally due to severe cardiac defects including double outlet right ventricle, atrial-septal and ventricular-septal defects. All these defects occurred with variable penetrance. Asymmetric expression of *Pitx2* is regulated by an enhancer that is located between exons 4 and 5, in which I identified a putative T-half site near an Nkx2.5 binding site. I show that Tbx1 can bind to this T-half site and in addition, can activate the *Pitx2* enhancer with the synergistic action of Nkx2.5. The results in this thesis link *Tbx1*, for the first time, to asymmetric cardiac morphogenesis and unravel a novel Tbx1-Pitx2 pathway in the secondary heart field which is indispensable for proper asymmetric heart development.

Contents

List of figures

List of tables

Abbreviations

°C	degree Celsius
22q11DS	22q11 deletion syndrome
aa	amino acid
ACTH	adrenocorticotrophic hormone
AHF	anterior heart field
AMP	adenosine monophosphate
Amp	ampicillin
ASD	atrial septal defect
ATP	adenosine triphosphate
AVN	atrioventricular node
BAC	bacterial artificial chromosome
BCIP	5'-bromo-4-chloro-3-indolylphosphate
bHLH	basic helix loop helix
bp	base pairs
BrdU	Bromo-deoxyuridine
BSA	bovine serum albumine
C-	carboxyl-
Ca	Calcium
CHD	congenital heart disease
cm	centimeter
CMV	Cytomegalo virus
CO_2	carbon dioxide
Co-IP	Co-immunoprecipitation
conc.	concentration
DGS	DiGeorge syndrome
DMEM	Dulbeco's Modified Eagle Medium
DMSO	Dimethylsulfoxide

DNA	desoxynucleic acid
dNTPs	deoxynucleoside triphosphates
DORV	double outlet right ventricle
DTT	Dithiothreitol
dUTP	deoxyuridine triphosphate
E	Embryonic day
E.coli	*Escherichia coli*
EDTA	Ethylenediaminetetraacetic acid
ELISA	Enzyme linked immuno-absorbent assay
EMSA	Electro mobility shift assay
EtOH	Ethanol
FCS	Fetal calf serum
fig	figure
g	gram
g	gravitational force
HCl	hydrochloric acid
HOS	Holt-Oram syndrome
hr	hour
ISH	*in situ* hybridization
IVS	interventricular septum
KCl	potassium chloride
kDa	Kilo Dalton
l	liter
LA	left atrium
LPM	left lateral plate mesoderm
LV	left ventricle
M	molar
Mb	mega bases
MeOH	Methanol
mg	milligram
Mg	Magnesium

$MgCl_2$	Magnesium chloride
min	minute
ml	milliliter
mM	millimolar
NaCl	sodium chloride
NaCl	Sodium chloride
NaOH	Sodium hydroxide
NCC	Neural crest cell
nm	nanometer
OFT	outflow tract
p	plasmid
PBS	Phosphate-buffered saline
PCR	Polymerase chain reaction
PFA	paraformaldehyde
pmol	picomol
RA	right atrium
resp.	respectively
RNA	ribonucleic acid
RNase	ribonuclease
rpm	rounds per minute
RSA	right subclavian artery
RT	room temperature
RV	right ventricle
SDS	sodium dodecyl sulfate
sec	second
SHF	secondary heart field
SPS	Small patella syndrome
SV	Simian virus
TBE	Tris-borate-EDTA-buffer
TBS	Tris-buffered saline
TE	Tris-EDTA

TEMED	N, N, N', N'-tetramethylethylendiamine
TGA	transposition of the great arteries
TOF	tetralogy of Fallot
tRNA	torula ribonucleic acid
U	unit
UMS	Ulnar-mammary syndrome
UV	ultraviolet
V	volt
VCFS	velo-cardio-facial syndrome
vol.	volume
VSD	ventricular septal defect
wt	wild type
µg	microgram
µl	microliter

1. Introduction

In this thesis the role of *Tbx1*, a member of the T-gene family of transcription factors, in heart development is discussed. *TBX1* is a strong candidate gene for the etiology of 22q11.2 deletion syndrome (22q11DS; also known as velo-cardio-facial syndrome (VCFS)/DiGeorge syndrome (DGS); MIM 192430/188400). Congenital heart defects occur prominently in this syndrome. The role of *Tbx1* in heart development, its genetic interaction with *Pitx2*, a homeobox transcription factor and putative down stream target of Tbx1, will be investigated by using mouse models and *in vitro* studies.

1.1 The mammalian heart

1.1.1 Structure of the adult heart

The mammalian heart is a modified muscular vessel, composed of separate but anatomically fused units: the right and left ventricle, and the right and left atrium. These four chambers are necessary to regulate the systemic and pulmonary circulation in the body (reviewed in Harvey, 2002). Venous blood from the body goes into the right atrium (RA) from where it enters the right ventricle (RV) through the tricuspid valve. From the RV the blood reaches the lungs through the pulmonary arteries. Then, oxygenated blood from the lungs flows through the pulmonary veins to the left atrium (LA) and passes through the mitral valve into the left ventricle (LV) from where it enters the arterial vascular circulation of the body through the aorta (Fig. 1.1 E) (reviewed in Harvey, 2002).

The heart consists additionally of specialized muscle cells that are responsible for the electrical conduction controlling the heart beat. These cells are organized into nodes or tracts. The electrical impulse is initiated at the so called sinuatrial node which lies at the junction between the RA and the superior caval

vein. This impulse spreads throughout the atria to the atrioventricular node (AVN) from where it is passed on to the ventricles. The bundle of His, its bundle branches and the Purkinje fibers are responsible for the rapid conduction to the apex of the ventricle and throughout the ventricle, respectively (reviewed in Harvey, 2002).

1.1.2 Development of the Heart

Congenital heart defects (CHDs) are found in ~ 1% of live births and are the most common of all birth defects (Hoffman and Kaplan, 2002), since the developing heart is very sensitive to genetic and environmental perturbation (reviewed in Harvey, 2002). The heart is the first organ to develop in the embryo and is essential for its survival. The development of the heart is a complex process, as its structures derive from three different cellular origins, the cardiac crescent, the anterior/secondary heart field and the cardiac neural crest. To understand the etiology of CHDs, it is therefore important to study cardiac development. Genetically engineered mice have proven to be a good model to gain insight into the complex processes during heart development and into the genes which are involved.

1.1.2.1 Early heart development

1.1.2.1.1 The cardiac crescent or primary heart field

Cardiac progenitor cells originate in the epiblast lateral to the primitive streak, from where they migrate into the splanchnic layer of the lateral pate mesoderm (LPM) and are recognizable as a crescent–shaped structure, the cardiac crescent or primary heart field, at 7.75 d.p.c. (Harvey, 2002) (Fig. 1.1 A). At day 8.25 p.c. the progenitors fuse ventrally to form the linear heart tube. The heart tube consists of an outer myocardial epithelium which surrounds an endothelial lining. At this time point the inflow tract of the heart lies caudally and the outflow tract (OFT) region is positioned cranially (Fig. 1.1 B). The heart is still connected to the

foregut through the dorsal mesocardium. At E8.5, the regions of the common atrium, atrioventricular canal (AVC), primitive ventricle and OFT are recognizable in the heart. At this stage the linear heart tube starts to undergo a process called cardiac looping in which the tube bends to the right side. During this process the inflow tract is progressively moved dorsally and cranially above the ventricles (reviewed in Harvey, 2002). The process of looping is almost completed at E10.5. At this stage, the endocardial cushions form in the atrioventricular canal (AVC) and in the OFT. They are the precursors of the tricuspid and mitral valves, the aortico-pulmonary septum, aortic and pulmonary valves. Massive cell proliferation occurs at the inner surface of the ventricles which results in the formation of the trabeculae. Between the ventricles the inter-ventricular septum is formed (Fig. 1.1 C). Remodeling of the heart is a process which starts concomitantly to the looping event and is almost completed by E12.5. Further spiraling of the heart tube positions the OFT ventrally between and the inflow tract dorsally from the two ventricles. The division of the heart to a four chambered unit is completed, around E14.5, through the fusion of the muscular inter-atrial and inter-ventricular septae with the non-muscular atrio-ventricular septum, which leads to clearly distinguishable LV, RV, LA and RA (reviewed in Harvey, 2002) (Fig. 1.1 D).

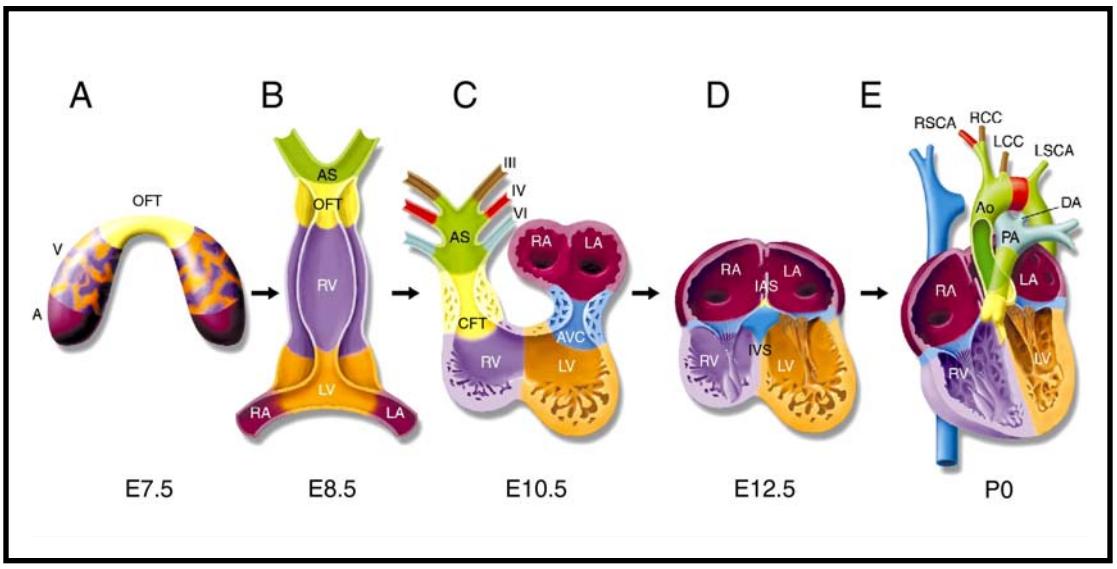

Modified after Srivastava and Olson, 2000

Fig. 1.1: Schematic representation of heart development

A: At E7.5, cardiac precursor cells form a crescent shape structure located in the mesoderm of the embryo. Specific regions of the cardiac crescent will give rise to certain structures in the heart (color coded). **B:** At E8.5, the linear heart tube forms, with the inflow tract located caudally and the outflow tract (OFT) located cranially. **C:** During the looping of the heart the atria are placed above the ventricles. And the ventricles balloon out form the outer curvature of the heart by massive trabeculation. The endocardial cushions, precursors of the valves and septae form in the atrio-ventricular canal (AVC) and the OFT. Cardiac neural crest cells migrate into the heart and contribute to the aortic arch arteries as well as to the OFT. Remodeling of the aortic arch arteries into the mature aortic arch begins. **D**: At E12.5, the inter-ventricular septum (IVS) and the inter-atrial septum (IAS) forms during the so called remodeling phase of the heart. **E:** At birth, the four-chambered heart is established. A, atrium; AS, aortic sac; DA, ductus arteriosus; LA, left atrium; LCC, left common carotid; LSCA, left subclavian artery; LV, left ventricle; PA, pulmonary artery; RA, right atrium; RCC, right common carotid; RSCA, right subclavian artery; RV, right ventricle; V, ventricle.

1.1.2.1.2 The anterior heart field (AHF) or secondary heart field (SHF)

The AHF or SHF is a recently discovered cell population of cardiac precursor cells in the pharyngeal mesoderm. This cardiac progenitor population expresses myocardial transcription factors such as *Nkx2.5*, *Gata4* and *Mef2c* that also can be found in cardiac precursor cells of the primary heart field (Waldo *et al*., 2001; Dodou *et al*., 2004). Lineage tracing experiments revealed contribution of cells from the pharyngeal mesoderm to the arterial as well as to the venous pole of the developing heart (Meilhac *et al*., 2004; reviewed in Kelly, 2005). It has been shown that they are added to the distal outflow tract myocardium (Kelly *et al*., 2001; Waldo *et al*., 2001; Mjaatvedt *et al*., 2001). In addition, recent studies provided evidence that SHF cells also contribute to the right ventricle, the interventricular septum (Kelly *et al*., 2001; Zaffran *et al*., 2004), the left ventricle, the atria and the inflow region of the heart (Meilhac *et al*., 2004). Perturbation or ablation of SHF cells leads to congenital heart defects (reviewed in Kelly, 2005; Ward *et al*., 2005). The understanding of the molecular pathways involved in the development of the cardiac progenitor cells in the pharyngeal/splanchnic mesoderm have just begun to be unraveled and implicate Lim homeobox, T-box, Mef2, Gata, Smads and forkhead genes (Cai *et al*., 2003; Yamagishi *et al*., 2003; Hu *et al*., 2004; Lee *et al*., 2004; Xu *et al*., 2004; Von Both *et al*., 2004).

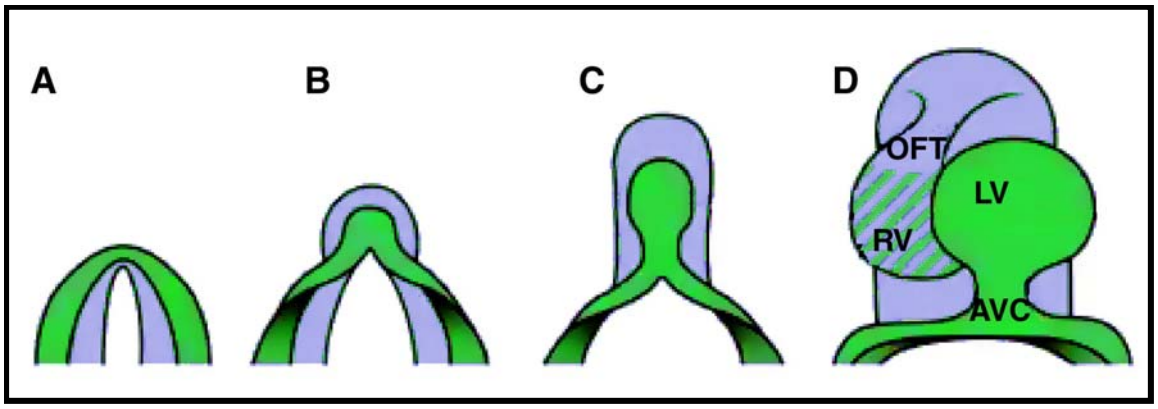

Modified after van den Hoff *et al*., 2004

Fig. 1.2: Relation between the primary heart field and the secondary heart field

The primary heart field or cardiac crescent is depicted in green. The SHF which lies anterior to the primary heart field is depicted in blue. A-D show the relative position of both cardiac regions between stage E7.5 - E8.5. The primary heart field gives rise to the left ventricle (LV) and the atrio-ventricular canal (AVC) and parts of the right ventricle (RV), whereas cells of the SHF give rise to the outflow tract (OFT) and the right ventricle (RV).

1.1.2.1.3 The cardiac neural crest

Neural crest cells (NCCs) originate in the developing neural tube in the embryo. During neural tube formation cells detach from the border of the neural and epidermal ectoderm and then migrate along specific pathways throughout the embryo. Finally, they will differentiate into various cell types depending on their destination. NCCs can be divided into two major groups, the cranial and the trunk neural crest (Gilbert, 2003). The cardiac neural crest derives from the caudal region of the cranial neural crest and contributes to the formation of the endothelium of the aortic arch arteries, the aortico-pulmonary septum in the outflow tract of the heart as well as the thymus, thyroid and parathyroid glands (Kirby, 1989; Kirby and Waldo, 1995; Waldo *et al*., 1998).

1.1.3 Formation of the septae during cardiac remodeling and associated defects

Formation of all the septae is a very crucial step during heart development, since abnormalities in endocardial cushions and subsequent failure in septum formation can cause a variety of life threatening cardiac malformations (Fig. 1.3) like atrial septal defect (ASD), ventricular septal defect (VSD), defects involving the great vessels, transposition of the great arteries (TGA) and tetralogy of Fallot (TOF) as well as persistent truncus arteriosus (PTA) (Sadler, 2000).

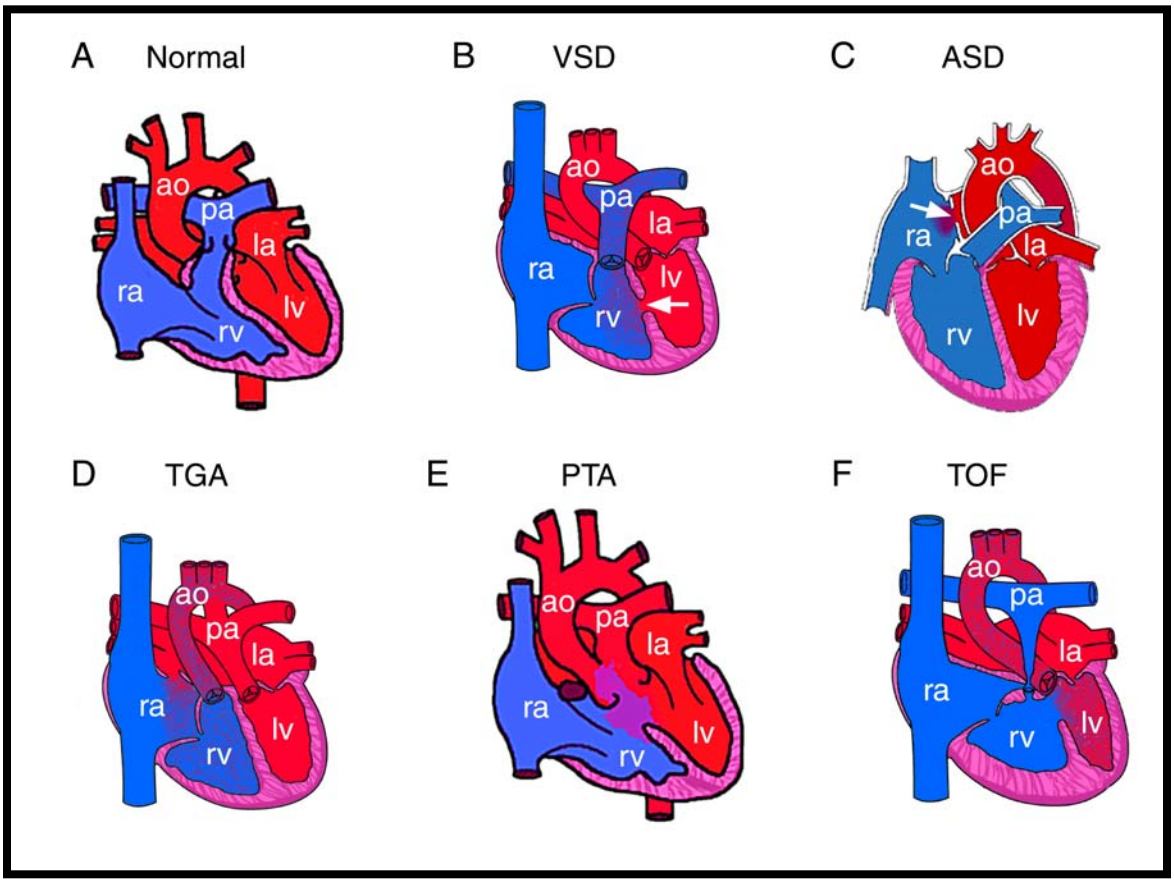

Fig. 1.3: Schematic representation of common cardiac malformations

A shows a normal heart. B depicts a VSD (arrow). The septum between the two ventricles is disrupted leading to mixing of oxygenated and deoxygenated blood from the left (lv) and the right ventricle (rv).

C represents an ASD (arrow), an opening between the left and the right atrium leading to mixing of oxygenated and deoxygenated blood from the left (la) and the right atria (ra). D shows TGA, where the aorta (ao) originates from the right instead of from the left ventricle and the pulmonary artery (pa) originates from the left instead of from the right ventricle. E illustrates a PTA. The pulmonary artery (pa) arises above an undivided truncus, caused by failure of the fusion of the endocardial cushions in the outflow tract. PTA is always associated with a VSD. F depicts TOF which is characterized by the stenosis of the infundiblum of the pulmonary artery (arrow), hypertrophy of the right ventricle, VSD and an overriding aorta that originates directly above the VSD.
A, E: modified after www.rch.org.au; B, D and F: modified after www.inova.org; C: modified after www.pediheart.org.

1.1.3.1 Formation of the atrial septum

The *septum primum* descends from the top of the common atrium and divides it. The two atria are still connected through an opening, the *ostium primum*. The latter will eventually be obliterated through the fusion of the *septum primum* with the endocardial cushions in the AVC. Cell death in the *septum primum* leads to a new opening, the *ostium secundum*. It ensures further communication between the atria. A new septum, the *septum secundum,* forms on the right side of the *septum primum*, as a consequence of the incorporation of the sinus horn into the right atrium. The *septum secundum* extends from the top into the lumen of the atrium and progressively overlaps with the *septum primum* but a small opening, the *foramen ovale*, persists. At birth the two septae are pressed against each other through increased blood pressure in the left atrium and the opening will be closed preventing mixing of deoxygenated and oxygenated blood (Sadler, 2000).

1.1.3.2 Formation of the mitral and tricuspid valves in the AVC

The AVC is surrounded by four endocardial cushions. The superior and the inferior cushions fuse and divide the common AVC into a left and right AVC. Failure in fusion leads to persistence of a common AVC. After fusion the cushion tissue becomes fibrous and forms the mitral valve in the left and the tricuspid valve in the right ventricle (Sadler, 2000).

1.1.3.3 Formation of the interventricular septum

The interventricular septum (IVS) consists of a myocardial and a mesenchymal part. The myocardial part is formed by the medial walls of the ventricles during extensive growth of the myocardium. The mesenchymal part is formed by the inferior endocardial atrial-ventricular cushion, the right and the left endocardial cushions in the outflow tract region. Fusion of all these parts results in formation of the IVS. A ventricular septum defect (VSD) occurs often in the mesenchymal part of the septum and is one of the most common birth defects (Fig. 1.3 B) (Sadler, 2000).

1.1.3.4 Formation of the aortico-pulmonary septum

The endocardial cushions on the left and right side in the outflow tract grow and finally fuse to form the aortico-pulmonary septum. The septum divides the outflow tract into the pulmonary trunk and the aorta. Defective division of the outflow tract can lead to abnormalities such as transposition of the great arteries (TGA) (Fig. 1.3 D). This means that the aorta originates from the right instead from the left ventricle and the pulmonary artery originates from the left instead of the right ventricle. Failure in fusion of the septum leads to persistent truncus arteriosus (PTA) (Fig. 1.3 E) (Sadler, 2000).

1.2 Cardiac defects in the 22q11DS

22q11DS has an incidence of 1 in 4,000 live births (Burn and Goodship, 1996). This makes it the most common interstitial deletion syndrome in humans (Scambler, 2000). Its main clinical features are outflow tract and aortic arch defects (see Table 1.1). In addition, patients have a characteristic facial appearance, learning disabilities, velopharyngeal insufficiency, hypernasal speech, cleft palate, (Sphrintzen *et al*., 1978), hypoplastic or absent thymus resulting in immunodeficiencies, and hypocalcemia (DiGeorge, 1965). Adult patients can develop schizophrenia and bipolar disorder (Karayiorgou *et al*., 1995). The majority of the deletions are sporadic, though 10-20% are autosomal dominant inherited (reviewed in Yamagishi, 2002).

Table 1.1: Frequency of cardiac defects in 22q11DS patients (n = 305) (after Emanuel *et al*., 2001)

Cardiac Defect	**%**
Tetralogy of Fallot (TOF)	20
Ventricular septal defect (VSD)	14
Interrupted aortic arch	12
Truncus arteriosus	6
Vascular ring	6
Atrial septal defect (ASD)	3
Right-sided aorta	2
Others incl. transposition of the great arteries, pulmonary atresia or stenosis, coarctation of aorta, hypoplastic left heart syndrome and heterotaxy	6

In approximately 90% of the cases the patients have a 3 Mb deletion encompassing ~30 genes, 8% have a nested 1.5 Mb deletion encompassing 27

genes (Morrow *et al*., 1995; Lindsay *et al*., 1995a; Carlson *et al*., 1997) Deletions of other sizes have also been described in a small subset of patients (reviewed in Yamagishi, 2002). However, there is no genotype-phenotype correlation. The phenotype is fully penetrant but with variable expressivity (Lindsay *et al.,* 1995a; Lindsay *et al*., 1995b). The deletions occur through chromosomal rearrangements. Chromosome 22q11 seems to be very prone to such chromosomal rearrangements, since three congenital malformation syndromes could be mapped to this region, 22q11DS, der(22) syndrome and cat eye syndrome (CES) (Edelmann *et al*., 1999a; 1999b; Funke *et al*., 1999; Edelmann *et al*., 2001). The reason for this susceptibility lies in certain regions of the chromosome, characterized by low copy repeats (LCRs), which are very susceptible to rearrangements (Edelmann *et al*., 1999a; 1999b; Shaikh *et al*., 2000).

1.2.1 Mouse models for 22q11DS

To understand the etiology of the 22q11DS several groups generated mouse models. A major part of the 3 Mb region including the 1.5 Mb deleted region of chromosome 22q11 is syntenic to a region on mouse chromosome 16 (MMU16). This advantage led to the generation of genetically engineered mice harboring different nested deletions of this region (Puech *et al*., 1997; Kimber *et al*., 1999; Lindsay *et al*., 2001; Merscher *et al*., 2001) (Fig. 1.4) The large deletion mouse (Lgdl/+) generated by Merscher *et al*. (2001) contains a 1.5 Mb deletion encompassing more than 24 genes. It mimics the human 1.5 Mb deletion.

Phenotypical analysis showed a reduced viability due to conotruncal heart defects in about 50% of the Lgdl/+ mice. To define the critical region that is responsible for the cardiac defects in the Lgdl/+ mouse mutant, complementation studies were carried out. Mice harboring smaller deletions as well as BAC (bacterial artificial chromosomes) transgenic mice over-expressing specific genes of 1.5 Mb region were used (Lindsay *et al*., 2001; Merscher *et al*., 2001). The mouse mutant containing a BAC harboring the 4 human genes *GP1Bβ*, *PNUTL1*,

TBX1 and *WDR14* was able to rescue most of the cardiac phenotype of Lgdl/+ mutant mice (Merscher *et al*., 2001). Out of the four genes, *TBX1* was the only gene that was expressed in the affected structure in patients during embryogenesis (see 1.3.3.1). Thus, *TBX1* was considered the only strong candidate for the phenotype in the mouse mutants and hence in the 22q11DS patients.

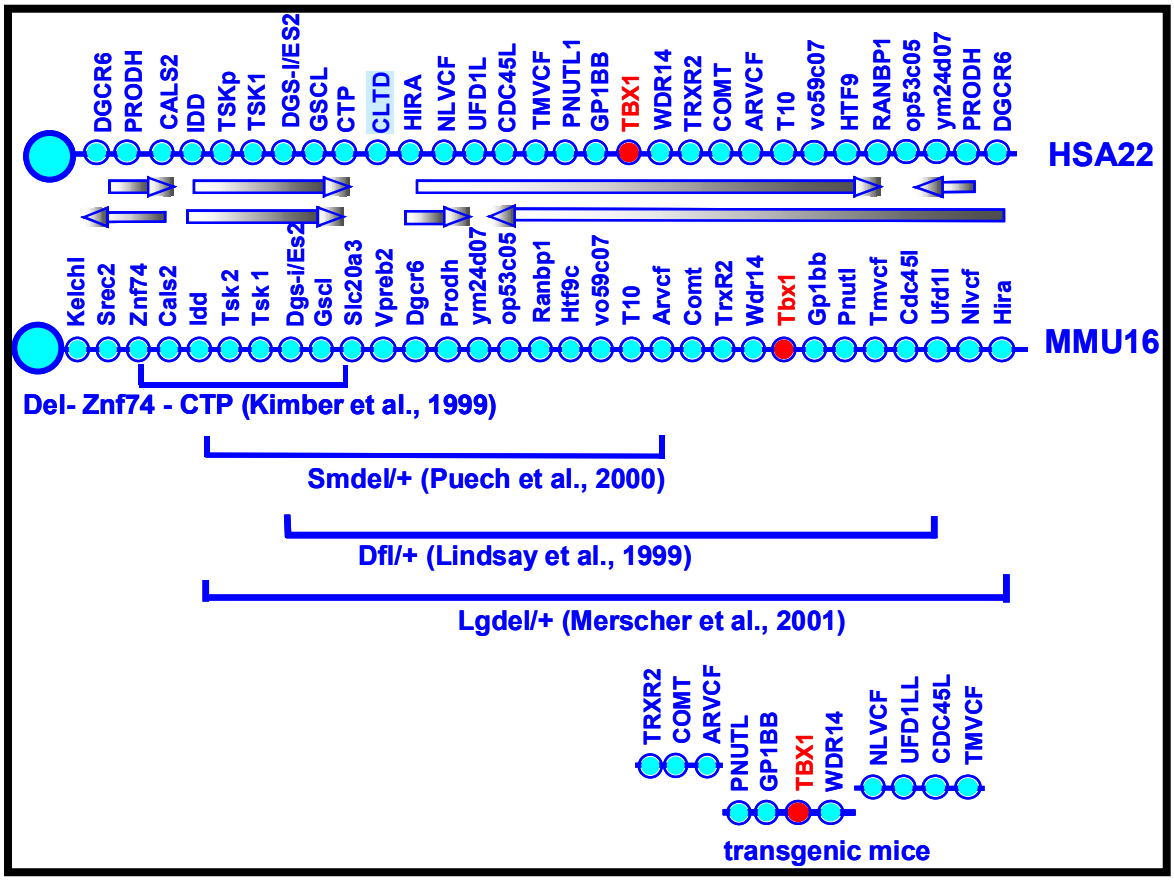

Modified after Merscher *et al*., 2001

Fig. 1.4: Map of part of human chromosome 22q11 (HSA22) affected in 22q11DS patients and its corresponding region on mouse chromosome 16 (MMU16).

The relative order of the genes (circles) is depicted on both chromosomes. The arrows indicate differences in orientation of the genes between the mouse and the human chromosome, respectively. Generated mouse models harboring different deletions of the region and genes of BAC transgenic mice are indicated and referenced.

1.2.2 Phenotype of the *Tbx1*+/- and *Tbx1*-/- mutant mouse

Based upon the fact that *Tbx1* was expressed in the structures affected in 22q11 patients, null mutants of *Tbx1* were generated. Haploinsufficiency of *Tbx1* in mice did not display the full spectrum of defects seen in 22q11DS patients as it had been expected. They only exhibited mild cardiovascular defects such as abnormal patterning of the great vessels, abnormal origin of the RSA, retroesophageal RSA and interrupted aortic arch. The difference in the phenotype is possibly due to different sensitivity to Tbx1 dosage of organ development in the mouse versus humans (Merscher *et al*., 2001; Liao *et al*., 2004).

The *Tbx1* null mutant however, exhibited a far more severe phenotype compared to 22q11DS patients. *Tbx1*-/- mice die perinatally and suffer from severe cardiovascular defects such as PTA, VSD and right sided aortic arch. An outer, middle and inner ear, masseter and pterygoid muscles are missing. In addition, they have craniofacial abnormalities, thymus and parathyroid gland aplasia as well as thyroid gland hypoplasia (Liao *et al*., 2004).

1.3 The T-box transcription factor, Tbx1

1.3.1 T-box transcription factors

Tbx1 belongs to the family of T-box genes, which are dosage sensitive transcription factors. T-genes serve different roles in many aspects of development and they are highly conserved throughout all animal species. The vertebrate genome contains at least 18 different T-box genes (Papaionnaou, 2001; Naiche *et al*., 2005). It is assumed that the T-box genes all derive from a single precursor gene and gene duplication led to the expansion of T-genes during evolution (Papaionnaou and Silver, 1998; Fig. 1.5). The T-genes are characterized through the T-box region which is homologous to the DNA-binding domain of *Brachyury* or *T*, hence their name. The *T*-gene was first discovered in 1927 (Dobrovolskaia-

Zavadskaia) and cloned in 1992 (Beddington *et al*.). Since then, many *T* related genes have been discovered in different species. Several T-box genes can be linked to human syndromes which emphasizes their significant role in development. Besides *TBX1,* which is involved, as mentioned above, in the etiology of 22q11DS (Merscher *et al*., 2001), mutations in *TBX3* cause Ulnar-Mammary-Syndrome (UMS). UMS is an autosomal dominant disorder which is characterized through upper limb malformations, mammary gland hypoplasia and/or dysfunction, dental and genital abnormalities (Bamshad *et al*., 1997; 1999). Mutations in *TBX5* lead to Holt-Oram syndrome (HOS), an autosomal dominant disorder. Patients exhibit cardiac and limb malformations (Li *et al*., 1997). *TBX19* or *T-PIT* was shown to be required for the expression of pro-opiomelanocortin (POMC), precursor of the adrenocorticotrophic hormone (ACTH) and melanocyte stimulating hormone in the corticotroph and melanotroph cell lineages in the pituitary. Mutations in *TBX19* lead to loss of ACTH resulting in adrenal insufficiency (Yi *et al*., 1999). *TBX4* has recently been linked to the small patella syndrome (SPS) which shows its important role in skeletal development of patella, pelvis and feet (Bongers *et al*., 2004).

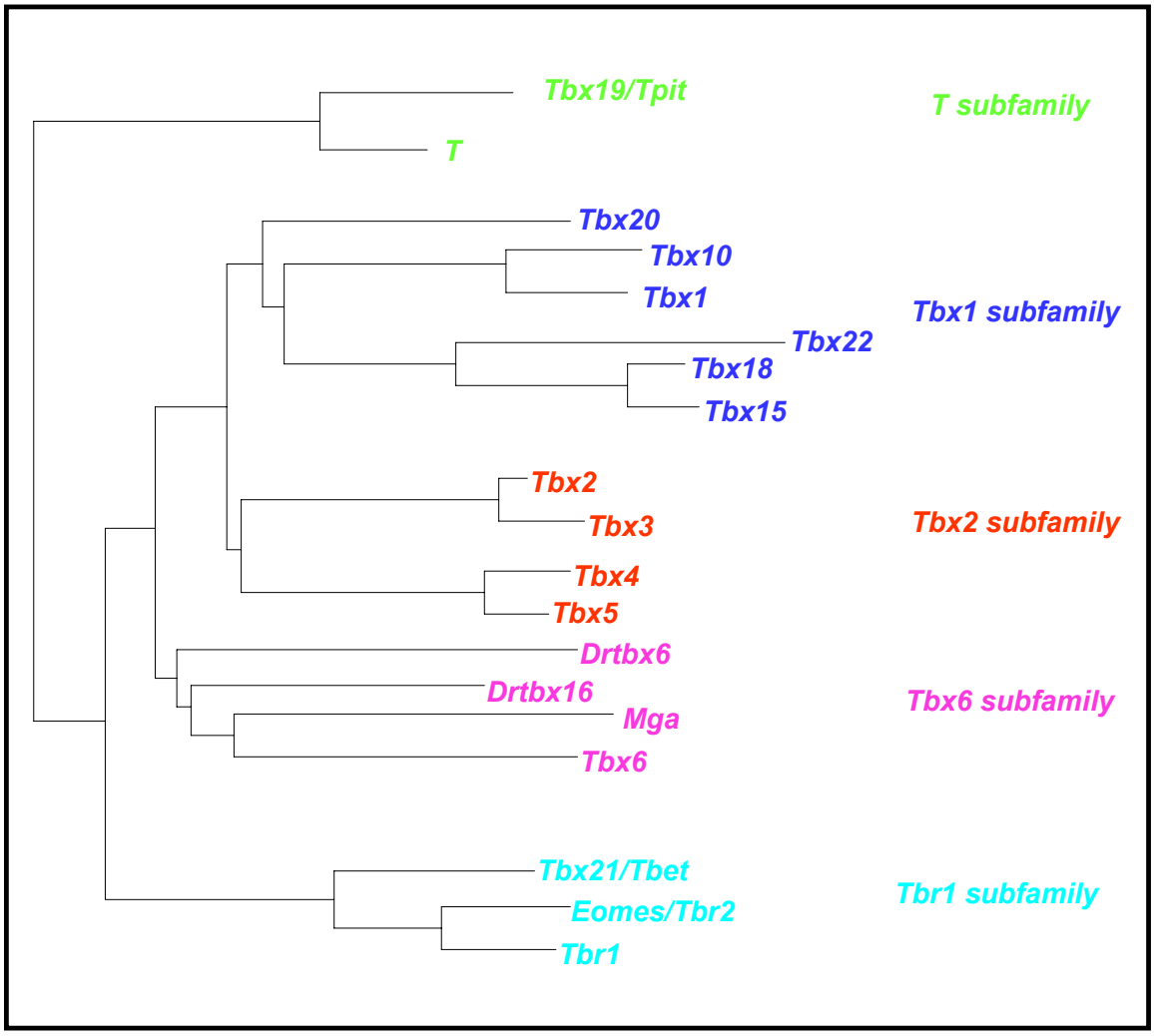

Modified after Papaioannou and Silver, 1998; Naiche *et al.*, 2005

Fig. 1.5: Phylogenetic tree of T-box genes

The T-box genes are an ancient family and have arisen through gene duplication from one ancestor gene. There are at least five different T-box subfamilies (each family is color coded) in animal species. Members of each subfamily have similar or overlapping expression patterns (Chapman *et al*., 1996).

1.3.2 Structure and function of T-box genes

The T-box proteins are about 50 – 78 kDa in size. They are characterized through a sequence-specific DNA binding domain, termed T-box, and a transcriptional activator or repressor domain (reviewed in Wilson and Conlon, 2002) (Fig. 1.6). The relative position of these domains is variable among the different T-box proteins. However, it is conserved in the T-box protein and its orthologs (reviewed in Wilson and Conlon, 2002). The T-box, a stretch of 180-190 aa residues, is defined as the minimal region that is necessary for the sequence-specific binding to the DNA (Papaioannou and Silver, 1998). It encompasses one third of the protein. All members, studied thus far, bind to the DNA consensus sequence 5′-AGGTGTGAAA-3′. Homology of the T-box domain varies between the different T-box proteins, though some specific residues are 100% conserved. The differences in the T-box region may reflect binding specificity to their target genes. T-box proteins have shown to be transcriptional activators, repressors or both, depending on the developmental context. The activator or repressor domain lies in the C-terminus of the protein, a region of low homology between T-box proteins (reviewed in Wilson and Conlon, 2002). The functional domain in Tbx1 has not been identified yet. It is likely that Tbx1 can act as both, repressor and activator (Raft *et al*., 2004; Takeuchi *et al*., 2005).

T-box proteins have been shown to interact with other transcription factors to regulate gene expression. Cooperative binding of promoters and synergistic activation of target genes have been demonstrated for T-box proteins and homeodomain, Lim domain and Gata zinc finger proteins (Stennard *et al*., 2003; Garg *et al*., 2003; Krause *et al*., 2005).

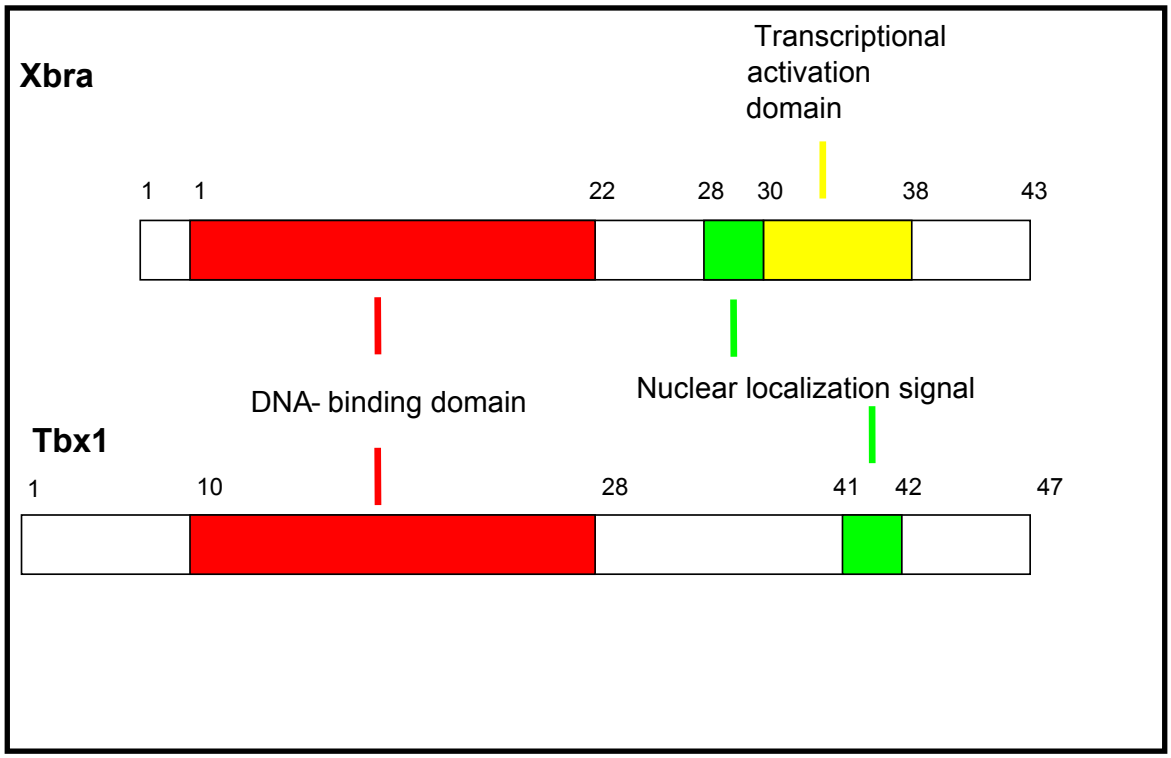

modified after Wilson and Conlon, 2002

Fig. 1.6: Protein structure of the T-box proteins Xbra and Tbx1

Depicted are the schematic protein structures of Xbra, the homolog of T in *Xenopus*, and Tbx1 in mouse. The structure of T-box proteins is conserved. The DNA-binding domain or T-box (red) encompasses one third of the protein and is necessary for binding specificity to downstream targets. Transcriptional regulatory domains are located in the C-terminus of the protein; Xbra has a transcriptional activation domain (yellow). A regulatory domain has not been described for Tbx1 yet. Xbra as well as Tbx1 contain a nuclear localization signal (green) enabling them to shuttle into and out of the nucleus.

1.3.3 *Tbx1* in mouse development

1.3.3.1 *Tbx1* expression in murine embryogenesis

Tbx1 expression can be detected as early as E7.5 in the mesoderm and splanchnopleura. The latter comprises the splanchnic mesoderm, a part of the LPM, and the endoderm in the developing embryo. At stages E9.5 - 10.5 it is expressed in the mesenchyme and endoderm of the pharyngeal arches, the head mesenchyme, the otic vesicle, the somites (Chapman *et al*., 1996, Nowotschin, unpublished data) as well as in the outflow tract of the heart (Vitelli *et al*., 2002). At later stages of embryogenesis *Tbx1* is found in the craniofacial muscles, including muscles of mastication and the pterygoid muscles, the tongue muscles, the tooth buds (Chapman *et al*., 1996; Nowotschin, unpublished data). Immunohistochemistry suggests that Tbx1 can shuttle between the nucleus and cytoplasm (Aggarwal, unpublished data; Braunstein, unpublished data, Nowotschin, unpublished data). Its nuclear localization signal has recently been published (Stoller and Epstein, 2005).

1.3.3.2 Role of *Tbx1* in development

Until now, the function of *Tbx1* in many developmental processes has been elusive. However, recent studies implicated important roles for *Tbx1* in the development of the ear, the craniofacial muscles, and the heart (Raft *et al*., 2004; Moraes *et al*., 2005; Kelly *et al*., 2004; Vitelli *et al*., 2002a; 2002b; Xu *et al*., 2004).

1.3.3.2.1 *Tbx1* is important for ear development

It has been proposed that *Tbx1* is necessary for patterning of the otocyst and proper morphogenesis of the inner ear sensory organs. It does so by suppressing *neurogenin* mediated neural fate determination of cells in the otocyst (Raft *et al*.,

2004). In addition, *Tbx1* was shown to be important for proper neural crest cell migration during middle and inner ear development (Moraes *et al*., 2005).

1.3.3.2.2 *Tbx1* plays a role in craniofacial development

Craniofacial development is based on interactions of the pharyngeal ectoderm, mesoderm and endoderm and neural-crest derived mesoderm. *Tbx1* is expressed in the pharyngeal core mesoderm which gives rise to craniofacial muscles. The development of the latter is perturbed in *Tbx1* null mutants. Early markers of the myogenic lineage, the bHLH transcription factors *MyoD* and *Myf5* are not expressed in the *Tbx1*-/- embryos. Therefore, it is hypothesized that *Tbx1* regulates the onset of branchiomeric myogenesis in the core mesoderm of the pharyngeal arches (Kelly *et al*., 2004).

In addition, a cell autonomous and a non cell autonomous role have been proposed for *Tbx1* in the pharyngeal pouch endoderm. *Tbx1* acts cell autonomously by propagating growth and patterning of the endoderm. The expression of *Tbx1* in the endoderm is assumed to be regulated by forkhead protein, Foxa2. Foxa2 and Foxc2/Foxc1 binding sites in the *Tbx1* promoter possibly drive its expression in the pouch endoderm and in the head mesenchyme, respectively (Yamagishi *et al*., 2003). Moreover, it is hypothesized that *Tbx1* supports the development of the pharyngeal pouch derivatives via signaling non cell autonomously through the neural crest cells. Though *Tbx1* is not expressed in neural crest cells, their migration pathways have shown to be defective in the *Tbx1* null mutants (Vitelli *et al*., 2002a)

1.3.3.2.3 Role of *Tbx1* in cardiovascular development

Since *Tbx1*-/- mice display severe cardiac defects *Tbx1* must play an important part in cardiovascular development. *Tbx1* is expressed in cells of the SHF. *Tbx1* has been implicated in controlling cell proliferation in the SHF and thereby regulating outflow tract development (Xu *et al*., 2004). Cell proliferation

in the SHF has been shown to be regulated by the fibroblast growth factor, *Fgf10*. (Kelly *et al*., 2001) There is evidence that *Fgf10* might be a direct downstream target of Tbx1 since it is down regulated in the pharyngeal mesoderm of *Tbx1* null mutants (Vitelli *et al*., 2002b; Xu *et al*., 2004). Further proof for this hypothesis comes from cell culture studies which showed activation of an *Fgf10*-reporter gene by Tbx1 (Xu *et al*., 2004). Further proof for a role of *Tbx1* in cardiovascular development provided the conditional knock out of *Tbx1* in *Nkx2.5*-expressing cells (Xu *et al*., 2004). *Nkx2.5* is a marker for cardiomyocytes and required for OFT development (Lyons *et al*., 1995). Loss of *Tbx1* in *Nkx2.5*-expressing cells led to the same OFT defects as in the complete knock out of *Tbx1* (Xu *et al*., 2004).

1.4 The homeobox gene *Pitx2* (*pituitary homeobox 2*)

The transcription factor PITX2 was first identified by positional cloning in humans. The gene was originally called *RIEG*, since point mutations in this gene can cause Rieger syndrome, the most extreme form of Rieger-Axenfeld syndrome (Semina *et al*., 1996). Most of the mutations found in Rieger syndrome affect the PITX2 homeobox region which plays a major part in the recognition and binding of DNA of target genes. Since then, *Pitx2* has been cloned from mouse and other species. The mouse homologue of *PITX2* was identified by a group of researchers who were looking for homeobox genes that are expressed in the pituitary (*Ptx2*) and brain (*Otlx2, Brx1*) (Gage and Camper, 1997; Mucchielli *et al*., 1996; Kitamura *et al*., 1997). In addition, it was identified to be a target gene (*ARP1*) of the human acute leukemia ALL1 protein (Arakawa *et al*., 1998). The official nomenclature in the Mouse Genome Database is now *Pitx2*.

Pitx2 belongs to the class of homeobox genes which share a highly conserved domain throughout evolution, called homeodomain which encompasses 60 aa. Homeobox genes play crucial roles in embryonic development of many

organisms. According to their similarities, they have been subdivided into different classes. *Pitx2* belongs to the *bicoid*-related *Pitx* gene family, a subdivision of the paired-class homeobox genes which includes three vertebrate paralogues *Pitx1, 2* and *3* and the fly cognate (Gage *et al*., 1999). All members of the paired-class have a characteristic aa residue at position 50 of the homeodomain, position 9 of the third helix, which is responsible for the recognition of DNA (Gehring *et al*., 1994; Hanes and Brent, 1991). All *Pitx* genes have a lysine residue at this position which recognizes the sequence 5′-TAATTTCC-3′, a *bicoid*-like sequence, hence their name (Gage and Camper, 1997). The amino acid sequence of the Pitx2 homeodomain shows high conservation between species. It is identical in *Homo sapiens*, *Mus musculus*, *Xenopus laevis* and *Danio rerio* (Campione *et al*., 1999) and shares homology with other bicoid-like homeodomain proteins like Otx1, Otx2, Otd, gsc and unc-30 (Semina *et al*., 1996). In addition to the homeodomain, another conserved region has been found within the *Pitx2* gene. It comprises a 14 aa stretch in the C-terminus of the coding region (Semina *et al*., 1996) and is important for protein-protein interactions (Amendt *et al*., 1998).

1.4.1 *Pitx2* and Rieger Syndrome

As mentioned above, mutations in human *PITX2* were found in patients with Rieger syndrome (RGS1; MIM 180500). This autosomal dominant disorder was first defined in 1935 (Rieger) and was mapped to chromosome 4q25 (Murray *et al*., 1992). It is the most extreme form of a family of diseases summarized as Axenfeld-Rieger syndrome. The most common feature of this syndrome is ocular anomalies like anterior chamber anomalies leading to glaucoma manifested in 50% of affected individuals. Rieger syndrome is further characterized by dental hypoplasia (missing, small or malformed teeth), mild craniofacial dysmorphism, and umbilical stump anomalies. Other features associated with Rieger syndrome but less common are abnormal cardiac, limb and pituitary development (Amendt

et al., 2000; Semina *et al*., 1996, Mammi *et al*., 1998). Expression studies of *Pitx2* during murine embryonic development showed its expression in all the affected structures in this syndrome.

1.4.2. Role of *Pitx2* in mouse development

1.4.2.1 Expression of *Pitx2* during embryogenesis

The earliest expression of *Pitx2* is detected at E7.5 in the head folds, in the left lateral plate mesoderm (LPM) and left splanchopleura (Piedra *et al*., 1998, Yoshioka *et al*., 1998; Campione *et al*., 1999). Later, during organogenesis from E9.5 through E14.5, *Pitx2* is expressed asymmetrically in handed organs such as heart, left lung bud, gut and vitelline vessels. Symmetric expression sites are the pharyngeal arches, the mesenchyme adjacent to nasal structures, the eye and the somites. Later in development, *Pitx2* expression can be found in the muscles of the trunk, craniofacial muscles, developing teeth, hind limb buds, the brain and pituitary (Kitamura *et al*., 1997; Mucchielli *et al*., 1997; Nowotschin, 1997). *Pitx2* expression in the pituitary and the brain has been studied extensively. In the pituitary it is detected as early as E9.5 in Rathke's pouch which develops into the anterior and intermediate lobes of the pituitary, in which its expression persists in distinct hormone producing cells (Gage and Camper, 1997). Early expression in the brain has been shown in areas such as the midbrain, zona limitans intrathalamica and ventral diencephalon. Later, the expression becomes restricted to certain brain nuclei (Kitamura *et al*., 1997; Mucchielli *et al*., 1996).

1.4.2.2 Isoforms of *Pitx2*

In humans as well as in mice three isoforms of *Pitx2* have been characterized: *Pitx2a*, *Pitx2b*, *Pitx2c* (Schweickert *et al*., 2000; Liu *et al*., 2001). A fourth one, *PITX2d*, has been found only in humans so far (Cox *et al*., 2002). The isoforms are generated either by alternative splicing (*Pitx2a* and *Pitx2b*) or by

alternative promoter usage (*Pitx2c)* and differ in their N-terminus while the C-terminus is identical in all isoforms (Fig. 1.7) The isoforms are differentially expressed during development (Kitamura *et al*., 1999; Schweickert *et al*., 2000; Yu *et al*., 2001). *Pitx2a* and *b* are co-expressed with *Pitx2c* in structures that are symmetric. *Pitx2c* is the only isoform that is asymmetrically expressed on the left side of LPM and later in the heart and other handed organs (see 1.4.2.4). It plays a major role in patterning of the left-right axis in vertebrates and in cardiac morphogenesis in early embryonic development (Logan *et al*., 1998; Piedra *et al*., 1998; Ryan *et al*., 1998; Campione *et al*., 1999).

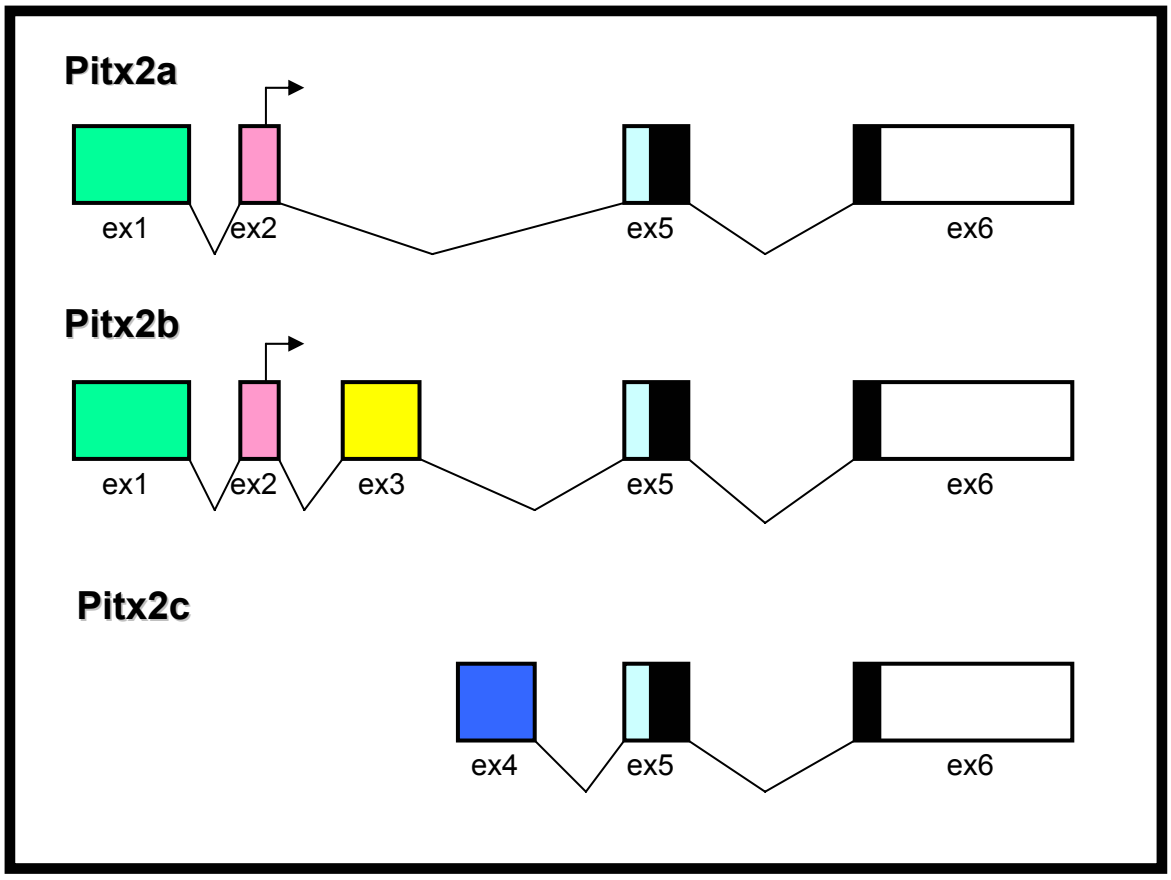

Fig. 1.7: Schematic representation of the *Pitx2* isoforms in the mouse

The C-terminus which contains the homeobox (black) in exon 5 and 6 is conserved in all *Pitx2* isoforms. The isoforms differ in their N-termini: *Pitx2a* and *b* share exons 1 and 2 (green and pink). Exon 3 (yellow) only included in *Pitx2b*. The N-terminus of *Pitx2c* consists of exon 4 (blue) which is unique to this isoform. ex, exon.

1.4.2.3 The *Pitx2* null mutant

To study the role of *Pitx2* during mouse development *Pitx2* deficient mouse lines were generated (Lin *et al*., 1999; Lu *et al*., 1999; Kitamura *et al*., 1999). The *Pitx2* null mutant is embryonic lethal. 35% of the homozygous mice die between day 9.5 p. c. and 10.5 p. c.. 100% of the *Pitx2*-/- embryos are dead by E15. Analysis of the phenotype showed that *Pitx2*-/- embryos fail to close the ventral

body wall leading to an external position of thoracic and abdominal organs. In 50% of the *Pitx2*-/- embryos embryonic turning was arrested though by E9 - E10. Severe cardiac defects, such as hypoplasia of the ventricles, ASD, DORV and PTA, were also a major component of the phenotype. In 50% of the *Pitx2*-/- mice the heart is positioned on the right instead on the left side (Lin *et al*., 1999; Lu *et al*, 1999; Kitamura *et al*., 1999; Kioussi *et al*., 2002). Other features of the *Pitx2* phenotype were craniofacial anomalies, reduction of the pituitary gland, right pulmonary isomerism, hypoproliferation of the spleen, the liver, the periorbital musculature and the lens. Moreover, the stomach of the null mutants turned to the left instead of to the right. Generation of allelic series of *Pitx2* mutations, null and hypomorphic alleles, showed varying severity of the above described phenotype suggesting a tissue specific dosage dependency on *Pitx2* for laterality and organogenesis (Gage *et al*., 1999).

1.4.2.4 *Pitx2c* is a mediator of left-right asymmetry

Vertebrates show a bilateral external symmetry but organs such as the heart, gut, lung, spleen and liver develop asymmetrically. The left-right positioning of these organs is conserved between species (*situs solitus*). Disturbances in patterning of the left-right axis can lead to full reversal of the body plan (*situs inversus*) or partly reversal of some organs (*situs ambiguus* or heterotaxia). In the last few years several publications shed light on the signaling events during left right patterning in the embryo.

Pitx2c is asymmetrically expressed early in the left LPM and in the heart, gut and lung during organogenesis. Though the upstream signals can vary between species the asymmetric expression in the LPM and later in the developing organs was shown to be conserved between chick, mouse, *Xenopus* and zebrafish making *Pitx2c* an important player in the evolution of the left-right signaling pathways of vertebrate asymmetry (Logan *et al*., 1998; Piedra *et al*., 1998; Ryan *et al*., 1998; Yoshioka *et al*., 1998; Campione *et al*., 1999).

Pitx2c continues to be asymmetrically expressed during organ morphogenesis. Therefore, it is believed that it transduces left-right identity to the organs. Evidence for this assumption came from studies of null mutants of the *transforming growth factors-β (Tgf-β)* related genes *lefty-1* and *Activin Receptor IIB*. Activin Receptor IIB is the receptor for Tgf-β-related factor nodal, which is expressed early in the left LPM and known to be upstream of *Pitx2*. Lefty-1 has been shown to restrict the expression of *nodal* and hence *Pitx2* to the left side (Meno *et al*., 1998).

In the *lefty-1* null mutant *Pitx2* is misexpressed on both sides of the heart leading to left-left isomerism of heart (Meno *et al*., 1998). Whereas in the *Activin Receptor IIB* knock out mouse (Oh and Li, 1997) *Pitx2* fails to be expressed leading to a right isomerism of the heart. However, absence of *Pitx2* in the gut does not cause isomerism but left-right reversal only. It still remains elusive how *Pitx2* translates the left identity into correct heart looping and gut coiling. Since *Pitx2* is also expressed in myocytes in these tissues, it is speculated that it can mediate changes in cell shape through contractile proteins in the cytoskeleton of these cells (Logan *et al*., 1998; Campione *et al*., 1999). However, null mutants of *Pitx2* did show a normal rightward looping, which questions the specific role of *Pitx2* in this process.

1.4.2.5 The role of *Pitx2c* in heart development and the *Pitx2c* null mutant

Analysis of *Pitx2*-/- mutants implies that it is more likely that *Pitx2* plays a crucial role in cardiac morphogenesis rather than in the process of looping. To understand its role in cardiac morphogenesis, the *Pitx2c* expression pattern in the heart was studied more closely (Campione *et al*., 2002; Franco and Campione, 2002). Earliest expression was seen in cardiac precursor cells in the left LPM at day E7.5. As the primitive heart tube forms, *Pitx2c* is expressed in its left part, subsequently as the heart begins its rightward looping *Pitx2c* expression is

maintained in those parts that derive from the left tubular heart components. At later stages during organogenesis its expression becomes restricted to the left inflow tract, the left atrial appendage myocardium and the left atrioventricular canal myocardium. In fetal stages *Pitx2c* is found in the left atrium, left AVC, the left superior caval vein as well as in the primary and secondary atrial septa (Fig. 1.8) (Campione *et al*., 2002; Franco and Campione, 2003). Besides in the heart, *Pitx2c* expression has been described in cardiac neural crest cells (Kioussi *et al*., 2002) as well as in cardiac precursor cells of the pharyngeal arch mesoderm, the presumptive SHF (Liu *et al*., 2002).

To assess the role of *Pitx2c* in development, *Pitx2c* null mutants were generated. Inactivation of the *Pitx2c* isoform leads to defects in remodeling of the pharyngeal arches arteries (right sided aortic arch and left innominate artery). In addition, *Pitx2c*-/- mice exhibit DORV, ASD, VSD, abnormal AV-cushions, valve defects, abnormal pulmonary and caval veins (Liu *et al*., 2002). These results suggest that that *Pitx2c* has distinct functions in the development of the aortic arch vessels, the outflow and inflow tract of the heart. It is needed for the correct asymmetric remodeling of the pharyngeal arch arteries. Moreover, Liu *et al*. could show that *Pitx2c* is necessary for patterning of the SHF as well as the outflow tract myocardium to ensure proper development of the conotruncus. Fate mapping experiments elucidated that the pulmonary and caval veins are populated by Pitx2 daughter cells which accounts for the defects in the null mutant (Liu *et al*., 2002).
Generation of *Pitx2ab* knockout mice with varying expression levels of *Pitx2c* revealed the importance of *Pitx2c* for cardiovascular development since only null mutants with normal *Pitx2c* expression levels did not display any cardiac defects. In addition, analysis of the hypomorphic mutants showed that different organs require different expression levels of *Pitx2c*. Low levels of *Pitx2c* expression were sufficient for normal atrial development, whereas organs such as the duodenum and the lungs required higher levels. Requirement of only low levels of *Pitx2* for

correct heart development could be an explanation for scarce incidences of cardiac abnormalities in Rieger syndrome patients (Liu *et al*., 2001).

Studies of the *Pitx2c* null mutants and hypomorphic allels showed that *Pitx2* is indispensable for proper heart development. Direct upstream regulators in the inflow and outflow tract of the heart have been elusive so far. Until now, direct upstream regulator genes of *Pitx2* are only known in the LPM, where *Pitx2* is activated initially through nodal signaling. Later, its expression is maintained by the homeobox transcription factor Nkx2.5 (Shiratori *et al*., 2001). However, it is not clear if Nkx2.5 is regulating maintenance of *Pitx2* expression by itself or whether there are other transcription factors involved.

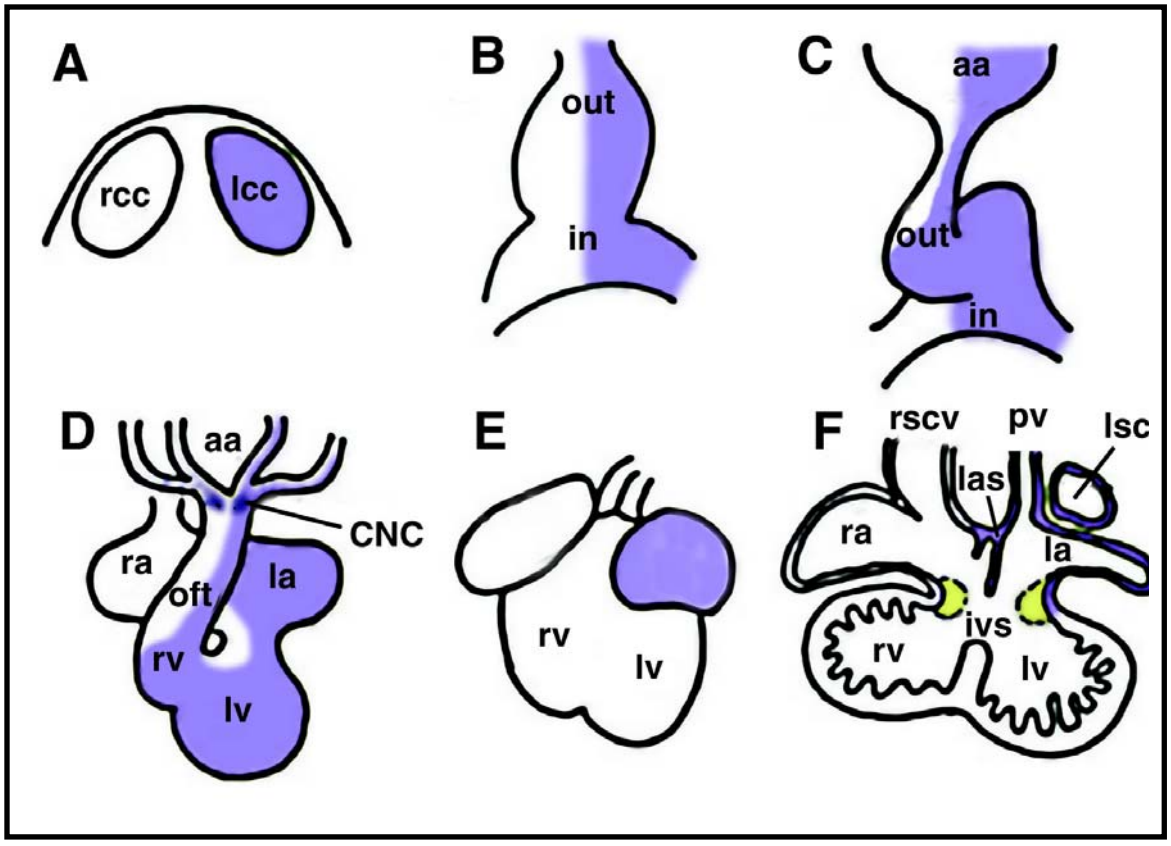

Modified after Franco and Campione, 2003

Fig. 1.8: Schematic representation of *Pitx2c* expression (blue) during cardiac development

A: *Pitx2c* is expresses at E7.5 in the left cardiac crescent (lcc).

B: *Pitx2c* is expressed exclusively in cells on the left side of the inflow (in) and outflow (out) region in the linear heart tube.

C and D: While the heart undergoes looping, *Pitx2* stays expressed in cells that originated from the left side of the linear heart tube. Thus, it is expressed in part of the outflow tract (oft), right ventricle (rv), left ventricle (lv) and left atrium (la). Expression can also be found in the aortic arches (aa) and in the cardiac neural crest cells (CNC) that migrate into the outflow tract.

E and F: Later in development, *Pitx2* expression is restricted to the left atrium (la), the interatrial septum (ias), pulmonary vein (pv) and the left superior caval vein (lsc). Endocardial cushions are depicted in green. ivs, interventricular septum; ra, right atrium; rcc, right cardiac crescent; rscv, right superior caval vein.

1.5 Rationale

Congenital heart diseases (CHD) make up 1:100 live births and are responsible for the majority of the prenatal deaths. The cause for CHD is mostly unknown. In the last few years genetically engineered mice have shed significant light on the genes involved in cardiac development. One of them is the transcription factor, *Tbx1*. Its human homolog, *TBX1* has been shown to be a strong candidate for the cardiac defects in 22q11DS patients. Expression analysis of *Tbx1* during murine embryogenesis as well as severe outflow tract and aortic arch patterning defects in the *Tbx1* null mutant point to an important role of *Tbx1* in cardiac morphogenesis. However, the molecular pathways of *Tbx1* are still elusive. To elucidate its role during early heart development, I took a candidate gene approach to identify possible downstream targets and pathways of *Tbx1*. One gene of particular interest was the homeobox transcription factor *Pitx2*, since it is expressed in cells of the SHF like *Tbx1*. Detailed analysis of the expression pattern of both genes should help to understand whether both genes are co-expressed in the same cells of the SHF. In addition, expression studies in *Tbx1* null mutants should elucidate if *Pitx2* expression is altered in those mice. Indeed, down regulation of *Pitx2* in cells of the SHF was found suggesting that *Pitx2* acts downstream of Tbx1. To ascertain whether *Pitx2* acts in the same genetic pathway like *Tbx1*, *Pitx2* heterozygous mice were intercrossed with *Tbx1* heterozygous mice. Double heterozygous mice displayed a more severe cardiac phenotype than single heterozygotes suggesting a genetic interaction between these two genes. To assess the nature of the interaction between Tbx1 and Pitx2, *in vitro* studies should be performed. Luciferase assays using a *Pitx2* enhancer reporter construct and a Tbx1 expression construct should determine whether Tbx1 could activate the *Pitx2* gene. Moreover, electromobility shift assays should be carried out to see whether

Tbx1 can directly bind to the *Pitx2* enhancer. The mouse model generated in this thesis should lead to more insight into the role of *Tbx1* in cardiac morphogenesis and serve as a basis to understand the etiology of cardiac defects in 22q11DS and CHDs in general.

2. Materials and Methods

2.1 Materials

2.1.1 Sources of chemicals, reagents and equipment

ABC (Avidin-biotinylated peroxidase complex)	DAKO, Carpinteria, CA
Agarose	ISC Bioexpress, Kaysville, UT
Alcian Blue	Sigma, St. Louis, MO
Alizaren Red	Sigma, St. Louis, MO
Ammonium hydroxide (NH_4OH)	Sigma, St. Louis, MO
Ammoniumpersulfate (APS)	BIORAD, Hercules, CA
Ampicillin	Sigma, St. Louis, MO
Anti-Flag Affinity Gel	Sigma, St. Louis, MO
Antigen Unmasking Solution	Vector laboratories, Burlingame, CA
Acrylamide/Bisacrylamide (37.5:1)	Roche, Indianapolis, IN
Axioskop 2 plus	Zeiss, Thornwood, NY
BM-Purple staining solution	Roche, Indianapolis, IN
Beta-Galactosidase reporter gene activity Kit	Sigma, St. Louis, MO
Beta-mercaptoethanol	BIORAD, Hercules, CA
Boehringer Block	Roche, Indianapolis, IN
Bovine Serum Albumine (BSA)	New England Biolabs, Beverly, MA Sigma, St. Louis, MO
Bradford Reagent	BIORAD, Hercules, CA
Bromphenol blue	Sigma, St. Louis, MO

Chaps (3-[(3-Cholamidopropyl)-dimethylammonio]-1-propane-sulfonate	Sigma, St. Louis, MO
Chloroform	Fisher, Pittsburgh, PA
Citric Acid	Fisher, Pittsburgh, PA
Citrate buffer 6%	Vector laboratories, Burlingame, CA
Competent cells INV110	Invitrogen, Carlsbad, CA
Competent cells Top10 one shot	Invitrogen, Carlsbad, CA
Cover slips	Fisher, Pittsburgh, PA
DAB substrate buffer and Chromogen	DAKO, Carpinteria, CA
Deoxycholate acid	Sigma, St. Louis, MO
Deoxy-nucleosidtriphosphates	Roche, Indianapolis, IN
Digoxigenin labeling Mix	Roche, Indianapolis, IN
Dimethylsulphoxide (DMSO)	Fisher, Pittsburgh, PA
Dissecting tools	Fine Science Tools, Foster City, CA
DNA Gel Purification Kit	Qiagen, Valencia, CA
DNA-Ladder 1Kb	Invitrogen, Carlsbad, CA
DNase, RNase free water	Gibco/Invitrogen, Carlsbad, CA
DNeasy Tissue Kit	Qiagen, Valencia, CA
Dry Milk (Blotting grade)	BIORAD, Hercules, CA,
Dulbecco's Mod Eagle Medium	Gibco/Invitrogen, Carlsbad, CA
ECL, Western Lightning Chemiluminescent Reagent	Perkin Elmer™, Wellesley, MA
EDTA 0.5 M	Gibco/Invitrogen, Carlsbad, CA
Embedding cassettes	Fisher, Pittsburgh, PA
Eosin B	Poly Scientific, Bayshore, NY
Ethanol 200 proof	Fisher, Pittsburgh, PA
Ethidium bromide	Sigma, St. Louis, MO
Fetal Bovine Serum	Gemini Bioproducts, Woodland, CA

Filtered pipette tips	Scitech Instruments, Franklin, NJ
Formalin, 10% Neutral Buffered (Accustain)	Sigma, St. Louis, MO
Formamide	Fisher, Pittsburgh, PA
G-50 Sephadex Spin Columns	Amersham, Pharmacia Biotech, Piscataway, NJ
Gel Slick	FMC Bioproducts, Rockland, ME
Glacial Acetic Acid	Fisher, Pittsburgh, PA
Glutaraldehyde 25%	Sigma, St. Louis, MO
Glycine	Gibco/Invitrogen, Carlsbad, CA
Glycine (Blotting Grade)	BIORAD, Hercules, CA,
Glycerol	Sigma, St. Louis, MO
Goat Serum	Sigma, St. Louis, MO
Hematoxylin	Poly Scientific, Bayshore, NY
Heparin	Sigma, St. Louis, MO
Hepes	Sigma, St. Louis, MO
Histowax Surgipath	Surgipath, Richmond, IL
Hotstart PCR kit	Qiagen, Valencia, CA
Hydrochloric acid 12.5 N	Fisher, Pittsburgh, PA
H_2O_2 3%	DAKO, Carpinteria, CA
Immunocal	Decal Chemical Corporation, NY
Isopropanol	Fisher, Pittsburgh, PA
Kanamycin	Sigma, St. Louis, MO
Kodak ultrasensitve film (Biomax MS)	Fisher, Pittsburgh, PA
L-Glutamine	Gibco/Invitrogen, Carlsbad, CA
Laemmli Buffer	BIORAD, Hercules, CA,
Ligase buffer (10x)	Roche, Indianapolis, IN
Lithiumchloride (LiCl)	Sigma, St. Louis, MO

Low mass DNA ladder	Gibco/Invitrogen, Carlsbad, CA
Luciferase Assay System	Promega, Madison, WI
Magnesium chloride (MgCl)	Sigma, St. Louis, MO
Magnesium chloride solution (PCR)	Roche, Indianapolis, IN
Maleic acid	Sigma, St. Louis, MO
Microtome, Leica RM 2155	Leica, Bannockburn, IL
Methanol	Fisher, Pittsburgh, PA
Microscopic slides Superfrost Plus	Fisher, Pittsburgh, PA
Mini Quick Spin Columns	Roche, Indianapolis, IN
N, N, N', N'-Tetramethylethylendiamine (TEMED)	BIORAD, Hercules, CA,
NBT/BCIP Staining solution	Roche, Indianapolis, IN
Oligonucleotides	Invitrogen, Carlsbad, CA
Paraformaldehyde	Sigma, St. Louis, MO
Pap pen	Vector Laboratories, Burlingame, CA
PCR tubes	USA Scientific, Ocala, FL
Penicillin/Streptomycin	Gibco/Invitrogen, Carlsbad, CA
Petri dishes	Fisher, Pittsburgh, PA
Permount, mounting medium	Fisher, Pittsburgh, PA
Peroxidase Block	DAKO, Carpinteria, CA
Phenol	Fisher, Pittsburgh, PA
Phosphate buffered saline with or without Calcium and Magnesium	Mediatech, Herndon, VA
Pipette tips	USA Scientific, Ocala, FL
Pipettes (1ml, 5ml, 10ml, 25ml)	Fisher, Pittsburgh, PA
Polyfect Reagent	Qiagen, Valencia, CA
Potassium chloride (KCL)	Sigma, St. Louis, MO
Potassium hydroxide (KOH)	Sigma, St. Louis, MO

Precision Plus Protein Dual Color Standard	BIORAD, Hercules, CA
Protran (Nitrocellulose membrane 0.45µm)	Schleicher und Schuell,
Protein G Agarose	Sigma, St. Louis, MO
Proteinase K	Roche, Indianapolis, IN
Qiagen buffers P1-P3	Qiagen, Valencia, CA
Restriction enzymes and buffers	New England Biolabs, Beverly, MA
RNase Inhibitor (RNase Out)	Invitrogen, Carlsbad, CA
Slide staining rack	EMS, Fort Washington, PA
Sodium acetate (NaAc)	Sigma, St. Louis, MO
Sodium chloride (NaCl)	Sigma, St. Louis, MO
Sodium dodecyl sulfate (SDS)	BIORAD, Hercules, CA,
Sodium hydroxide	Sigma, St. Louis, MO
SSC (Saline-sodium citrate) Buffer 20 x	Sigma, St. Louis, MO
Stereomicroscope	Leica, Bannockburn, IL
Surgipath Histowax	Surgipath, Richmond, Il
T3, T7 and SP6-Polymerase and 10 x Transcription buffer	Roche, Indianapolis, In
T4 Kinase & 10 x Kinase Buffer	New England Biolabs, Beverly, MA
T4 Ligase & 10 x Ligation buffer	Roche, Indianapolis, IN
Taq polymerase	Roche, Indianapolis, IN
TBE-(Tris-Borate-EDTA-) Buffer, 10 x	Sigma, St. Louis, MO
Tissue culture plates	Fisher, Pittsburgh, PA
Torula-RNA	Sigma, St. Louis, MO
Tris buffered Saline (pH 8)	Sigma, St. Louis, MO
TGS-(Tris-Glycine-SDS-) Buffer, 10 x	BIORAD, Hercules, CA,

Tris HCl, Tris Base	Sigma, St. Louis, MO
Tris-HCL (10%) SDS Gels	BIORAD, Hercules, CA,
Triton X-100	Sigma, St. Louis, MO
Trizol	Invitrogen, Carlsbad, CA
Trypsine	Gibco/Invitrogen, Carlsbad, CA
Tween 20	Sigma, St. Louis, MO
Whatman 3MM paper	Fisher, Pittsburgh, PA
Xylene	Fisher, Pittsburgh, PA

2.1.2 Plasmids

pBluescript II KS +/-	Stratagene, La Jolla, CA
pGl3 SV40 luciferase vector	Promega, Madison, WI
pcDNA 3.1	Invitrogen, Carlsbad, CA
pCR II Topo Vector	Invitrogen, Carlsbad, CA
pEGFP-N1	Clontech,
CMV-β-Gal	Obtained from Dr. L. D'Adamio
Flag-Nkx2.5 in pCI	Obtained from Dr. V.M. Christoffels

2.1.3 Bacteria

Top 10 *E.coli*	Invitrogen, chemical competent cells, F*mcr*A Δ(*mrr-hsd* RMS-*mcr*BC) Φ80*lac*Z ΔM15 ΔlacX74 *rec*A1 *ara*Δ139 Δ(*ara-leu)*7697 *gal*U *gal*K *rps*L (Str^R) *end*A1 *nup*G

Inv 110 *E.coli*	Invitrogen, chemical competent cells, F'*tra* Δ36*pro*AB *lac*I9ZΔM15 *rps*L (Str^R) *thr leu end*A *thi*-1 *lac*Y *gal*K *gal*T *ara ton*A *tsx dam dcm dup*E44 Δ(*lac-pro*AB) Δ(*mcr*C-*mrr*102::Tn10 (Tet^R)

2.1.4 Cell lines

Cos 7	fibroblast-like cell line from monkey kidney
293T	Human kidney carcinoma cell line

2.1.5 Mouse lines

FVB	Taconic laboratories, Germantown, NY
C57/Bl	Jackson laboratories, Bar Harbor, ME
Pitx2+/- mice in C57/Bl	Obtained from Dr. Philip Gage, (Gage *et al*., 1999)
Tbx1+/- in C57/Bl	Merscher *et al*., 2001
Tbx1+/- in FVB	Liao *et al*., 2004

2.1.6 Probes used for *in situ* hybridization

m*Pitx2* full length in pBluescript SK	Obtained from Dr. Marina Campione, (Campione *et al*., 1999)
m*Tbx1* full length in pCRII Topo	was cloned in pCRII TOPO by PCR
m*Nkx2.5*	Obtained form Dr. Richard Harvey, (Lyons *et al*., 1995)
m*Islet-1*	Obtained form Dr. Silvia Evans, (Cai *et al*., 2003)

2.1.7 Antibodies

Anti-bromodeoxyuridine (monoclonal, mouse)	Roche, Indianapolis, IN
Anti-Pitx2 (polyclonal, rabbit)	Received from Dr. Tord Hjalt (Hjalt *et al*., 2000)
Anti-Tbx1 (polyclonal, rabbit)	Zymed, San Francisco, CA
Anti-Digoxigenin, Fab-Fragments coupled with Alkaline Phosphatase	Roche, Indianapolis, IN
Goat-anti-rabbit, biotinylated	DAKO, Carpinteria, CA
Goat-anti-mouse, biotinylated	DAKO, Carpinteria, CA

2.1.8 Oligonucleotides

2.1.8.1 Tbx1 genotyping primers

Set1:

Tbx1KO1-F	5′-TTGGTGACGATCATCTCGGT-3′
Tbx1KO2-R	5′-ATGATCTCCGCCGTGTCTAG-3′
mut2-R	5′-AGGTCCCTCGAAGAGGTTCA-3′

Set2:

Tbx1-WT-F	5′-AGTCTTGGGCAGGTGCATAA-3′
Tbx1-WT-R	5′-CACAGAACATGTTAAGCGGG-3′
Hygro-F	5′-CCATCACAGTTTGCCAGTGA-3′
Hygro-R	5′-GATTCCGGAAGTGCTTGACA-3′

2.1.8.2 Pitx2 genotyping primers

Set1:

Pitx2-31130	5′-TCGTGTCTTAAAAGGATGTGTTTCTTC-3′
Pitx2-30266	5′-TTCTGGAGGGTTTTCTTGTTCTAGG-3′
Pitx2-30265	5′-AGACTAGTGAGACGTGCTACTTCCATTTGT-3′

Set2:

Pitx2-F	5′-GTGTCTGTAAAACACGCGCATG-3′
Pitx2-R	5′-GTCTCCAGTGAAGCCAAGCCT-3′

2.1.8.3 Oligonucleotides in EMSA

Wt-short:	5′-CAATCAGGTGTAAAGAGGAA-3′
M1-short:	5′-CAATCAGATTTGAAGAGGAA-3′
M2-short:	5′-CAATCAAATTTGAAGAGGAA-3′
Cons-short:	5′-CAATCAGGTGTGAAAAGGAA-3′

2.1.9 Solutions for whole mount and section *in situ* hybridization

PBSw	PBS (-Ca^{2+}/Mg^{2+}), 0.1% Tween-20
Hybridization buffer	0.5 g Boehringer Block, 25 ml Formamide, 20 x SSC pH 7.0, dissolve at 65°C while stirring, then add 6 ml ddH_2O, 5 ml 10 mg/ml torula RNA, 100µl 50 mg/ml Heparin, 250µl 20% Tween-20, 10% CHAPS, 500µl 0.5 M EDTA pH 8.0; store at -20°C
Maleic acid buffer	100 mM Maleic acid, 150 mM NaCl, pH 7.5 adjusted with NaOH
BM-Block buffer	10% Goat serum, 1% Boehringer Block, dissolve in PBSw at 65°C for 1 hr

AP1-buffer, NTM-buffer	100 mM Tris pH 9.5, 100 mM NaCl, 50 mM $MgCl_2$

2.1.10 Solutions for immunohistochemistry

1 x TBS	10 x TBS (Sigma) in 1 l H_2O
ABC	5 ml 1 x TBS plus 1 drop avidin and 1 drop Biotin (DAKO)
DAB solution	1 ml Substrate buffer plus 1 drop Chromogen
Blocking solution	5% Serum, 2% BSA and 0.1% Triton X-100 in TBS
Solution for secondary antibody	2.5% Serum in TBS
Antigen retrieval solution	2 ml Antigen Unmasking Solution (Vector), 213 ml dH_2O

2.1.11 Solutions and media

Ethidium bromide solution	10 mg/ml Ethidium bromide
5 x Loading Dye for agarose gels	40 ml Glycerol, 50 ml 10 x TBE, 5 ml 10% Bromphenol Blue, 5 ml 1% Xylene Cyan
1 x LB-Medium	0.5% yeast extract, 2% Bacto-Tryptone, 10 ml NaCl, add dH_2O up to 1 l and autoclave afterwards
SOC Medium	Invitrogen, Carlsbad, CA

2.1.12 Media and Solutions for cell culture

Culture medium for COS7 and 293T cells	DMEM (GIBCO/Invitrogen), 10% FCS, 1% L-Glutamine, 1% Penicillin/Streptamycin
Freezing medium for COS7 and 293T cells	DMEM, 1% DMSO, 1% FCS
Cell lysis buffer	For cell extracts of luciferase assays and EMSAs: Passive cell lysis buffer (Promega) For CoIP: RIPA-Buffer (50 mM Tris pH 7.5, 200 mM NaCl, 1% Triton X-100, 0.25% DOC, 1 mM EDTA)

2.1.13 Radioactivity

γ-^{32}P-dCTP	Amersham Pharmacia Biotech

2.1.14 Solutions for Western blot

Transferbuffer 1x	3.03 g Tris, 14.4 g Glycine, 20%MeOH in 1 l H_2O
Blocking buffer	PBS, 0.1% Tween-20, 5% Dry milk

2.1.15 Solutions for EMSA

DNA-binding buffer	5% glycerol, 10 mM Hepes pH 7.5, 25 mM KCl, 1 mM DTT, 1 mM EDTA, 5 mM $MgCl_2$

2.2 Methods

2.2.1 Analysis of nucleic acids

2.2.1.1 Phenol/Chloroform extraction of nucleic acids

The DNA was extracted with an equal amount of a phenol/chloroform/isoamyl (25:24:1) alcohol mixture to remove contaminating proteins. The mixture was then vortexed vigorously for 30 sec and centrifuged for 5 min at 12,000 x g. The top (aqueous) phase was removed and transferred into a new tube and was extracted again with an equal volume of chloroform. After extraction the top phase was removed and transferred into a new tube for EtOH precipitation.

2.2.1.2 Precipitation of nucleic acids out of aqueous solutions

In order to precipitate nucleic acid from an aqueous solution, it had to be adjusted to a 0.2 M salt concentration with 3 M Sodium acetate (pH 4.8). Then 2.5 vol. of 100% EtOH was added and the nucleic acids were precipitated for 0.5 hr at -20°C. Afterwards the sample was centrifuged for 10 min at a speed of 10,000 x g. To remove excessive salt the pellet was washed with 70% Ethanol. Finally, the pellet was air dried at RT or in speed vacuum. Nucleic acids were stored in H_2O or in TE-Buffer at -20°C.

2.2.1.3 Precipitation of nucleic acids out of aqueous solutions with isopropanol

DNA in an aqueous solution was precipitated with an equal volume of isopropanol. The mixture was precipitated on ice for 20 min and centrifuged at 10,000 x g for 10 min. The DNA pellet was washed with 70% Ethanol to

remove salts, air dried and resuspended in an appropriate volume of H_2O or TE-buffer.

2.2.1.4 Determination of nucleic acid concentration

The concentration of DNA in a sample was measured in a spectrophotometer where its absorbance of UV light at a wave length of 260 nm and 280 nm was measured against a blank (solvent of the DNA). One absorption unit at 260 nm equals 50 µg/ml of DNA, 40 µg/ml of RNA and 20 µg/ml of single stranded oligonucleotides. The quotient of the absorption at 260 nm and 280 nm is a measurement for the purity of the nucleic acid solution. The measurement should be at ~ 1.8 for DNA and ~ 2 for RNA.

2.2.2 DNA-Preparation

2.2.2.1 Preparation of small amounts of plasmid DNA (Mini-Prep)

A volume of 1.5 ml of a 3 ml over night culture (1 x LB-medium) was transferred into an 1.5 ml tube, centrifuged for 1 min at 12,000 x g and the supernatant except for 100 µl discarded. The bacterial pellet was resupended and lysed in 50 µl Phenol/Chloroform (1:1). The suspension was vortexed. After centrifugation at 12,000 x g for 5 min the upper, aeqeous phase which contained the DNA and bottom, organic phase that contained proteins had separated. The upper phase (~ 100 µl) was transferred into a fresh tube. To precipitate the DNA, 2 µl of 5 M NaCl and 200 µl of EtOH were added and incubated for 30 min at -20°C. The sample was then centrifuged at 12,000 x g for 10 min, the supernatant discarded and the pellet washed with 70% EtOH. After air drying the DNA was resuspended in 20 µl - 50 µl H_2O.

2.2.2.2 Preparation of large amounts of DNA (Maxi-Prep)

Large amounts of DNA were prepared using the commercially available Qiagen buffers. An over night culture of 30 ml (1 x LB-Medium, containing antibiotics for selection) was distributed into 1.5 ml tubes and centrifuged for 1 min at 12,000 x g. Supernatant was completely discarded and the bacterial pellet was resuspended in 150 µl P1-Buffer (10 mM EDTA pH 8.0, 50 mM Tris/HCl, 100 µg/ml, and RNase A). Subsequently, two tubes were combined to one, containing 300 µl of lysed bacteria. A volume of 300 µl P2-Buffer (200 mM NaOH, 1% SDS) was added to each tube to lyse the cells. The tubes were inverted 5 to 6 times and the suspension was incubated for 5 min at RT. To precipitate proteins and genomic DNA, 300 µl P3-Buffer (2.6 M KAc, pH 4.8) were added, samples incubated on ice for 15 min and centrifuged at 12000 x g for 6 min. Supernatant was transferred to fresh 1.5 ml tubes, filled with isopropanol and incubated 30 min – 1 hr on ice to precipitate the DNA. To collect the DNA, the samples were centrifuged at 12,000 x g for 15 min at 4°C. The DNA pellets were washed in 70% EtOH, air dried and resuspended in an appropriate amount H_2O and then combined. Plasmid DNA was stored at -20°C.

2.2.3 Gel electrophoresis of DNA and RNA

2.2.3.1 Agarose gel electrophoresis

Dependent on the size of the fragment of interest, a 0.8% - 2% agarose gel was made. The appropriate amount of agarose was dissolved completely in 1 x TBE buffer in a microwave (volume was dependent on size of gel tray). After adding 5 µl ethidium bromide (10 mg/ml) per 100 ml, the solution was poured into an appropriate gel apparatus.

Dependent on sample volume, a comb with the appropriate size was used. After polymerization of the gel was put into a gel box filled with 1 x TBE buffer and samples were loaded in 5 x Loading Dye (40 ml Glycerol, 50 ml 10 x TBE, 5 ml 10% Bromphenol Blue, 5 ml 1% Xylene Cyan). Final concentration of Loading Dye was 1 x. The voltage used to separate the DNA or RNA bands ranged between 70 and 190 volt dependent on the size of the gel.

2.2.3.2 Isolation and purification of DNA fragments from agarose gels

The DNA band of interest was cut out with a razor blade under UV light. The DNA bands are visible under UV light because the ethidium bromide in the gel intercalates with DNA. Purification of the DNA from the gel was done using the Qiagen DNA Gel Purification Kit according to the manufacturer's protocol.

2.2.4 Cloning techniques

2.2.4.1 Restriction digests of DNA

A total of 3 units of restriction enzyme per 1 μg of DNA were used for a restriction digest. One U defines the amount of enzyme that is necessary to digest 1 μg lambda DNA in 1 hour. The volume of a restriction digest was at least 10 times larger than the volume of the enzyme in order to dilute the glycerol, contained in the enzyme mix. The digest was done in the appropriate buffer and at the recommended temperature for 4 - 6 hrs or over night.

2.2.4.2 Ligation of DNA fragments

The DNA fragment to be ligated was used in a four fold molar excess to the vector. The appropriate amount of T4-Ligase and Ligase buffer were added and the ligation was incubated in a water bath over night at 16°C.

2.2.4.3 LB/Ampicillin or LB/Kanamycin plates

A total of 5 g yeast extract, 10 g bacto tryptone, 10 g NaCl and 15 g bacto-agar was dissolved in 1 l ddH_2O and autoclaved. Before pouring, the agar was cooled down to 60°C. Ampicillin, kanamycin, or both (final conc. 50 µg/ml (Amp), 25 µg/ml (Kan)) were added for antibiotic selection and the agar was poured into Petri dishes (10 cm in diameter).

2.2.4.4. Transformation of DNA into competent bacterial cells

To transform DNA into competent bacteria, chemically competent TOP10 one shot cells or INV 110 cells from Invitrogen were used. About 100 ng DNA were added to 50 - 100 µl competent cells and incubated for 30 min on ice. Cells were heat shocked in a 42°C water bath for 30 sec. (Top 10) or 45 sec. (INV 110), respectively. Then, cells were immediately quenched on ice. 250 µl of SOC medium was added and cells were shaken in an incubator at 37°C for an hour. Cells were plated on LB agar plates with the appropriate antibiotics.

2.2.5 Isolation of genomic DNA from mouse tails and yolk sacs for genotyping

Mouse tails or yolk sacs from embryos were used for genotyping. Isolation of genomic DNA from these tissues was done using the DNeasy Tissue Kit from Qiagen. Tails and yolks sacs were incubated in 180 µl ATL-Lysis Buffer and 20 µl Proteinase K at 55°C in a heat block shaking for 6 hrs

- over night to break down the tissue. The purification of the DNA was done according to the manufacturer's protocol, except for yolk sacs isolated from embryos E7.5 - E8.5. Here, the genomic DNA was eluted from the column using 50 µl Elution buffer (Qiagen). Genomic DNA of tails and yolk sacs was stored at 4°C.

2.2.6 Polymerase chain reaction (PCR)

The PCR is used to amplify exponentially DNA of interest. A standard reaction in total volume of 25 µl contains 2.5 pmol of each primer, 0.4 µl of Taq Polymerase (5 U/µl) (HotStart Taq, Qiagen, for Pitx2 genotyping) FastStart Taq; Roche, for Tbx1 genotyping), 3 µl $MgCl_2$ (25mM) 4µl dNTPs (1.25 mM), 2.5 µl Reaction buffer (10 x), and 20 ng of template DNA. Tails or yolk sacs were used for genotyping mice and embryos, respectively (see 2.2.5). PCR conditions varied depending on primer pairs used.

PCR conditions for Pitx2 genotyping using the primers: Pitx2-F, Pitx2-R or Pitx2-31130, Pitx2-30266 and Pitx2-30265

94°C	15:00 min	1 cycle
94°C	0:30 min	
60°C	0:30 min	37 cycles
72°C	2:30 min	
72°C	10:00 min	1cycle

PCR conditions for Tbx1 genotyping using the primers: Tbx1KO1-F, Tbx1KO2-R and mut-2-R

94°C	10:00 min	1 cycle
94°C	0:30 min	
55°C	0:30 min	35 cycles
72°C	2:30 min	
72°C	10:00 min	1 cycle

PCR conditions: Genotyping for Tbx1 using the primers: Hygro-F, Hygro-R, Tbx1wt-F and Tbx1wt-R

94°C	10:00 min	1 cycle
94°C	1:00 min	
60°C	1:00 min	35 cycles
72°C	1:00 min	
72°C	10:00 min	1 cycle

2.2.7 Histology of mouse embryos

2.2.7.1 Isolation of mouse embryos

Mice were anesthetized using CO_2 and then killed by cervical dislocation. The animal was laid on its back and its abdomen soaked in 70% EtOH, which reduces the risk of contaminating the dissection. A lateral incision on the ventral side of the animal was made using scissors. The skin could be pulled away so that the entire abdomen was exposed. Using fine scissors and Dumont forceps the peritoneum was cut open and the uterus duplex was isolated and transferred into PBS on ice. Embryos still in the uterus were separated from each other and each single embryo was isolated under the stereomicroscope in ice cold PBS. The uterus, the decidua and the yolk sac were removed using extra fine Dumont forceps. The yolk sac was used for genotyping the embryo.

2.2.7.2 Fixation of mouse embryos and newborns

Embryos E7.5 - E11.5 and E10.5 hearts for whole mount *in situ* hybridization as well as embryos for *in situ* hybridization (ISH) on sections were fixed in 4% PFA in PBS (-Ca^{2+}/-Mg^{2+}) at 4°C. Fixation times depended on embryonic stage and varied between 4hrs -16hrs. After fixation embryos for whole mount ISH were washed twice in PBS, 0.1% Tween-20 (PBSw) and then dehydrated in a MeOH series (25%, 50% and 75%) each step 10 min. Embryos for ISH on sections were washed twice in PBS (-Ca^{2+}/-Mg^{2+}) and then dehydrated in an EtOH series (25%, 50% and 70%). The times for the dehydration steps varied according to the size of the embryo. Newborns and embryos for histological analysis and antibody staining were fixed in 10% neutral buffered formalin. Fixation times varied according to the size of

the embryo (see Table 2.2.1). After fixation embryos were dehydrated through an EtOH series (25%, 50% and 70%).

Table 2.2.1: Fixation times for mouse embryos and newborns in 10% neutral buffered Formalin

Age	Fixation time
Newborns	3 days
E15.5 – E18.5	2 days
E11.5 – E14.5	16 hrs
E9.5 – E10.5	6 hrs

2.2.7.3 Embedding of mouse embryos and newborns

Specimens in 70% EtOH were put into embedding cassettes to be processed in an embedding machine using vacuum to make tissues or embryos permeable for wax. Newborns and fetuses (E16.5 - E18.5) had to be decalcified in Immunocal (Fisher) for 4 hrs prior to embedding. Specimens were dehydrated and incubated in wax according to Table 2.2.2. Then, specimens were transferred into embedding molds, where they were oriented in the desired position and submerged in melted wax (60°C). A microtome holding cassette was put on top. The mold was transferred onto a cold plate for 30 min. until the wax had hardened. A scalpel was used to remove the mold. The wax block was trimmed to be ready for sectioning with a microtome.

Table 2.2.2: Incubation times for tissue processing

Reagent	**Stages E15.5 – E16.5**	**Newborns and decidual swellings**	**Stages E10.5 – E14.5**	**Stages E7.5 - E9.5** (processed manually)
70% Ethanol	5 min	5min	5min	5min
70% Ethanol	15min	20min	5min	5min
80% Ethanol	15min	20min	5min	5min
95% Ethanol	15min	20min	5min	5min
100% Ethanol	8min	20min	5min	5min
100% Ethanol	10min	20min	5min	5min
100% Ethanol	15min	25min	7min	5min
Xylene	10min	20min	5min	10min
Xylene	10min	25min	5min	10min
Xylene	15min	25min	7min	-
Paraffin	15min	30min	15min	15min
Paraffin	15min	35min	20min	15min
Paraffin	15min	40min	20min	15min

2.2.7.4 Sectioning of tissue

Tissue blocks were trimmed with a razor blade. The wax block with the specimen to be cut was then fixed to the microtome via the holding cassette. Specimens for *in situ* hybridization on sections were cut at 10-12 µm, specimens for immunohistochemistry and histological analysis were cut at 7 µm. Ribbons of sections for immunohistochemistry or histological analysis were transferred into a 40°C water bath, so that sections could spread on the surface of the water. Sections were then transferred onto a slide and dried vertically at room temperature. Ribbons of sections for *in situ* hybridization on sections were transferred onto prepared slides with a drop of sterile water. These slides were put on a slide warmer (50°C) for 30 min to spread the sections. Finally, sections were dried vertically at RT.

2.2.8 Analysis of the phenotype of mutant mice

2.2.8.1 Hematoxylin and eosin staining of histological sections

Counterstaining with hematoxylin and eosin of histological sections of mouse embryos and newborn mice was used to analyze the morphology and histology of the mouse mutants. Sections of embryos or newborns were deparaffinized in xylene (1 x 8 min, 1 x 7 min), rehydrated in an 2 x 100% (3 min), 95% (2 min), 80% (2 min) and 70% (1 min) EtOH series and rinsed under running tap water for 3 min. Sections were then stained in hematoxylin (1/3 dilution in H_2O) for 2 -5 min and washed again under running tap water to get rid of an excess of hematoxylin. A destaining step in acid alcohol (1% HCl (12.5 N) in 70% EtOH) followed for 5 sec. Slides were washed again in running tap water for 5 min and stained again in Mordant stain (1.5 ml of 28% NH_4OH in 600 ml H_2O) for 5 sec. Slides are subsequently washed under running tap water (8 min) and 80% EtOH (1 min) and then stained in eosin (8 min). Finally, sections were rehydrated through an 80% (30 sec), 95% (45 sec), 95% (1 min), 2 x 100% (1 min) EtOH series and 2 steps in xylene (7 and 8 min). Slides were mounted using Permount. Morphology of the specimens was examined under a light microscope (Axioskop 2 Plus, Zeiss) and pictures were taken using a digital camera (Leica DC300).

2.2.8.2 Immunohistochemistry on paraffin sections

Immunohistochemistry was used to examine the spatial and temporal expression of proteins in embryos as well as in adult tissue. Compared to *in situ* hybridization for which RNA probes can be synthesized for basically any gene of interest, the immunohistochemistry is strongly dependent on a well working antibody for the protein of interest. Alternatively, frozen sections instead of paraffin sections and immunofluorescence instead of

immunohistochemistry can be used. To dewax the tissue, slides were incubated at 60°C for 30 min and then processed through 2 x 10 min xylene and then rehydrated through a 2 x 100%, 95%, 80% and 70% EtOH series (2 min each). Subsequent washings steps were done in H_2O and 2 x TBS (Sigma) for 2 min each. To block endogenous peroxidase activity, slides were treated with 3% H_2O_2 (DAKO) for 15 min at RT. Then, slides were washed with TBS for 2 min and incubated in citrate buffer (pH 6.0; Vector) in a steamer for 20 min to retrieve the antigen and then cooled down for 30 min before continuing with the blocking step. To reduce unspecific binding, the sections were blocked in 5% goat serum (The type of serum used in the blocking buffer depends on where secondary antibody was raised in.), 2% BSA, 0.1% Triton X-100 for 1 hr at RT. Incubation of primary antibody was carried out for 1 hr (rabbit-anti-Tbx1) and 2 hrs (rabbit-anti-Pitx2) at RT. Working dilution of the used antibodies were: Tbx1: 1/500 and Pitx2: 1/50. After the incubation slides were washed in TBS (6 x 5 min) and then the secondary antibody, a biotinylated goat-anti-rabbit antibody (DAKO), was applied in a dilution of 1/500 in TBS and 2.5% goat serum and incubated for 1 hr. Two washing steps for 5 min followed and then the avidin-biotinylated peroxidase complex (ABC from DAKO; pre-incubated in TBS for at least 30 min) was put onto the sections and incubated for 30 min. After two more washes in TBS for 5 min the sections were exposed to the substrate, the chromogen (DAKO) to stain the sections through an enzymatic reaction. Slides were rinsed in H_2O, counterstained in hematoxylin for 10 sec, dehydrated through an EtOH series and xylene and subsequently mounted.

2.2.8.3 BrdU staining (cell proliferation assay) on sections

BrdU is incorporated into transcribed RNA and hence, serves for detection of proliferating cells. BrdU was injected intraperitoneal into pregnant mice 2 hrs prior isolation of embryos. Embryos were fixed and sectioned using standard protocols. Sections were then subjected to the same procedures mentioned in the protocol for immunohistochemistry, with the following exceptions. After the antigen retrieval the sections were treated additionally in 3 N HCl for 45 min at RT to denature the DNA and then washed in TBS (2 x 3 min) to neutralize the pH value. Blocking buffer consisted of 5% rabbit serum, 2% BSA 0.1% Triton X-100. As a primary antibody a mouse anti-BrdU (Roche) was used in a 1/50 dilution in blocking buffer. As a secondary antibody a biotinylated rabbit-anti-mouse antibody (DAKO) was used in a 1/500 dilution in 2.5% rabbit serum in TBS.

2.2.8.4 Digoxigenin-labeling of RNA probes for *in situ* hybridization by *in vitro* transcription

Sense and antisense riboprobes are synthesized from a linearized cDNA using T7, T3 or SP6 RNA polymerase depending on which vector the template is cloned in. During the *in vitro* transcription digoxigenin-labeled dUTP will be used for the synthesis of the riboprobe. Later the labeled RNA can be detected through a color reaction using an enzyme coupled anti-digoxigenin antibody.

For the synthesis of the antisense or sense RNA probe 10 µg of the plasmid of interest were linearized with the appropriate enzyme and purified by phenol/chloroform extraction with subsequent EtOH precipitation. The purified linearized plasmid was resuspended in nuclease free ddH_2O (Gibco). For the labeling reaction 1 µg of the linearized plasmid was added to 2 µl of 10 x transcription buffer, 2 µl of Digoxigenin Labeling Mix (Roche), 2 µl of the appropriate RNA-Polymerase and 1 µl RNase Inhibitor. The reaction was

carried out in total volume of 20 µl in nuclease free water. The reaction was incubated for 3 hrs at 37°C. To get rid of an excess of free nucleotides, the labeled RNA probe was run through a mini quick spin sephadex column (Roche).

2.2.8.5 Non-radioactive *in situ* hybridization

In situ hybridization to RNA is used as a tool to determine the spatial and temporal expression pattern of a gene of interest. Non-radioactive *in situ* hybridization is based on the use of a digoxigenin-labeled anti-sense RNA probe of the gene of interest, which is hybridized to the endogenous RNA in the embryo or tissue. The RNA is detected indirectly via an anti-digoxigenin-antibody, conjugated to alkaline phosphatase. Addition of the substrate BM-Purple, leads to conversion of the chromogen in an enzymatic reaction by the alkaline phosphatase to a blue precipitate in the tissues where the RNA is expressed. *In situ* hybridization methods are used to detect RNA in whole embryos, embryonic tissues as well as on embryonic sections.

2.2.8.5.1 Whole mount *in situ* hybridization (modified after Belo *et al*., 1997)

All of the following steps were carried out on ice, except for those stated otherwise. Embryos which had been stored in 75% MeOH/PBSw were rehydrated through a 50% and 25% MeOH series in PBSw (5 - 10 min depending on age of embryos). After washes in PBSw (3 x 5 min) embryos were treated with 4.5 µg/ml Proteinase K in PBSw at RT to permeable the embryo which facilitates entering of the RNA probe. Depending on the age of the embryos or tissue size the time of Proteinase K treatment varied (**E6:** 3 min; **E7.5:** 5 min; **E8.5:** 7 min; **E9.5:** 9 min; **E10.5:** 11 min; **E11.5:** 20 min). Digestion with Proteinase K was stopped by adding freshly prepared 2 mg/ml glycine in PBSw. Embryos were rinsed and washed in PBSw (2 x 5 min) and

then refixed in freshly prepared 4% PFA/0.2 % glutaraldehyde in PBS for 15 min. After fixation the embryos were washed in PBSw (3 x 5 min), in 1 ml 50% PBSw; 50% hybridization solution for 3 min and in 1 ml of hybridization solution for 3 min. After replacing 900 µl of hybridization solution with fresh solution embryos were pre-hybridized for 2 - 3 hrs at 65°C. The RNA probe was denatured in 100 µl hybridization solution at 95°C (final conc. of RNA probe was 200 ng/ml) and then added to the embryos. Hybridization was carried out over night at 70°C in a water bath.

On the second day the hybridization solution was replaced with 800 µl of fresh solution and embryos were incubated for 5 min at 70°C. Subsequently, 400 µl 2 x SSC (pH 4.5) (3 x 1 min) were added. The low pH stabilizes negative charges of the riboprobe and facilitates the hybridization. Next, the solution was removed and 2 x 30 min washes in 2 x SSC (pH 7.4) at 70°C in the water bath followed. To reduce background, the samples were subsequently washed in Maleic Acid Buffer (2 x 10 min at RT and 2 x 30 min at 70°C). Additional washing steps were carried out in PBSw (2 x 10 min, 1 x 5 min) at RT. Embryos were then incubated in 1 ml BM-block-mouse antibody buffer for 2 hrs at 4°C to block unspecific binding sites. Following the blocking step, 1.5 ml of a 1:10,000 dilution of the anti-Digoxigenin antibody was added and incubated at 4°C over night. The antibody had been pre-absorbed in the BM-blocking buffer for 2 hrs at 4°C.

On the third day the samples were washed in 0.1% BSA/PBSw 5 x 45 min to reduce unspecific binding of the antibody, 2 x 30 min in PBSw and 2 x 10 min in AP1-Buffer. All the washes were carried out at RT. Samples were then transferred into 1 ml BM-Purple solution and placed into the dark for the staining reaction. Specimens were stained until background appeared. The staining reaction was stopped by washing in PBS (at least 3 times). Embryos were post-fixed in 4% PFA and then stored in PBS at 4°C. Pictures

of whole mount embryos were taken using the stereomicroscope (Leica M12) and digital camera Leica DC300.

2.2.8.5.2 *In situ* hybridization on paraffin wax sections (after Franco *et al*., 2000)

Fixation, embedding and sectioning of the tissues were done according to standard procedures (2.2.7.2 - 2.2.7.4). Paraffin sections were cut as thick as possible ranging from 10 µm - 12 µm depending on age of the embryo to enhance the signal.

Slides with paraffin sections were pretreated in xylene (3 x 7 min) and 50% xylene/50% EtOH to remove the wax from the tissue. Sections were then rehydrated in a 2 x 100% (2 min), 1 x 96%, 1 x 90%, 1 x 70% and 1 x 50% (each 1 min) EtOH series. After washing in PBS (2 x 5 min) sections were treated with Proteinase K (20 µg/ml) in PBS for 10 - 15 min (depending on tissue size) at 37°C in a water bath to facilitate the entering of the RNA probe. Proteinase K treatment was stopped by transferring slides into 0.2% glycine in PBS. After 2 washes in PBS for 5 min sections were refixed in 4% PFA/0.2% glutaraldehyde in PBS for 20 min. Then, slides were washed in PBS (2 x 5 min). Subsequently, sections were surrounded with a PAP pen and the hybridization solution was put on each section for the pre-hybridization for 1 hr at 70°C.

The digoxigenin-labeled probe was diluted in the hybridization solution to a final conc. of 200 ng – 4 µg/ml (each probe has its own optimal concentration) and denatured at 95°C for 5 min and quenched on ice. The prepared probe was then added to each section and incubated over night at 70°C. The following day the slides were rinsed in 2x SSC (pH 4.5) and washed in 50% formamide/2 x SSC (pH 4.5) for 3 x 30 min at 65°C to facilitate hybridization of the RNA probe. Sections were washed in PBSw (3 x 5 min) and then incubated in BM-block-mouse antibody buffer for 1 hr at

RT in a humidity chamber. The anti-digoxigenin antibody was diluted in BM-block-mouse antibody buffer 1:1,000 (The anti-digoxigenin antibody can also be used at lower conc. (1:3,000) to reduce background). Sections were incubated with the diluted antibody for 2 hrs at RT in a humidity chamber. Following washes in PBSw (3 x 5 min) and NTM buffer (2 x 5 min), sections were incubated with a 1:50 dilution of NBT/BCIP in NTM buffer (staining solution) over night or longer in a humidity chamber in the dark at RT. Afterwards, slides were rinsed in H_2O and dehydrated through a 50%, 70%, 90%, 96%, 2x 100% EtOH series, 50% xylene/50% EtOH (1 min) and xylene (3 x 5 min). Slides were mounted using Permount. Pictures of stained sections were taken using a light microscope with DIC (Axioskop, Zeiss) and the digital camera (Leica DC300).

2.2.8.6 Alizarin Red and Alcian Blue staining of bone and cartilage in 18.5 dpc embryos

This staining technique is used to reveal skeletal structures of embryos or newborns. Cartilage is stained in blue and bone in red. E18.5 mouse fetuses were delivered by cesarean section and euthanized in CO_2. Then, their skin was peeled off with forceps and fetuses were fixed in 95% - 100% EtOH over night. Specimens were stained for cartilage in Alcian Blue stain (15 mg Alcian Blue 8GX (Sigma), 80 ml 95% EtOH, 20 ml glacial acetic acid) for 24 hrs. After rinsing twice in 95% EtOH, the soft tissue of the fetuses was dissolved in 2% KOH for 6 hrs. Through the alkaline treatment the bones become visible. The bones were counterstained in Alizarin Red (75 µg/ml Alizarin Red S (Sigma) in 1% KOH over night. Samples were cleared using 20% glycerol in 1% KOH for 3 - 7 days, changing the solution daily. Loose tissue was dissected away if necessary. The skeletal preparations were transferred into 20% glycerol, 20% EtOH over night and then into 50% glycerol, 50% EtOH for further clearing and storage.

2.2.9 Cell culture

2.2.9.1 Culture of 293T cells and COS7 cells

293T cells (human kidney carcinoma cells) and COS7 were cultured in DMEM medium containing 10% FCS, 1% L-Glutamine and 1% Penicillin/Streptomycin. Cells were split every second day 1:10. They were trypsinized and subsequently centrifuged in 5 ml culture medium at 1000 rpm for 3 min. Supernatant was discarded and cells were resuspended in culture medium and distributed on cell culture dishes.

2.2.9.2 Freezing and thawing of 293T and COS7 cells

Cells were trypsinized with 0.25% Trypsin, EDTA, pH 8 and centrifuged in 5 ml culture medium at 1,000 rpm for 3 min. Supernatant was discarded and cell pellet was resuspended in freezing medium (1% DMSO, 1% FCS, 8% DMEM-Medium). Cells were then stored at -80°C.

Cells were thawed in a 37°C water bath, washed with DMEM-Medium containing 10% FCS, 1% L-Glutamine and 1% Penicillin/Streptomycin and then plated on tissue culture dishes.

2.2.9.3 Transient transfections of COS7 cell and 293T cells

Constructs used in transfection for Luciferase Assays:

- 900 bp enhancer element of Pitx2c isoform (Pitx2-ASE) (Shiratori *et al*., 2001) cloned into pGl3 SV40 luciferase vector (Promega)
- Full length cDNA Tbx1 cloned into pcDNA3.1
- Flag-Nkx2.5 cloned into in pCI (Promega)
- CMV-βGal construct

Transfections were performed in 6-well plates using Polyfect Reagent (Qiagen) according to manufacturer's protocol.

COS7 cells were transfected with 0.15 μg of the Pitx2-ASE luciferase construct and with 0.3 μg of the expression constructs Tbx1 in pcDNA3.1, Nkx2.5 in pCI, respectively. The empty vectors pcDNA3.1 and pCI were used as controls. A total of 0.03 μg of CMV-βGal construct was co-transfected to normalize transfection efficiency. Cells were lysed in 1 x Lysis buffer (Promega) and harvested after 48 hrs. Luciferase and β-Galactosidase activity were assayed using Luciferase assay system (Promega) in a TD-20/20 luminometer and β-Galactosidase reporter gene activity detection Kit (Sigma), respectively.

Construct used in tranfections for EMSA:

- Full length cDNA Tbx1 in pcDNA3.1

A total of 8 μg of Tbx1 expression vector was tranfected into a 10 cm dish of 80% confluent 293T cells. Untransfected cells were used as controls. The transfection was carried out in 10 cm tissue culture dishes using Polyfect Reagent (Qiagen) according to manufacturer's protocol.

Constructs used in transfection for CoIp:

- Tbx1-GFP cloned into pEGFP-N1 (Clontech)
- Flag-Nkx2.5 cloned into in pCI (Promega)

A total of 4 μg of Tbx1-GFP and 4 μg of Flag-Nkx2.5 were co-transfected into 293T cells. Cells transfected with 8 μg Tbx1-GFP, cells transfected with 8 μg Flag-Nkx2.5 and untransfected cells were used as controls. Transfections were carried out in 10 cm tissue culture dishes using Polyfect Reagent (Qiagen) according to manufacturer's protocol.

2.2.9.4 Determination of Luciferase reporter gene activity

To determine the luciferase reporter gene activity, the Luciferase Assay System (Promega) was used to measure the activity of Firefly luciferase. The Firefly luciferase oxidizes its substrate beetle luciferin using ATP, Mg^{2+} and O_2 to oxyluciferin, AMP, PP_i, CO_2 and light. The emission of light is quantified in a luminometer. Transfected cells were lysed in 1 x passive lysis buffer (Promega) for 15 min on a shaker at RT. (For 6-well plates 500 µl and for 10 cm dishes 1 ml of 1 x Passive Lysis Buffer (Promega) were used.) The lysates were transferred to 1.5 ml tubes and cleared by centrifugation for 30 min at 12,000 x g. 20 µl of cell lysate was added to 50 µl of Luciferase Reagent II (Promega) and the luciferase activity was measured in a TD-20/20 luminometer (Turner Design).

2.2.9.5 Determination of β-galactosidase reporter gene activity

For normalization of the efficiency of transfections a CMV-β-gal expression construct was transfected into cells along with other reporter and expression construct (2.2.9.3). Cell lysates were tested for β-galactosidase activity using the β-galactosidase reporter gene activity Kit (Sigma) according to the manufacturer's protocol. Cells were lysed in 1 x Passive Lysis Buffer (Promega). 50 µl of each cell lysate was pipetted into a well of a 96-well plate. 50 µl of 1 x Lysis buffer were used as blank. 50 µl 2 x assay buffer (200 mM sodium phosphate buffer (pH 7.3), 2 mM $MgCl_2$, 100 mM β-mercaptoethanol, 1.33 mg/ml o-nitrophenyl β-D-galactopyranoside (ONPG)) were added to each well and mixed. β-Galactosidase uses ONPG as substrate and catalyzes its hydrolysis to yellow colored o-nitrophenol. Samples were incubated at 37°C until yellow color developed. The reaction was stopped by adding 150 µl stop solution (1 M $NaCO_3$). The β-galactosidase activity was measured in an ELISA reader (Victor 2 1420 Multilabel Counter; Perkin Elmer™) at a wave length of 420 nm.

2.2.9.6 Determination of Protein concentration (Bradford assay)

The protein concentration of cell lysates was determined using the Bradford protein assay (BIORAD). A total of 5 µl cell lysate was added to 795 µl H_2O. Protein concentrations were measured against a standard curve using 2, 5, 10, 15, and 20 µg/ml BSA. 5 µl of 1 x Passive Lysis buffer (Promega) in 795 µl H_2O was used as blank. A total of 200µl of BIORAD reagent was added to each sample and incubated for 15 min. The absorbance was read at 595 nm in a spectrophotometer to determine the protein concentration.

2.2.10 Co-Immunoprecipitation (Co-IP)

The Co-IP identifies protein-protein interactions. Proteins of interest are transfected into cells and the cells are harvested under conditions that preserve protein-protein interactions. The protein is immunoprecipitated from the cell extract and then subjected to SDS-PAGE for separation. The identity of the protein is detected by Western blot analyis.

For this analysis, 293T cells transfected with either the expression construct Tbx1-GFP cloned in pEGFP-N1 (Clontech), a Flag-Nkx2.5 (obtained from Dr. V. M. Christoffels) or both using Polyfect Reagent (Qiagen). Cells were lysed and harvested after 48 hrs in RIPA-buffer (50 mM Tris pH 7.5, 200 mM NaCl, 1% Triton X-100, 0.25% DOC, 1 mM EDTA). Cell lysates were pre-cleared using 30 µl Protein G Agarose per 500 µl cell extract for 30 min rotating at 4°C. Co-Ip was performed with an Anti-Flag M2 affinity gel (Sigma) according to manufacturer's protocol.

Co-IPs were subjected to SDS-PAGE (see 2.2.11) to separate proteins according to size. After blotting, proteins were detected by Anti-Flag M2 (Sigma) and Anti-Tbx1 (Zymed) antibodies. Blots were exposed to Kodak film (Biomax MS).

2.2.11 SDS-PAGE

Proteins were separated using denaturing polyacrylamide gel electrophoresis (SDS-PAGE). SDS denatures proteins. These are consequently separated in the gel according to their molecular weight only. The mobility of the proteins in the gel also depends on the pore size of the gel and the voltage used.

Cell lysates or Co-Ip samples were loaded into wells of a 10% Tris-HCl-SDS-Gel (BIORAD). The gel was positioned vertically in gel chamber filled with 1x Tris-glycine-SDS running buffer (BIORAD). The SDS-Gel was electrophoresed at 100 V for 1.5 hrs. To determine the molecular weight of the protein, a Protein marker (BIORAD) was loaded. Gels were subsequently subjected to Western blotting.

2.2.12. Western blot and immunodetection of proteins

To detect the identity of proteins separated on SDS-Gels, they were transferred to a nitrocellulose membrane (Protran, Schleicher-Schuell). Proteins on the membrane could then be detected by specific antibodies. SDS-gels and membranes were pre-soaked in transfer buffer (3.03 g Tris, 14.4 g Glycine and 20% MeOH in 1 l H_2O) prior to transfer. The transfer was performed in a wet blot apparatus. The wet blot apparatus consists of a tank holding the blot sandwich in vertical position between the two electrodes. The blot sandwich was completely submerged in transfer buffer. The blot sandwich for the transfer was set up as follows: anode, cushion, blotting paper, gel, membrane, blotting paper, cushion, and cathode. Proteins were transferred to the membrane at 100 V for 2 hrs at 4°C.

Membranes were incubated in blocking buffer (25 g Blotting Grade Dry Milk in 500ml PBS, 0.1% Tween-20) to block unspecific binding of the antibodies. Incubation of the primary antibody (Anti-Tbx1, Zymed and Anti-Flag M2, Sigma) was performed on a shaker over night at 4°C. The Anti-Tbx1 antibody was used in a dilution of 1:500. Anti-Flag M2 was used in a dilution of 1:5,000. Membranes were washed in PBSw (3 x 15 min) and then incubated with the secondary antibody. Biotin-labeled anti-rabbit-IgG and biotin-labeled anti-mouse-IgG were used for detection of Anti-Tbx1 and Anti-Flag, respectively. Both secondary antibodies were used in a dilution of 1:3,000. Membranes were subsequently washed in PBSw (3 x 15 min). Protein signals on the membranes were detected performing ECL (Perkin Elmer) according to the manufacturer's protocol and exposure to Kodak film (Biomax MS)

2.2.13 Electro-Mobility-Shift Assay (EMSA)

2.2.13.1 Annealing of oligonucleotides for the DNA-binding assay

A total of 100 pmol of each oligonucleotide were added to 5 µl annealing buffer (100 mM Tris pH 8, 500 mM NaCl, 10 mM EDTA pH 8) and 43 µl H_2O. The reaction was boiled for 15 min and slowly annealed by cooling down to room temperature.

2.2.13.2 Radioactive end-labeling of DNA-oligonucleotides using T4 Polynucleotide Kinase

The T4 Polynucleotide Kinase is used to phosphorylate DNA ends. It catalyzes the transfer of the γ-phosphate of ATP to the 5' hydroxyl terminus of the DNA and can thereby label 5'ends of DNA.

A total of 20 pmol of double stranded oligonucleotides were radio-labeled with 5µl [γ-^{32}P]dATP using 1 µl T4-Kinase (NEB), 2 µl 10 x Kinase Buffer (NEB) and 11 µl H_2O. The kinase reaction was incubated for 30 min at 37°C and then purified on Sephadex G-50 spin columns (Amersham).

2.2.13.3 DNA-Binding Assay

The DNA binding assay uses non-denaturing polyacrylamide gel electrophoresis (PAGE) to detect specific binding of proteins from cell extracts or purified proteins to DNA. Proteins that bind to radioactively end-labeled oligonucleotides slow down the mobility of the oligonucleotide in the gel which results in discrete bands.

For the DNA-binding assay, radioactive-labeled oligonucleotides were used containing the T- half site of the Pitx2-ASE (WT), mutated (M1, M2) or a consensus (Cons) T- half site. The sequences of the oligonucleotides are as follows:

WT: CAATCAGGTGTAAAGAGGAA
M1: CAATCAGATTTGAAGAGGAA
M2: CAATCAAATTTGAAGAGGAA
Cons: CAATCAGGTGTGAAAAGGAA.

Full length cDNA of Tbx1 was cloned into pcDNA3.1 (Invitrogen) and transfected into 293T cells. Crude cell lysates of Tbx1 transfected 293T cells were used for DNA binding assay and incubated for 30 min on ice in a reaction containing 5% glycerol, 10 mM Hepes pH 7.5, 25 mM KCl, 1 mM DTT, 1 mM EDTA and 5 mM $MgCl_2$ (DNA-Binding buffer), 1 µg dIdC and 0.1 pmol radio-labeled probe of either Wt, M1, M2 or Cons, respectively. In a competition assay unlabeled wild type competitor oligonucleotides in a 100 fold molar excess were added. In this case samples were pre-incubated for 20 min on ice before adding radio-labeled probe. When adding the Tbx1

antibody to the DNA binding assay to perform a supershift assay, samples were again pre-incubated for 20 min on ice before radio-labeled probe was added. The DNA-protein complexes were resolved on a 6% non-denaturing polyacrylamide gel in 0.5 x TBE. Gels were exposed to Kodak film (Biomax MS).

3. Results

A candidate gene approach was used to screen for downstream targets of the T-box transcription factor, *Tbx1* to investigate its role during early cardiac morphogenesis in the mouse. Possible downstream genes should be identified by up or down regulation in the *Tbx1* homozygous mutants using whole mount *in situ* hybridization (ISH) of E8.0 - 10.5 mouse embryos. Genes that are co-expressed with *Tbx1* during early development were considered as candidates. One gene of particular interest was the homeobox gene *Pitx2,* which is important for asymmetric development of the heart. It is expressed in the SHF where *Tbx1* has recently been implicated to play major role in (Vitelli *et al*., 2002b; Hu *et al*., 2004; Xu *et al*., 2004). In this thesis, I present a detailed analysis of *Tbx1* and *Pitx2* co-expression in the left SHF during early embryogenesis. Furthermore, I show down-regulation of *Pitx2* in the *Tbx1* null mutants suggesting a possible interaction of both genes. Crosses of *Pitx2* heterozygous and *Tbx1* heterozygous animals result in severe cardiac defects and consequent neonatal lethality in the *Pitx2*+/-; *Tbx1*+/- mice. Subsequent molecular studies reveal a direct activation of the *Pitx2* gene through Tbx1 by interaction with Nkx2.5. In summary the results in this thesis provide evidence for a novel Tbx1-Pitx2 pathway in the left SHF.

3.1 Co-expression of *Tbx1* and *Pitx2* in the cardiac precursor cells of the secondary heart field (SHF) during early mouse embryogenesis

Whole mount *in situ* hybridization of E7.75 embryos revealed *Pitx2* and *Tbx1* co-expression in the lateral plate mesoderm (LPM) during early mouse embryogenesis (Fig. 3.1) To investigate co-expression in more detail, *in situ* hybridization on sections were performed of wild type embryos of stages E8.0 – 9.5 using *Tbx1*, *Pitx2*, *Nkx2.5* as a marker for cardiomyocytes (Lyons *et al*., 1995) as well as the LIM homeodomain transcription factor *Islet-1* (*Isl-1*). The latter has been previously described as a marker for cardiac progenitor cells of the SHF (Cai *et al*., 2003). *In situ* hybridization on sections showed that *Tbx1* and *Pitx2* are co-expressed in the arterial and the venous pole of the heart as early as E8.0 until E9.5. Co-expression of both genes occurred in *Nkx2.5* and *Isl-1* positive regions meaning that they are expressed in cardiac precursor cells of the SHF. At E8.0, co-expression of *Tbx1, Pitx2, Nkx2.5* and *Isl-1* occurred at the venous pole of the developing heart in the left horn of the sinus venosus (lsv) (Fig. 3.2 A-D) and at the arterial pole in the ventricular region (vr) and the pharyngeal mesoderm (pm) (Fig. 3.2 E-H). At day E8.5, co-expression of all four genes persisted in the left sinus venosus (lsv), the pharyngeal mesoderm (pm) and in the inner curvature of the common ventricle (cv) (Fig. 3.2 I-P). In addition, *Tbx1*, *Pitx2*, *Nkx2.5* and *Isl-1* were co-expressed in the outflow tract at this stage. *In situ* hybridization of sagittal sections of embryos of stage E9.5 showed that co-expression persisted in the pharyngeal mesoderm (pm), in cells of the common ventricle (cv) and the outflow tract (oft) (Fig. 3.2 Q-T).

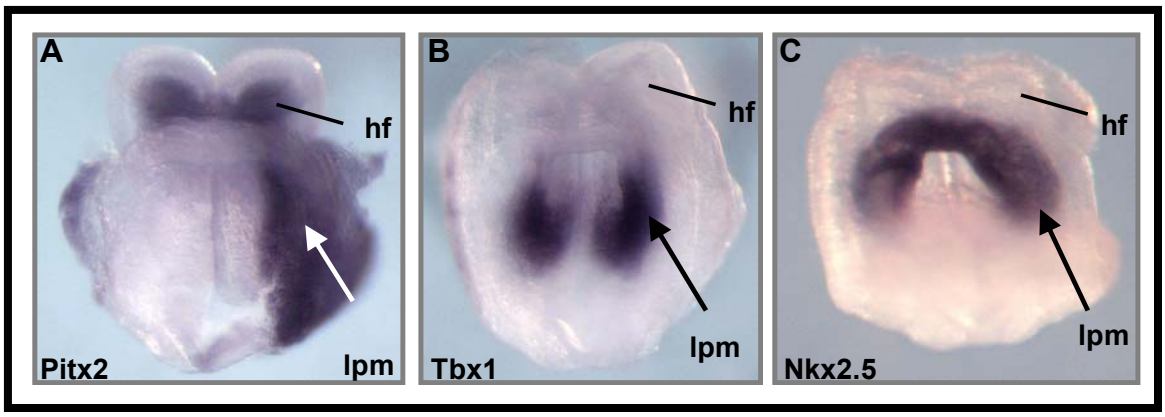

Fig. 3.1: Co-expression of *Tbx1* and *Pitx2* in cardiac precursor cells

Whole mount *in situ* hybridization of wt embryos stage E7.75 show co-expression (arrows) of *Pitx2* (A) and *Tbx1* (B) in *Nkx2.5* (C) expressing cells in the left lateral plate mesoderm (lpm). hf, head folds.

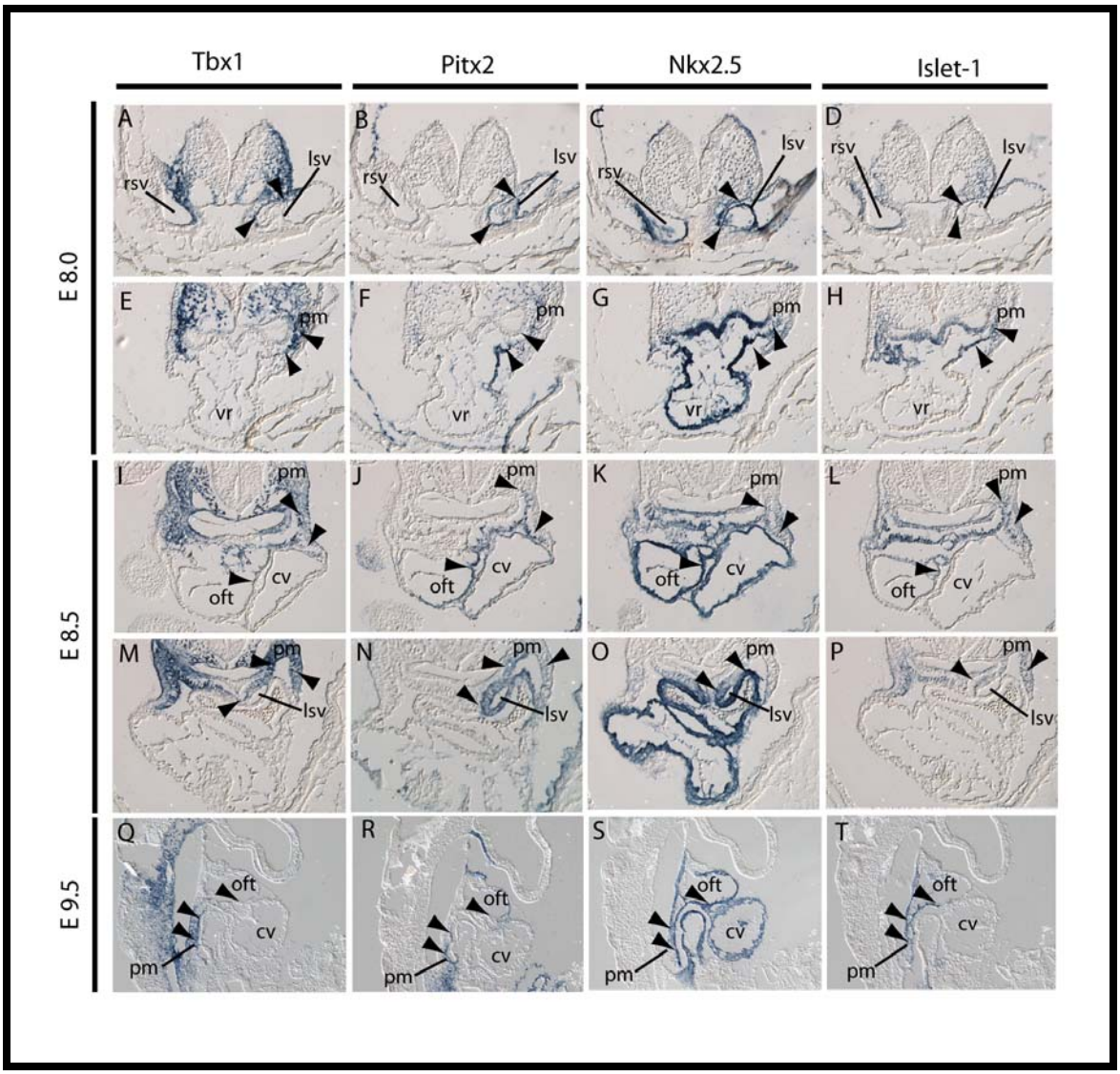

Fig. 3.2: Co-expression of *Tbx1* and *Pitx2* in cardiac precursor cells in the SHF

In situ hybridization on transverse sections of E8.0 and E8.5 embryos and sagittal sections of E9.5 embryos show co-expression of *Tbx1* (A, E, I, M, Q) and *Pitx2* (B, F, J, N, R) within the *Nkx2.5* (C, G, K, O, S) and *Islet-1* domains (D, H, L, P, T). Overlapping expression of *Tbx1, Pitx2, Nkx2.5* and *Islet-1* was found in the left horn of sinus venosus (lsv) at stages E8 - E8.5 (A-D; M-P) and in the left pharyngeal mesoderm (pm) at stages E8 - E9.5 (E-T), in the inner curvature of the common ventricle (cv) at stages E8 – E8.5 (E-L;) and in the outflow tract (oft), at stages E8.5 (I-L) – E9.5 (Q-T). rsv, right horn of sinus venosus; vr, ventricular region. Arrowheads mark regions of co-expression.

3. 2 Transient asymmetric expression of *Tbx1* in early mouse development

Pitx2 has been reported to be asymmetrically expressed in the left splanchnic/pharyngeal mesoderm and in the heart on the left side (Piedra *et al*., 1998; Yoshioka *et al*., 1998; Campione *et al*., 1999). Later, during remodeling of the heart its expression will be maintained in cells that originated from the left side. *Pitx2* expression can thus be found in the left atrium, parts of the right ventricle and the outflow tract (Franco and Campione, 2002). Closer examination of *Tbx1* expression at stage E9.0 using sections of whole mount *in situs* showed a transient asymmetric expression of *Tbx1* in *Pitx2* positive regions, the left pharyngeal mesoderm (pm) (Fig. 3.3 C) and the left atrium (la) (Fig. 3.3 D).

In addition, *in situ* hybridization of sagittal sections of stage E9.0 showed that the left-sided *Tbx1* expression in the pharyngeal mesoderm (pm) extends more caudally compared to its expression on the right side (Fig. 3.3 A-B). Thus, left asymmetric co-expression of *Pitx2* and *Tbx1* indicates that this aspect of their regulation might be shared.

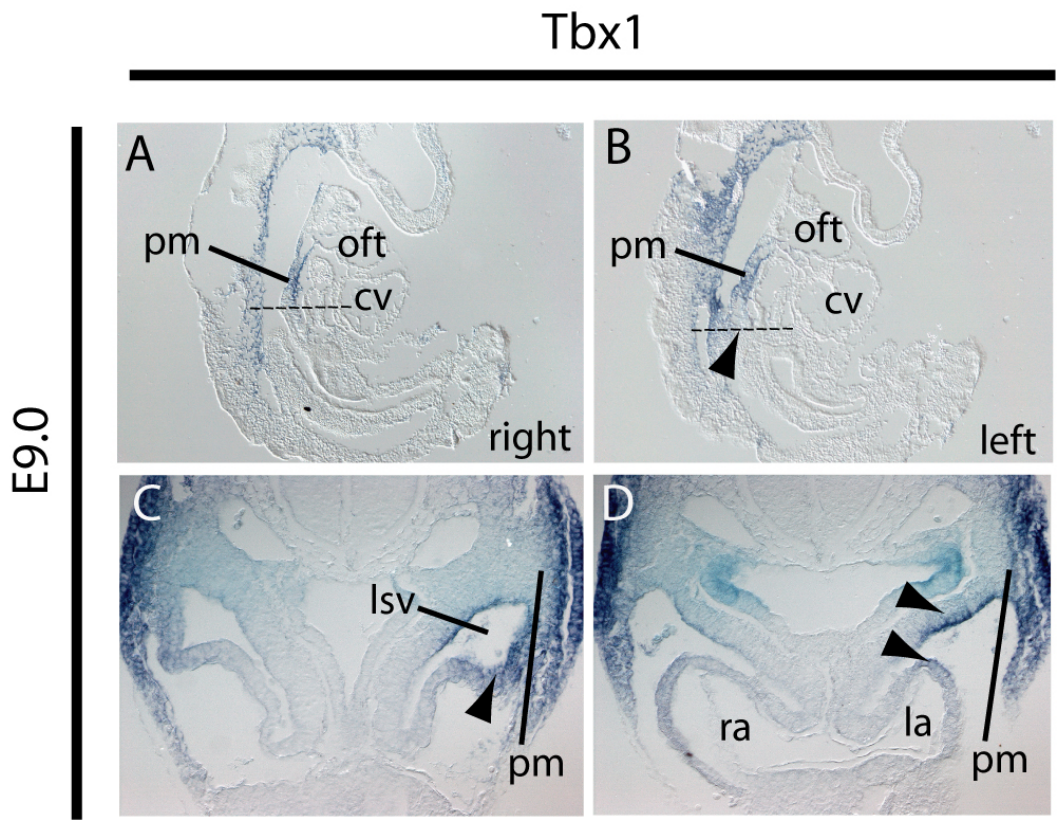

Fig. 3.3: Transient asymmetric *Tbx1* expression during embryogenesis

In situ hybridization with a *Tbx1* probe of E9.0 sagittal sections and sections of whole mount *in situs* of E9.0 wt embryos show asymmetric expression of *Tbx1*. *Tbx1* is asymmetrically expressed on the left side in the pharyngeal mesoderm (pm) (arrowhead in C and D) and in the left atrium (la) (arrowhead in D). Note that *Tbx1* expression in pharyngeal mesoderm extends more caudally on the left side (arrowhead in B) compared to the right side (A). Dotted line marks end of expression. cv, common ventricle, ra, right atrium, oft outflow tract.

3.3. Down-regulation of *Pitx2* in *Tbx1* null mutants during stages E8.0 and E10.5

To ascertain whether there is a potential epistatic relationship between the two genes, I performed expression studies in *Tbx1* null mutants. *In situ* hybridization in *Tbx1*-/- embryos revealed reduced expression of *Pitx2*. At E8.0 *Pitx2* expression was down-regulated in the outflow tract (oft) (Fig. 3.4 A-B) and in the region of the left SHF, the left splanchnic mesoderm (sm) (Fig. 3.4 C-D). At this stage *Pitx2* expression in the head mesenchyme (hm) was also reduced in the *Tbx1*-/- embryos (Fig. 3.4 A-B). This was possibly due to fewer cells in this region in *Tbx1* null mutants. However, *Pitx2* expression was unaltered in other regions of the embryo (data not shown). To determine whether *Pitx2* expression was also changed later in heart development, I examined embryos of stages E10.0 - E10.5. Whole mount *in situ* hybridization of dissected hearts and *in situ* hybridization of sections through the heart revealed that *Pitx2* expression was down-regulated in the left atrium (la), the ventral portion of the right ventricle (rv), the inner curvature and the outflow tract (oft) of the *Tbx1* null mutants (Fig. 3.4 E-J). However, down-regulation was variable in the null mutants, ranging from total absence (Fig. 3.4 J) of expression to general down-regulation (Fig. 3.4 G, H). Thus, these studies implicate that *Pitx2* acts downstream of Tbx1 in a genetic pathway during early cardiac morphogenesis.

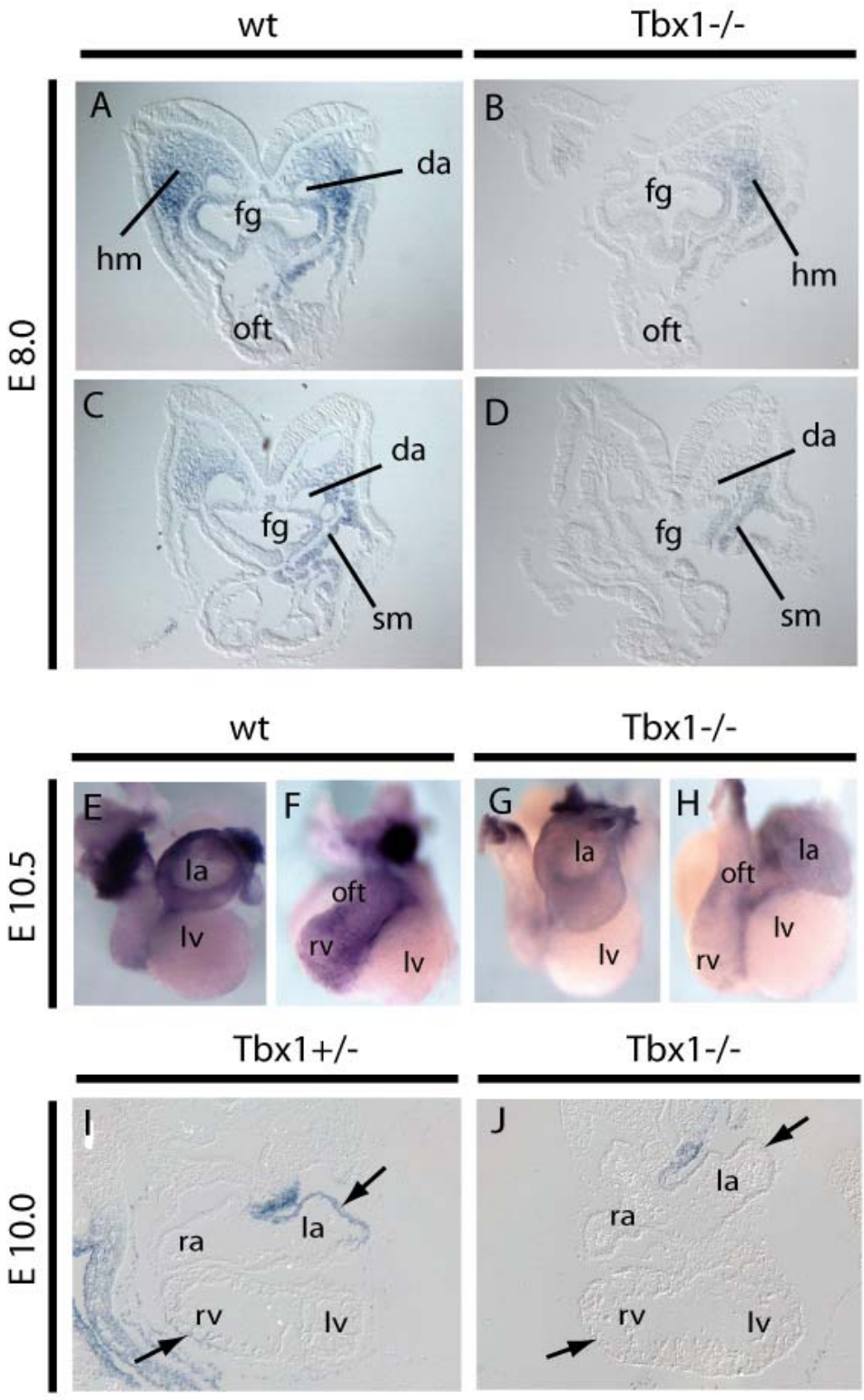
wt
Tbx1-/-
E 8.0
A
da
fg
hm
oft
B
fg
hm
oft
C
da
fg
sm
D
da
fg
sm
wt
Tbx1-/-
E 10.5
E
la
lv
F
oft
rv
lv
G
la
lv
H
oft
la
lv
rv
Tbx1+/-
Tbx1-/-
E 10.0
I
ra
la
rv
lv
J
la
ra
rv
lv

Fig. 3.4: Down-regulation of *Pitx2* in *Tbx1*-/- embryos at stages E8.5 and E10.
Transverse sections of whole mount *in situs* of stage E8.5 show down-regulation of *Pitx2* in the outflow tract (oft) and in left splanchnic mesoderm (sm) in the *Tbx1*-/- (B, D) compared to corresponding wild-type sections (A, C). Whole mount *in situ* hybridization of embryonic hearts of stage E10 show reduction of *Pitx2* expression in the left atrium (la), the outflow tract (oft) and right ventricle (rv) in *Tbx1*-/- (G, H) compared to wild type hearts (E, F). *In situ* hybridization on transverse sections of E10 *Tbx1*+/- (I) and *Tbx1*-/- (J) hearts show absence of *Pitx2* expression in the left atrium (la) and the right ventricle (rv) in the null mutant (arrows). lv, left ventricle; ra, right atrium. da, dorsal aorta; fg, foregut; hm, head mesenchyme.

3.4 Determination of a genetic interaction of Tbx1 and Pitx2 by crossing *Tbx1*+/- and *Pitx2*+/- mice

To validate the hypothesis that *Pitx2* acts downstream of Tbx1 in the same genetic pathway, I generated *Pitx2*+/-; *Tbx1*+/- mice. If there is a genetic interaction the phenotype of the double heterozygous mice should be more severe than that of the single heterozygous animals. Previous work on *Tbx1*+/- mice has shown that these mice survive in normal Mendelian ratios and exhibit only mild cardiovascular effects, primarily of the aortic arch such as abnormal origin of the right subclavian artery (RSA), or retroesophageal RSA (Jerome and Papaioannou, 2001; Lindsay *et al*., 2001; Merscher *et al*., 2001; Liao *et al*., 2004). Cardiovascular defects have never been reported in *Pitx2*+/- mice (Gage *et al*., 1999; Kitamura *et al*., 1999), nor have I seen any in my study. Analysis of the genotype distribution of the offspring of the *Pitx2*+/- and *Tbx1*+/- crosses at P10 revealed a significantly reduced viability of the double heterozygous mice compared to wt, *Tbx1* and *Pitx2* single heterozygous mice (Table 3.1). This

suggested that the double heterozygous mice die during embryogenesis or in the neonatal period.

Table 3.1: Genotype distribution of crosses between *Pitx2*+/- and *Tbx1*+/- mice at P10

Genotype	*Pitx2*+/-	*Pitx2*+/-; *Tbx1*+/-	*Tbx1*+/-	WT	Total
Number of mice analyzed (percentage)	28 (26.92%)	2 (1.92%)	27 (25.96%)	47 (45.19%)	104 (100%)
Number of mice expected according to Mendelian ratio (percentage)	26 (25%)	26 (25%)	26 (25%)	26 (25%)	104 (100%)

3.5 Phenotype analysis of the *Pitx2*+/-; *Tbx1*+/- mice

To assess the time point when *Pitx2*+/-; *Tbx1*+/- are dying, fetuses during late gestation were isolated and genotyped. Genotyping of E17.5 fetuses showed normal Mendelian ratios of all genotypes (Table 3.2). Consequent closer examination of the newborn mice revealed that the *Pitx2*+/-; *Tbx1*+/- mice survived embryogenesis. However, the majority of the double heterozygous mice became cyanotic in the early neonatal period and died due to respiratory distress.

Table 3.2: Genotype distribution of crosses between *Pitx2*+/- and *Tbx1*+/- mice at E 17.5

Genotype	*Pitx2*+/-	*Pitx2*+/-; *Tbx1*+/-	*Tbx1*+/-	WT	Total
Number of mice analyzed (percentage)	14 (33.3%)	11 (26.19%)	6 (14.29%)	11 (26.19%)	42 (100%)
Number of mice expected according to Mendelian ratio (percentage)	10.5 (25%)	10.5 (25%)	10.5 (25%)	10.5 (25%)	42 (100%)

3.5.1 Analysis of the craniofacial and skeletal structures of *Pitx2*+/-; *Tbx1*+/-

To exclude any malformation of the rib cage and craniofacial region, bone and cartilage staining of E17.5 embryos of wt, *Pitx2*+/-, *Tbx1*+/- and *Pitx2*+/-; *Tbx1*+/- was performed. Examination of the bone and cartilage of the skeleton showed neither malformations in the craniofacial region nor in the trunk region of the double heterozygous mice (Fig. 3.5).

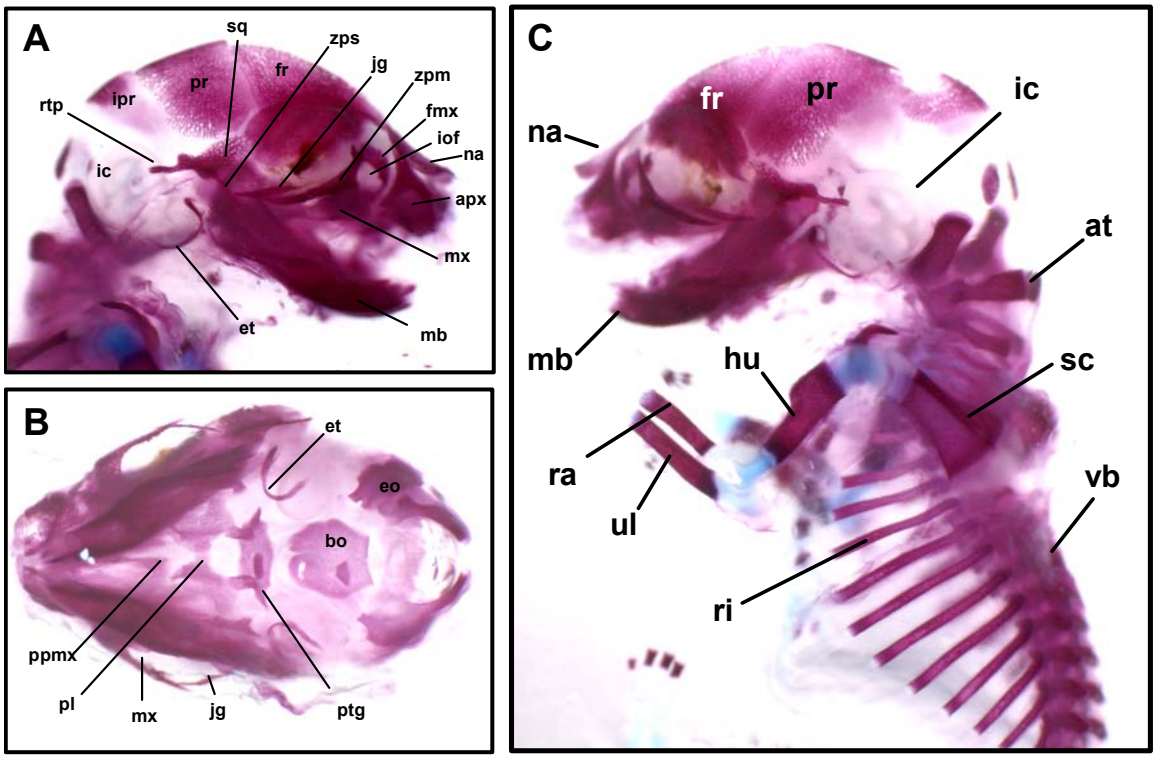

Fig. 3.5: *Pitx2*+/-; *Tbx1*+/- do not exhibit any craniofacial anomalies

A-C show bone and cartilage staining of an E18.5 *Pitx2*+/-; *Tbx1*+/- embryo. A: lateral view of the head, B: ventral view of the head C: lateral view of the fetus. No malformations could be detected in the craniofacial and trunk region of *Pitx2*+/-; *Tbx1*+/-. apx, alveolus of premaxilla; at, atlas; bo, basioccipital bone; et, ectotympanic; eo, exoccipital bone; fmx, frontal process of maxilla ; fr, frontal bone; hu, humerus; ic, inner ear capsule; iof, infraorbital foramen; ipr, interparietal bone; jg, jugal bone; mb, mandible; mx, maxilla; na, nasal bone; pl, palate; ppmx, palatal process of maxilla; pr, parietal bone; ptg, pterygoid bone; ra, radius; rtp, retrotympanic process; sc, scapula; sq, squamosal bone; ul, ulna; vb, vertebrae; zpm, zygomatic process of maxilla; zps, zygomatic process of squamosal.

3.5.2 Histological analysis E18.5 mice

Histological analysis of E18.5 embryos and newborns (n = 25) revealed severe cardiac defects in the double heterozygous animals. The defects though occurred with variable expressivity, possibly due to genetic modifiers or stochastic factors, because the mice were in a mixed background.

Double heterozygous mice displayed double outlet right ventricle (DORV), where both, the aorta and the pulmonary artery arise from the right ventricle (arrow in Fig. 3.6 A). DORV was not observed in either *Tbx1* (Fig. 3.6 B) or *Pitx2* (Fig. 3.6 C) single heterozygous mice in the genetic background analyzed. Stenosis of the infundibulum (the upper angle of the right ventricle where the pulmonary artery arises) of the pulmonary trunk (pt) (arrow head in Fig. 3.6 A) was found in the double mutants. Atrial septal defcts (asd), ventricular septal defects (vsd) (Fig. 3.6 D) and atrio-ventricular valve defects (vad) (Fig. 3.6 E) were present in the *Pitx2*+/-; *Tbx1*+/- mice, whereas in *Tbx1* (Fig. 3.6 G) and *Pitx2* (Fig. 3.6 H) single heterozygous mice, the atrial and ventricular structures were normal. In addition, abnormal drainage of the pulmonary vein into a common (Fig. 3.6 F) instead into a left atrium (Fig. 3.6 H) were found. Moreover, malpositioning of the aorta, malformation of the coronary vessels, pulmonary and caval vein atresia did occur in the mutant mice (data not shown). The severe cardiac phenotype found in the *Pitx2*+/-; *Tbx1*+/- mice compared to normal heart structures in the *Tbx1* or *Pitx2* single heterozygous mice provides evidence for a genetic interaction between *Tbx1* and *Pitx2*.

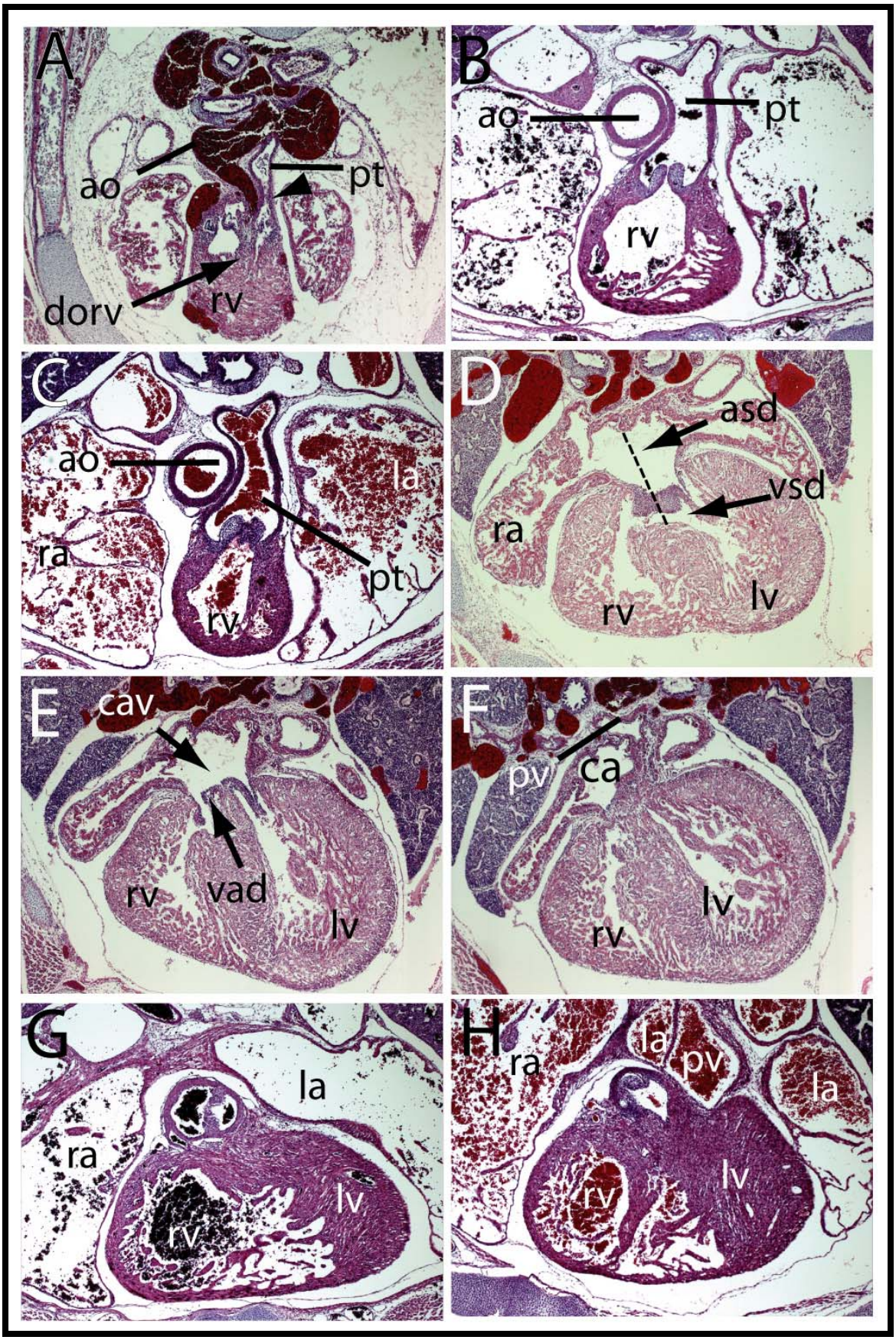
A
ao
pt
dorv
rv
B
ao
pt
rv
C
ao
la
ra
pt
rv
D
asd
vsd
ra
rv
lv
E
cav
rv
vad
lv
F
pv
ca
lv
rv
G
la
ra
lv
rv
H
ra
la
pv
la
lv
rv

Fig. 3.6: *Pitx2*+/-; *Tbx1*+/- newborns exhibit cardiac defects.
Histological analysis reveals that *Pitx2*+/-; *Tbx1*+/- exhibit double outlet right ventricle (dorv; arrow) and stenosis of the infundibulum (arrowhead; A), atrial septal defect (asd) and ventricular septal defect (vsd) (D), atrio-ventricular valve defects (vad), a common atrio-ventricular junction (cav) (E) and abnormal drainage of pulmonary vein (pv) (F) into a common atrium (ca) instead of into the left atrium (la; H). *Pitx2*+/- (B, G) and *Tbx1*+/- (C, H) mice served as controls. They do not show any malformations in the heart. Dotted line in D marks the location of the missing inter-atrial septum and inter-ventriuclar septum, respectively. ao, aorta; la, left atrium; lv, left ventricle; pt, pulmonary trunk; ra, right atrium; rv, right ventricle.

3.5.3 Histological analysis of *Pitx2*+/-; *Tbx1*+/- of stage E10.5

To determine the developmental onset of these defects, I analyzed *Pitx2*+/-; *Tbx1*+/- embryos at E10.5. At this stage in embryogenesis, as a consequence of the looping process of the heart, the common atrium is located dorsally to the ventricles. Within the heart the endocardial cushions form, which give rise to the septae in the atrio-ventricular canal as well as in the outflow tract. Shape and size differences of the hearts of the double heterozygotes were already visible at this stage (Fig. 3.7 A-D). An enlarged atrio-ventricular canal (avc), reduced ventricular expansion, abnormal ventricular shape (Fig. 3.7 A-B) and malformation of the outflow tract (oft) (Fig. 3.7 C-D) were observed. The severity of the malformation was also variable between the different double heterozygous mice at this stage, consistent with the later variable phenotype.

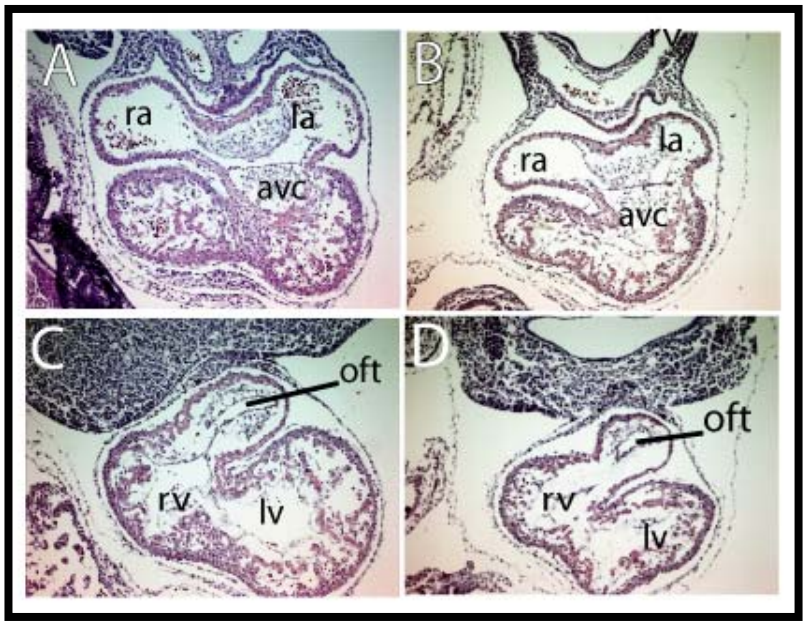

Fig. 3.7: *Pitx2*+/-; *Tbx1*+/- embryos exhibit malformation of the heart at E10.5

Pitx2+/-; *Tbx1*+/- embryos of stage E10.5 (B, D) have grossly malformed hearts if compared to wild type (A, B) embryos. They display an enlarged atrio-ventricular canal (avc), a reduced ventricular expansion and abnormal shape of the outflow tract (oft). la, left atrium; lv, left ventricle; ra, right atrium; rv, right ventricle.

3.6 Molecular studies to examine direct genetic interaction of Tbx1 and *Pitx2*

There exist three *Pitx2* isoforms in the mouse. *Pitx2c* is the only isoform that is asymmetrically expressed. Its expression is regulated by a 900 bp enhancer (Pitx2-ASE) located between exon 4 and 5 of the *Pitx2* gene (Fig. 3.8). The Pitx2-ASE contains one Nkx2.5 binding site as well as three binding sites for the forkhead transcription factor FAST. The FAST binding sites are Nodal-responsive elements and are required for activation of asymmetric *Pitx2* expression through Nodal in the left lateral plate mesoderm, whereas the Nkx2.5 binding site is

required later for the maintenance of the *Pitx2* expression during organogenesis (Shiratori *et al.*, 2001).

Sequence analysis revealed a putative T-half site (AGGTGTAAAG) in the enhancer, 26 bp downstream of the Nkx2.5 binding site (Fig. 3.8). The site differs from the T-consensus sequence only in two bases (AGGTGTGAAA), which do not belong to the most critical bases for the binding. Thus, I hypothesized that *Pitx2c* might be a direct downstream target of Tbx1. To test this hypothesis, I performed *in vitro* assays.

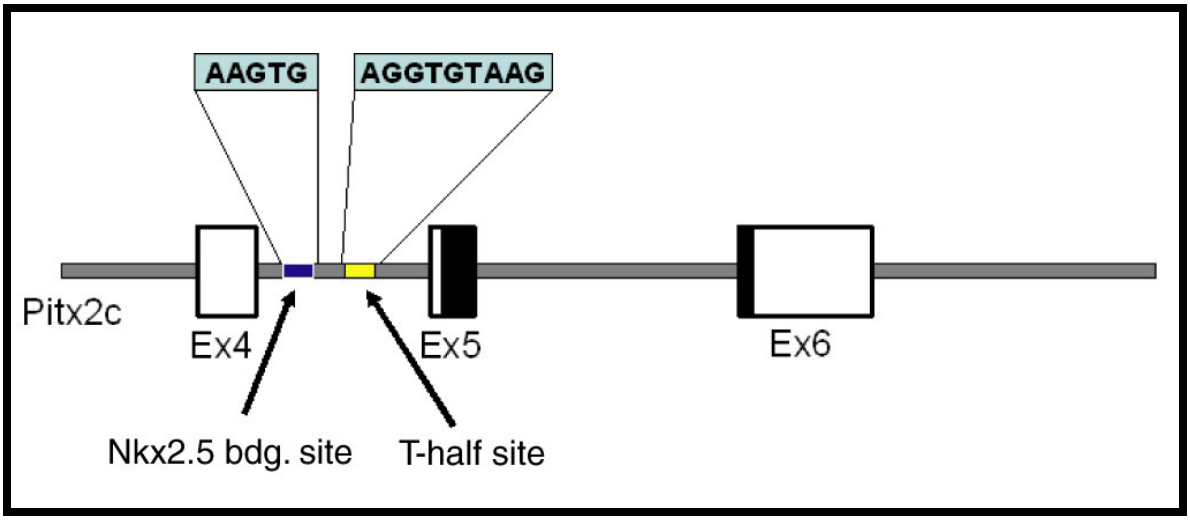

Fig. 3.8: Location of the T-half site in the *Pitx2c* enhancer

The *Pitx2c* enhancer (Pitx2-ASE) is located in the intron between exons 4 and 5 of the *Pitx2* gene (Shiratori *et al*., 2001). Sequence analysis revealed that it contains a putative T-half site close to an Nkx2.5 binding site.

3.6.1 Luciferase assays using the *Pitx2c* enhancer (Pitx2-ASE)

The Pitx2-ASE was cloned into pGL3 SV40 vector (Promega), which contains a minimal promoter and a luciferase reporter gene. Moreover, the full length cDNA of Tbx1 was cloned into the expression vector pcDNA3.1 and a Flag-Nkx2.5 expression vector (pCI) was obtained from Dr. V. M. Christoffels (Fig. 3.9). COS7 cells were co-transfected with the Pitx2-ASE luciferase reporter construct and either Tbx1 or Flag-Nkx2.5 expression vectors. In both cases transfection of the expression vector resulted only in a weak activation of the *Pitx2c* enhancer. The empty expression vectors, pcDNA3.1 and pCI were transfected as controls (Fig. 3.10).

T-box transcription factors often require co-factors to regulate transcription. It has previously been shown that Nkx2.5 can interact with other T-box proteins to repress or activate gene function. For example, during development of the cardiac chamber myocardium Tbx2 and Nkx2.5 form a complex on the *atrial natriuretic* (*ANF*) or *Nppa* promoter to repress its activity (Habets *et al*., 2002). A similar interaction has been reported for the T-box protein Tbx5. It interacts with Nkx2.5 on the *Nppa* promoter and this complex synergistically activates the *Nppa* gene (Bruneau *et al*., 2001; Hiroi *et al.,* 2001). In light of this fact, I co-transfected both expression constructs, Tbx1 and Flag-Nkx2.5 with the Pitx2-ASE reporter. This resulted in strong activation (~12-fold) of the *Pitx2c* enhancer. The empty expression vectors pcDNA3.1 and pCI were co-transfected as a control and did not lead to any activation of the reporter (Fig. 3.10).

Though Tbx1 alone is able to activate the *Pitx2c* enhancer only weakly, in combination with Nkx2.5, however, strong activation occurs. This indicates that Tbx1 and Nkx2.5 can synergistically activate the *Pitx2c* enhancer. These *in vitro* experiments provide evidence that Tbx1 acts upstream of *Pitx2c*.

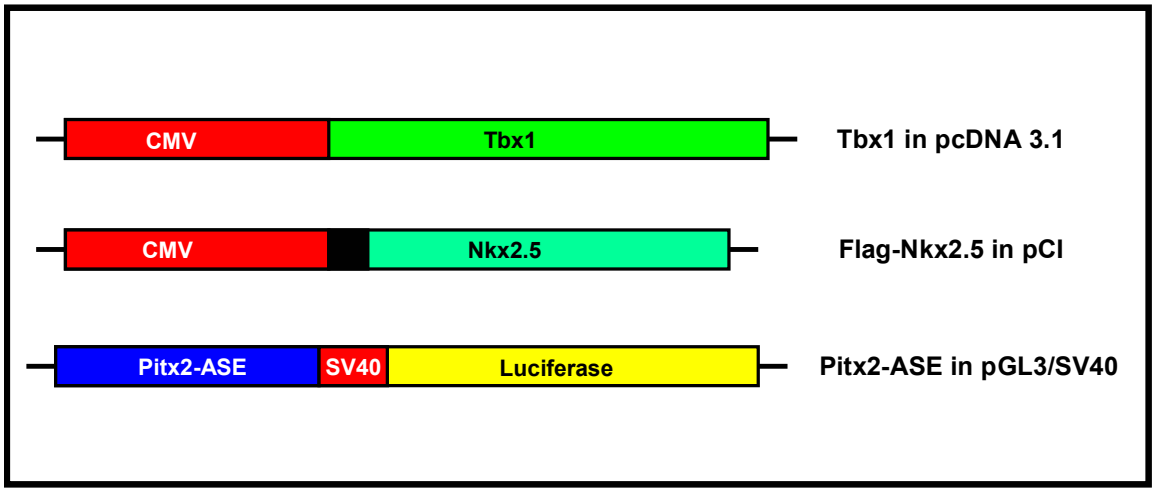

Fig. 3.9: Expression and reporter constructs used in luciferase assays.

In transfections for luciferase assays the following constructs were used: a full length cDNA of Tbx1 cloned into the expression vector pcDNA3.1. A fusion of Flag (black box) and Nkx2.5 in the expression vector pCI. Both expression constructs are driven by a CMV promoter. The Pitx2-ASE (900 bp) was cloned into the pGl3-promoter vector, which contains a SV40 minimal promoter upstream of the luciferase gene.

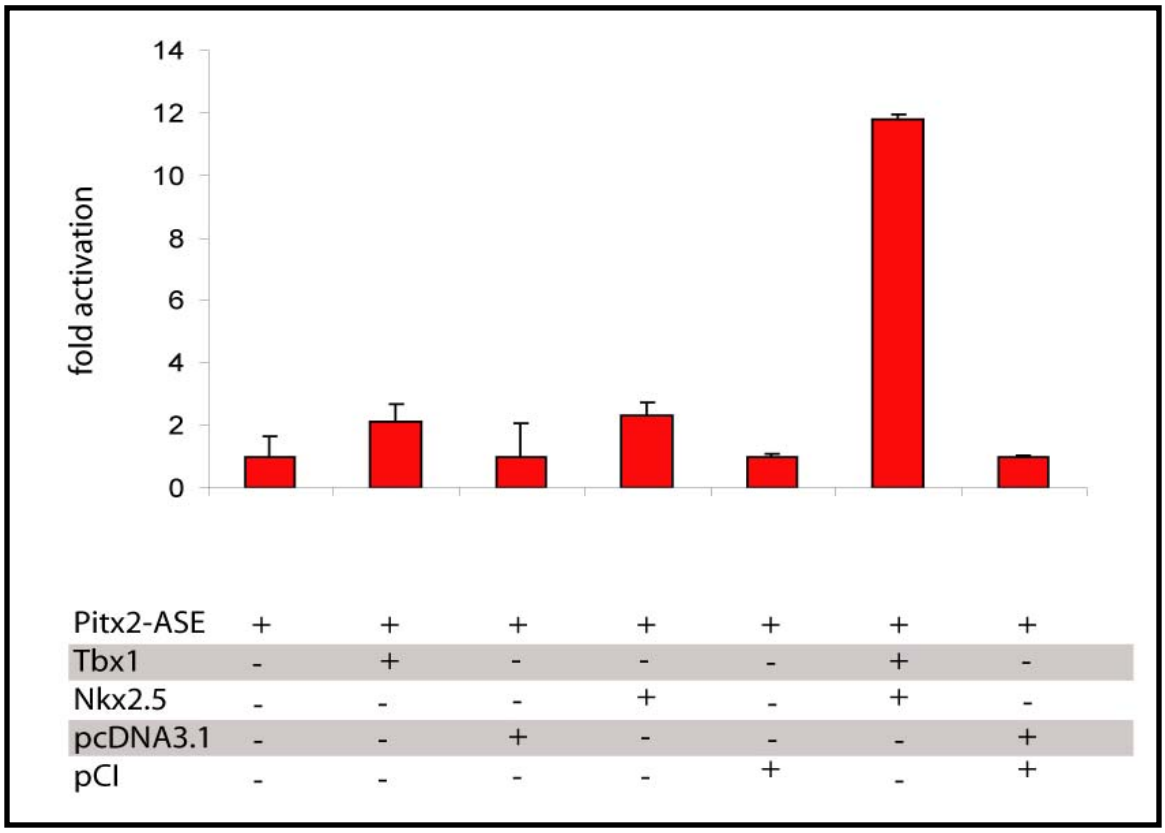

Fig. 3.10: Tbx1 activates the *Pitx2c* enhancer (Pitx2-ASE)

Luciferase reporter assays using the *Pix2c* enhancer and Tbx1 and Nkx2.5 as expression vectors shows weak activation of the Pitx2-ASE by either Tbx1 or Nkx2.5 in COS7 cells. Co-transfection of both, Tbx1 and Nkx2.5 leads to a 12-fold activation of the Pitx2-ASE. Data are presented as means and error bars for three independent experiments are indicated.

3.6.2 Tbx1 binds specifically to the T-half site in the Pitx2-ASE

Specific binding of Tbx1 to the T-half site of the Pitx2-ASE was assayed using gel shift experiments (Fig. 3.13). Whole-cell extracts of 293T cells transfected with a Tbx1 expression vector (*Tbx1* full length cDNA in pcDNA3.1) and synthesized oligonucleotides either containing the T-site of the Pitx2-ASE (Wt-oligo), mutated T-half sites (M1, M2) or a consensus T-half site, were used in the DNA-binding assay. Mutated oligonucleotides were designed as such they contained mutation in bases most critical for T-box protein binding (compare Fig. 3.11 and 3.12).

Lysates transfected with the Tbx1 expression vector resulted in the formation of a Tbx1-DNA complex in the presence of Wt-oligo (arrow in Fig. 3.13). To prove the specificity of the binding, 100-fold excess of non-labeled Wt-oligo was added, resulting in loss of the signal. Addition of a Tbx1 antibody, which recognizes a peptide in the carboxyl terminal third of the Tbx1 protein, outside the conserved T-box, resulted in a supershift of the Tbx1-DNA complex (arrowhead in Fig. 3.13), whereas addition of pre-immune serum as a control did not. Part of the DNA-protein complex had not been supershifted. This is possibly due other T-genes present in the cell extract that can bind to the same sequence. For example, it has recently been reported that Tbx20 can also activate the *Pitx2c* enhancer (Takeuchi *et al*., 2005); it is likely that it binds to the same T-half site. A DNA-protein complex that could not be supershifted with the Tbx1 antibody was also visible in control experiments in non-Tbx1 transfected 293T cells, suggesting that endogenous T-box proteins may be present in these cells (data not shown). Lysates transfected with Tbx1 expression vector resulted in a weak Tbx1-DNA complex in the presence of an oligonucleotide containing the consensus T-half site. Addition of 100-fold excess of the consensus oligonucleotide resulted in loss

of the signal (Fig. 3.13). The oligonucleotides, M1 and M2 which contain mutated T-sites did not lead to the formation of a T-box protein-DNA complex (Fig. 3.13).

In summary, the EMSA demonstrates that Tbx1 can specifically bind to the T-half site detected in the sequence of the *Pitx2c* enhancer. Mutations of critical bases of the T-half site lead to loss of Tbx1 binding. Thus, *Pitx2* is likely to be direct downstream target of Tbx1.

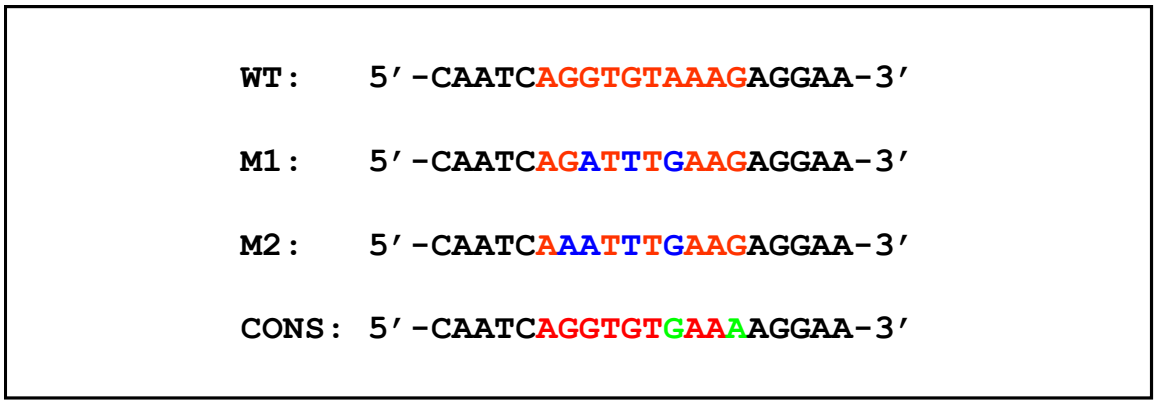

Fig. 3.11: Oligonucleotides used in electromobility shift assays (EMSAs).
Oligonucleotides of 20 bp were used in EMSAs. Oligonucleotides contained either the T-half site (red) found in the Pitx2-ASE (Wt), mutated T-half sites, (M1, M2, resp.; mutated sites are highlighted in blue) and a consensus T-half site (Cons). Note that the T-half site in the Pitx2-ASE (Wt) differs only in two bases (green) from the consensus T-half site (Cons).

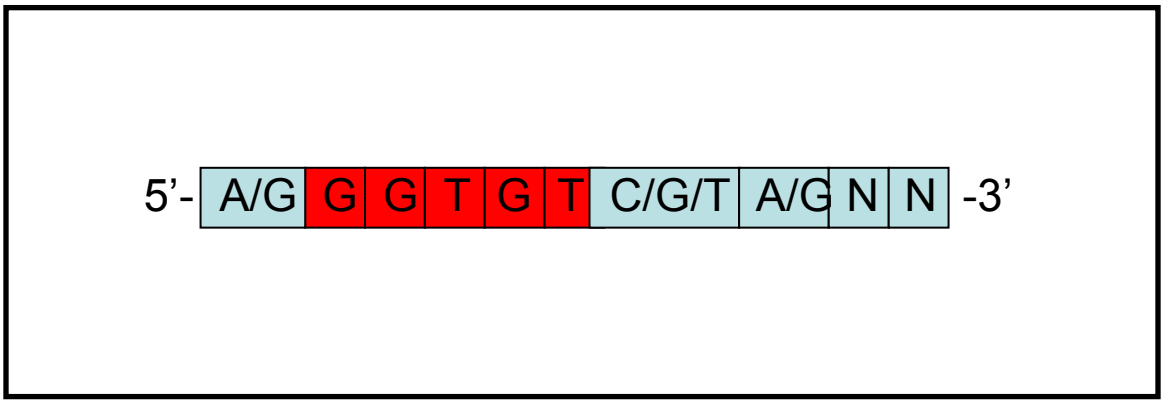

Fig. 3.12: Critical bases in the consensus T-half site
Critical bases for T-box protein binding that have been evaluated for TBX5 (Ghosh *et al.*, 2001) are the bases 2-6 (red) of the T-half site. Other bases in the T-site are subject to variation suggesting they are not essential for the binding. Mutated oligonucleotides in the EMSA (Fig. 3.13) have mutations in these bases.

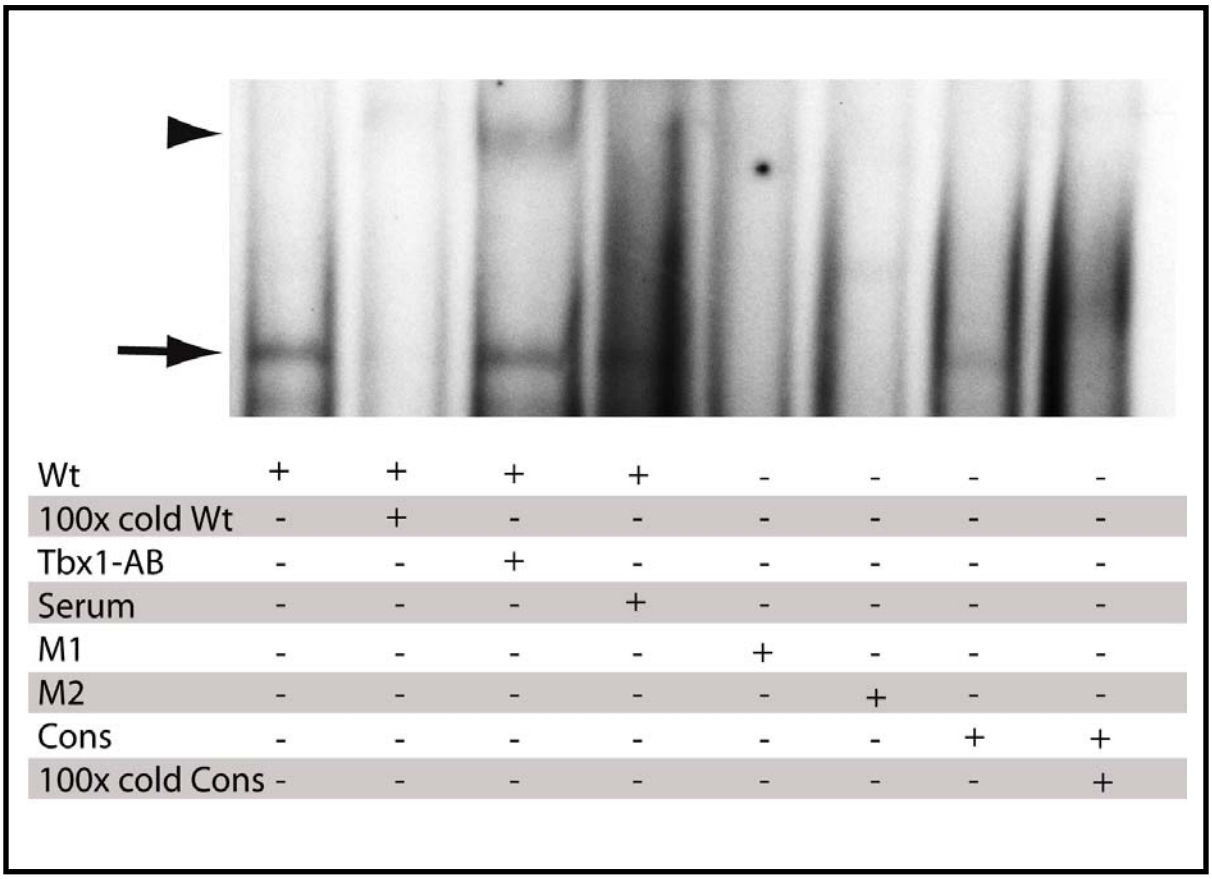

Fig. 3.13: Tbx1 binds to a T-half site within the *Pitx2c* enhancer

Electromobilty shift assays using whole cell extracts of Tbx1 transfected 293T cells confirms binding of Tbx1 to the T-half site within the *Pitx2* enhancer (WT) (arrow). Addition of Tbx1-antibody results in a supershift of the complex (arrowhead). Mutation of the T-half site (M1, M2) does not lead to the formation of a Tbx1-DNA complex. Binding of Tbx1 to the consensus T-half site (Cons) is weak.

3.6.3 Interaction of Tbx1 and Nkx2.5

To ascertain whether Tbx1 and Nkx2.5 interact physically with each other, I performed co-immunoprecipitation experiments using cell lysates of 293T cells transfected with the expression vectors Tbx1-GFP (cloned in EGFP-N1, Clontech) and Flag-Nkx2.5. Cell extracts of 293T cells transfected with Tbx1-GFP alone, Flag-Nkx2.5 alone and untransfected cells were used as controls. The immunoprecipitation was performed with an antibody directed against the Flag epitope. The Tbx1 protein was then detected by immunoblotting with an anti-Tbx1 antibody. Cell lysates transfected with either both, Tbx1 and Nkx2.5, Tbx1 alone, Nkx2.5 alone or untransfected cells served as controls for Tbx1 protein expression. Tbx1 expression could only be detected in Tbx1, Nkx2.5 co-transfected and Tbx1 transfected cells. After co-immunoprecipitation with anti-Flag antibody, Tbx1 protein could be detected in cell lysates transfected with Flag-Nkx2.5 and Tbx1 (arrow in upper blot in Fig. 3.14). No Tbx1 protein was found in co-immunoprecipitation with an antibody directed against Flag using cells that were either untransfected or transfected with Tbx1, or Nkx2.5 only (upper blot in Fig. 3.14). The Flag-Nkx2.5 fusion protein was detected by immunoblotting with the Anti-Flag M2 antibody (Sigma). Control lysates showed protein expression of Nkx2.5 in cells transfected with Tbx1 and Nkx2.5 or with Nkx2.5 only (Fig. 3.14; arrow in bottom blot). No protein was found in lysates of untransfected and Tbx1 transfected cells. After co-immunoprecipitation with anti-Flag antibody, Flag-Nkx2.5 was detected in samples of Tbx1 and Nkx2.5 as well as Nkx2.5 transfected cells. Controls using untransfected and Tbx1 transfected cells did not show Flag-Nkx2.5 protein expression (Fig. 3.14; bottom blot).

Indeed, co-transfection of both, Tbx1 and Nkx2.5 expression vector constructs revealed interaction between Tbx1 and Nkx2.5. Thus, from the above

studies it can be concluded that Tbx1 might physically interact with Nkx2.5 on the *Pitx2c* enhancer and in that way synergistically activates the *Pitx2* gene in cells.

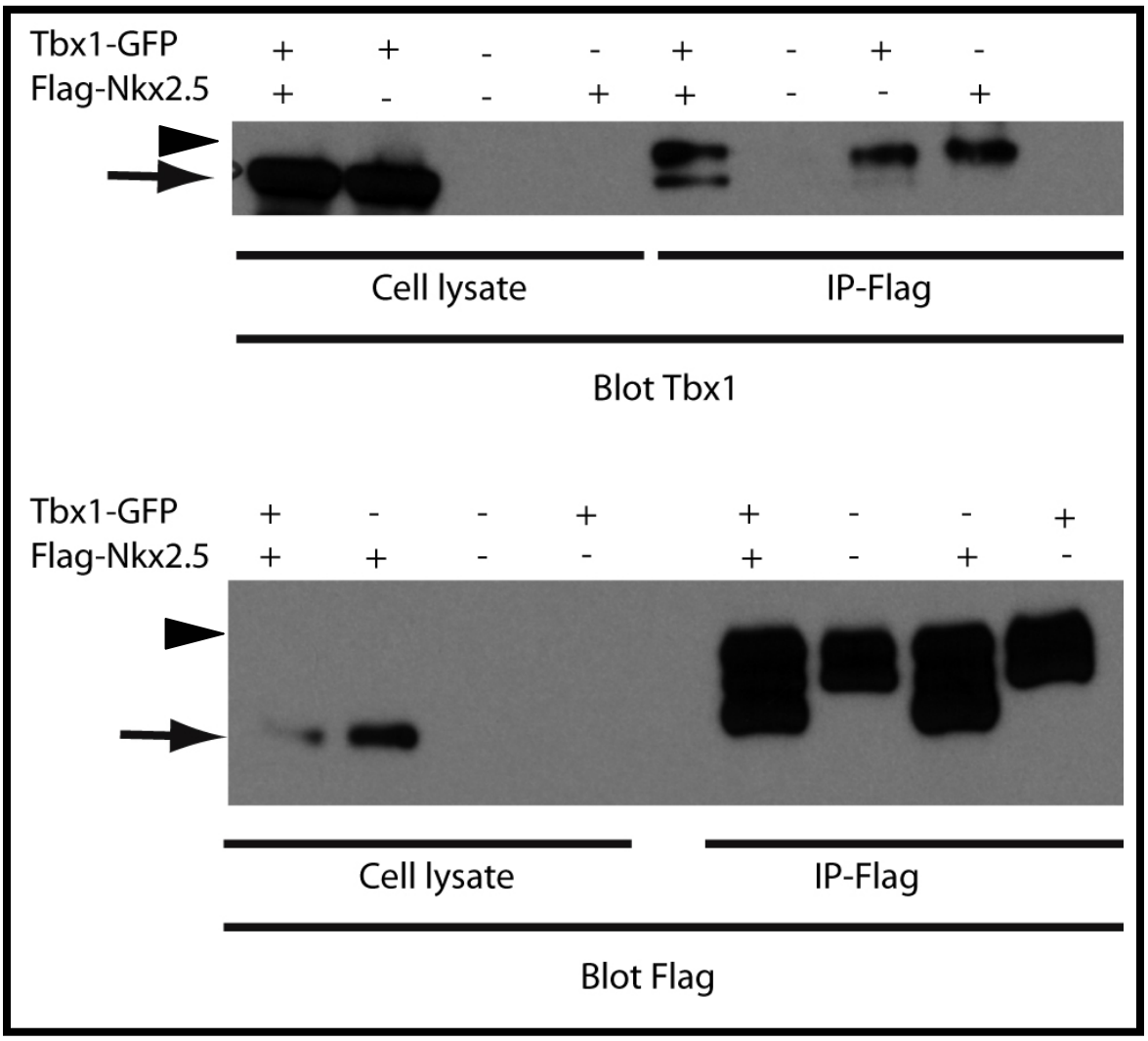

Fig. 3.14: Interaction of Tbx1 and Nkx2.5

Co-transfection of Tbx1-GFP and Flag-Nkx2.5 in 293T cells and subsequent co-immunoprecipitaton (Co-Ip) reveals interaction of Tbx1 and Nkx2.5. Upper blot shows immunoblot of Co-Ip followed by detection of Tbx1 protein (arrow). Bottom blot shows immunoblot of Co-Ip followed by detection of Flag protein (arrow). Co-IP of cell extracts transfected with Tbx1-GFP or Flag-Nkx2.5 alone or untransfected were used as controls and do not show interaction. Arrowhead marks unspecific bands.

3.7 Conservation of T-half site in the *Pitx2* enhancer in mammals but not other vertebrates

Pitx2 is a highly conserved gene throughout species. Its left-sided asymmetrical expression during early development is conserved in vertebrates (reviewed in Hamada *et al*., 2002). It is therefore of interest to understand if the regulatory elements driving the asymmetric *Pitx2* expression are also conserved throughout the vertebrate species.

Comparative sequence analysis using *UCSC Genome Bioinformatics* (http://genome.ucsc.edu) revealed that the T-half site, which I discovered in the murine *Pitx2c* enhancer, is not conserved in all vertebrate species. It is only found in mammalian species (mouse rats, human, and chimp) (Fig. 3.15). Sequence analysis revealed that a T-half site is not present in the Pitx2-ASE of *Xenopus laevis* (Fig. 3.16). A Pitx2-ASE in zebrafish has not been published yet. The genomic sequence of zebrafish *pitx2* did not reveal any matches for a T-half site. This leads to the conclusion that the Tbx1-Pitx2 pathway discovered in this thesis has evolved recently.

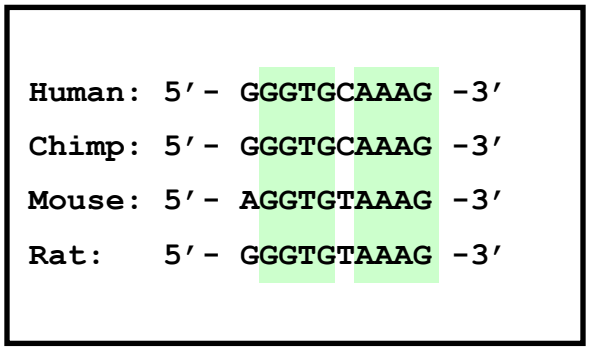

Fig. 3.15: The T-half site in the Pitx2-ASE is conserved in mammals

Sequences of T-half site in human, chimp, mouse and rat are shown. T-half site is conserved 100% in human and chimp. The T-half site in the rat differs from that in

the mouse only in the first base, whereas mouse and human/chimp differ in 2 bases. Rat and human differ in one base.

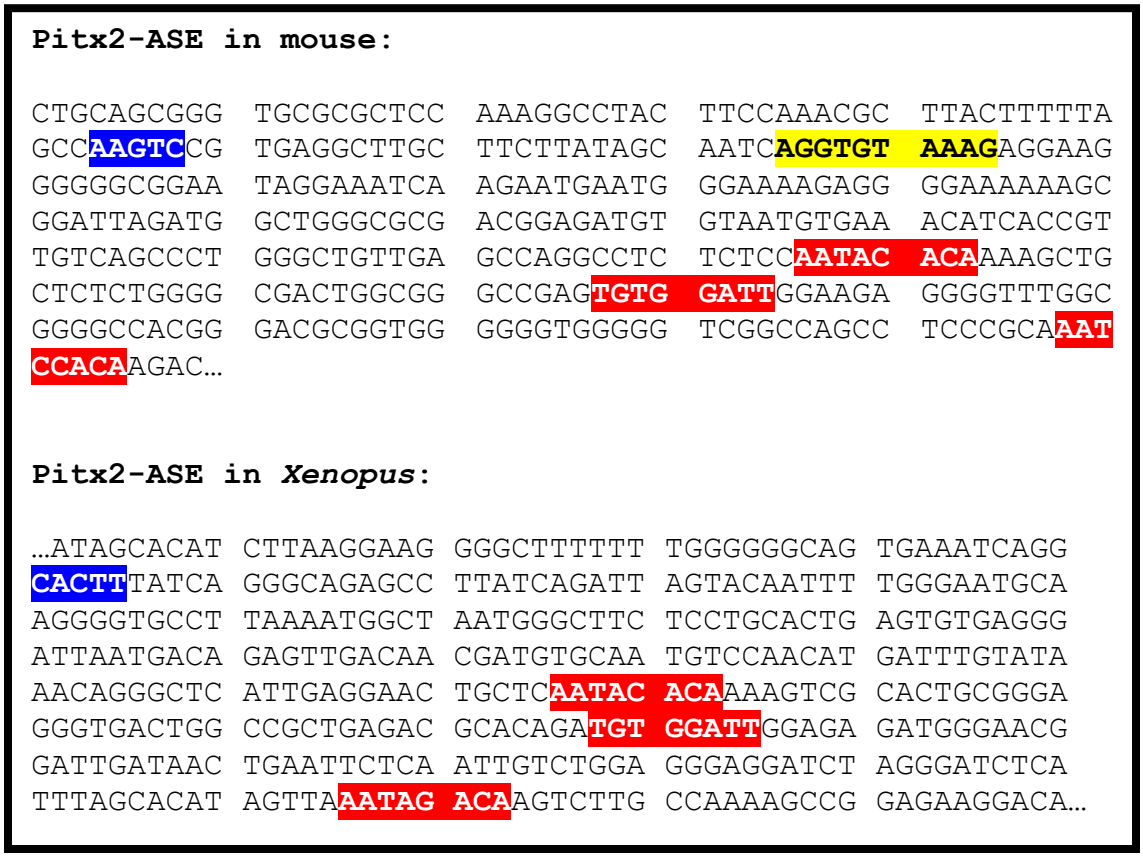

Modified after Shiratori *et al*., 2001

Fig. 3.16: The T-half site in the Pitx2-ASE is only found in mouse but not in Xenopus

Part of the sequences of the Pitx2-ASE in mouse and *Xenopus* are shown. Both have conserved Nkx2.5 binding sites (highlighted in blue) and conserved Fast binding sites (highlighted in red). However, the T-half site (highlighted in yellow), which Tbx1 binds to, is only found in the Pitx2-ASE of the mouse.

4. Discussion

My studies provide *in vivo* as well as *in vitro* evidence for a novel Tbx1-Pitx2 pathway, in the SHF. I have shown that genetic interaction of these two genes is crucial for proper asymmetric cardiac remodeling during early heart development. Perturbation of the Tbx1-Pitx2 pathway leads to severe cardiac defects. *Pitx2*+/-; *Tbx1*+/- mice exhibit defects that are common in several congenital heart diseases, and are reminiscent of the cardiac defects found in human patients with 22q11DS, for which TBX1 is a strong candidate. The *Pitx2*+/-; *Tbx1*+/- mice, therefore provide new insight into how cardiac defects occur in 22q11DS patients and which signaling pathways are involved during development. In addition, I have provided evidence for direct activation of the *Pitx2c* enhancer by Tbx1 in co-operation with Nkx2.5 in the SHF.

4.1 Cardiac defects in *Pitx2*+/-; *Tbx1*+/- mice

I have shown that hemizygous deletion of *Tbx1* and *Pitx2* together lead to severe defects of the arterial and venous pole of the heart. These defects resemble those previously described for the *Pitx2c* null mutant (Liu *et al.,* 2002). Both mutants, *Pitx2c*-/- and *Pitx2*+/-; *Tbx1*+/- mice, display VSD, DORV, malformation of the atrio-ventricular canal, pulmonary and caval veins. However, *Pitx2c* null mutants have much more severe defects occurring in the aortic arch vessels. Apart from DORV, they also exhibit right aortic arch, left innominate artery and left dominant double aortic arch (Liu *et al*., 2002).Thus, *Pitx2* has also a major part in asymmetric patterning and remodeling of the branchial arch arteries, besides its function in cardiac remodeling. Severe aortic arch patterning defects occur also in *Tbx1*-/- mice, whereas the Tbx1 single heterozygous animals have only mild defects, such as retroesophageal right subclavian artery with variable expressivity

(Merscher *et al*., 2001). However, the *Pitx2*+/-; *Tbx1*+/- mice do not show more severe defects in the aortic arches than the Tbx1 single heterozygous. What could be the reason for this? One explanation could be that one copy of *Pitx2* and/or *Tbx1* are sufficient for proper remodeling of the aortic arches. Both transcription factors have been shown to be dosage sensitive (Gage *et al*., 1999; Liao *et al*., 2004) suggesting that only low levels of both transcription factors are required for branchial arch patterning and remodeling. In addition, it has been shown that *Tbx1* is expressed in the pharyngeal endoderm where it acts upstream of the *fibroblast growth factor*, *Fgf8*. This Tbx1-Fgf8 pathway is thought to be important for branchial arch patterning (Abu-Issa *et al*., 2002; Frank *et al*., 2002; Hu *et al*., 2004; Xu *et al.,* 2004). Since this pathway is independent of the Tbx1-Pitx2 pathway, Tbx1 signaling through *Fgf8* could be sufficient to establish the correct branchial arch remodeling in the embryo.

As mentioned above, *Pitx2*+/-; *Tbx1*+/- mice exhibit defects in the valves of the AV canal and in the pulmonary veins. It has been demonstrated by lineage tracing experiments that these structures are populated by *Pitx2* daughter cells (Liu *et al*., 2002). It is likely that their precursor cells originate in the SHF meaning that they are descendants from cells expressing *Tbx1* and *Pitx2*. A role for *Pitx2* involving cellular migration has been shown in cardiac neural crest cells (Kioussi *et al*., 2002). Thus, one can speculate that the Tbx1-Pitx2 pathway in the SHF might be required for cell movement of SHF cells into the pulmonary veins. Alternatively, the Tbx1-Pitx2 pathway could regulate proliferation of the precursors of the cells migrating into the veins. Lineage tracing of these cells would help to answer this question.

Another defect shared between *Pitx2*-/- and *Pitx2*+/-; *Tbx1*+/- mice is a severe defect in the central mesenchymal mass that forms the AV-cushion and the valves (Kitamura *et al*., 1999; Liu *et al*., 2001). This results in a common AV-canal. Similarly to the *Pitx2* function in the morphogenesis of the pulmonary veins, it has been claimed that *Pitx2* is as well required for cellular movement in

the AV-cushions. The AV-cushions are surrounded by *Pitx2* expressing cells in the inner curvature myocardium of the heart. It has been shown that these myocardial cells invade the mesenchymal AV-cushions (van den Hoff *et al*., 2001). However, it is speculated that another source of *Pitx2* expressing cells in the AV-cushion could originate from the dorsal mesocardium (Liu *et al*., 2002), a structure that attaches the developing heart to the foregut. It is likely that cells, entering the heart through the dorsal mesocardium and invading the AV-cushions, derive from the SHF. The Tbx1-Pitx2 pathway could then be responsible for regulating the migration of these cells.

As mentioned above, cardiac defects displayed by the *Pitx2*+/-; *Tbx1*+/- mice resemble the ones of the *Pitx2c*-/- mice (Liu *et al*., 2002). *Pitx2* is essential for proper asymmetric cardiac remodeling (reviewed in Campione *et al*., 2002; Franco and Campione, 2003). In addition, I could present transient asymmetric *Tbx1* expression in the SHF and in the left atrium, both *Pitx2* expressing regions. The results of this thesis link *Tbx1*, for the first time, to asymmetric cardiac morphogenesis. Thus, defects resulting from perturbation of the Tbx1-Pitx2 pathway can be considered as laterality defects. Hence, many forms of CHDs, especially in the 22q11DS can therefore be termed laterality defects.

4.2 Interaction of Tbx1 and Nkx2.5

This work shows for the first time *in vitro* evidence for the interaction of Tbx1 with the transcription factor Nkx2.5. I hypothesize that this interaction is necessary to synergistically activate the Pitx2-ASE (Fig. 4.1). Interactions of other T-genes with Nkx2.5 have already been reported previously. Tbx5 and Tbx2 have been shown to interact with Nkx2.5 on the promoter of the gene *Nppa* (*ANF, atrial natriuretic factor*) during cardiac chamber development (Bruneau *et al*., 2001; Hiroi *et al*., 2001; Habets *et al*., 2002) The promoter of *Nppa* contains an Nkx-

binding site and several T-half sites. Tbx5 binds to the T-half site and interacts with Nkx2.5 to synergistically activate the *Nppa* promoter (Bruneau *et al*., 2001; Hiroi *et al*., 2001). In contrast, binding of Tbx2 and subsequent interaction with Nkx2.5 leads to repression of the *Nppa* gene (Habets *et al*., 2002). Interaction with Nkx2.5 has also been shown for another T-gene, Tbx20 on the *connexin 40* promoter (Stennard *et al.,* 2003). These studies show that interactions of T-genes and Nkx2.5 are conserved in various processes during cardiac development and are indispensable for patterning the developing heart.

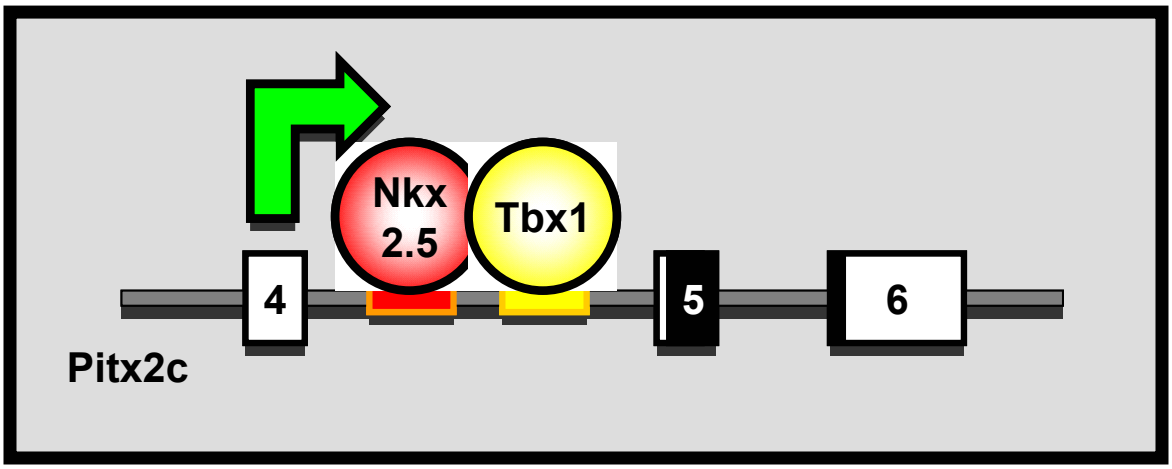

Fig. 4.1: Interaction of Tbx1 and Nkx2.5 on the *Pitx2c* enhancer (Pitx2-ASE)

The Pitx2-ASE in mouse contains an Nkx2.5-binding site (red box) and a T-half site (yellow box). Interaction of the transcription factors Nkx2.5 and Tbx1 on the enhancer lead to synergistic activation of the *Pitx2c* isoform. Activation through Nkx2.5 and Tbx1 may be required for maintenance of *Pitx2c* expression in the left SHF.

4.3 Interaction of Nkx2.5 and Tbx1 leads to activation of the *Pitx2c* enhancer

Establishing the left-right axis in the vertebrate embryos involves four steps: the determination of the left right polarity in or near the node, signals that transfer the left-right identity from the node to the lateral plate mesoderm (LPM), expression of signaling molecules Nodal and lefty in the left LPM and activation of *Pitx2*, which regulates asymmetric organ morphogenesis (Hamada, 2001). The asymmetric expression of *Pitx2c* is mediated by a specific left-side enhancer, called Pitx2-ASE, which is located in the intron between exons 4 and 5. The Pitx2-ASE contains three FAST-binding sites and an Nkx2.5-binding site, which are necessary for asymmetric regulation of *Pitx2*. First, *Pitx2* expression is initiated through Nodal signaling from the node through FAST transcription factors. It has been shown that Nodal is only transiently expressed between stages E 7.25 and E 8.0 (Collignon *et al*., 1996; Lowe *et al*., 1996; Meno *et al*., 1996; 1997). *Pitx2* expression comes on around E 7.5 in the LPM but stays on much longer until E 10.5 on the left side of primordia of asymmetric structures such as the sinus venosus, left atrium, cardinal veins and *septum transversum*, which gives rise to the liver and in a specific region of the foregut which gives rise to the lung and the gut (Meno *et al*., 1998; Yoshioka *et al*., 1998; Campione *et al*., 2000). After *Nodal* expression has ceased, *Pitx2* expression is maintained by the transcription factor Nkx2.5 (Shiratori *et al*., 2001). The mechanism by which *Pitx2* expression is maintained later is mainly unknown.

It is likely that in different organs there are different transcription factors that interact with Nkx2.5 to maintain *Pitx2* expression. This thesis elucidates one of them, the transcription factor Tbx1. Tbx1 interacts with Nkx2.5 and is most likely necessary to maintain *Pitx2* expression in the SHF to regulate cell proliferation or migration to ensure correct asymmetric cardiac remodeling (Fig.

4.2). One can conclude that *Pitx2* expression is established in two ways in the left SHF. First, *Pitx2* becomes activated in the left LPM through Nodal and second, its expression is maintained through Tbx1 and Nkx2.5 (Fig. 4.2). It is tempting to speculate that *Pitx2* expression is maintained in other asymmetric organs in a similar way, through interactions of other T-box genes, or other transcription factors with Nkx2.5 or other members of the Nkx2-family in organs, where Nkx2.5 is not expressed.

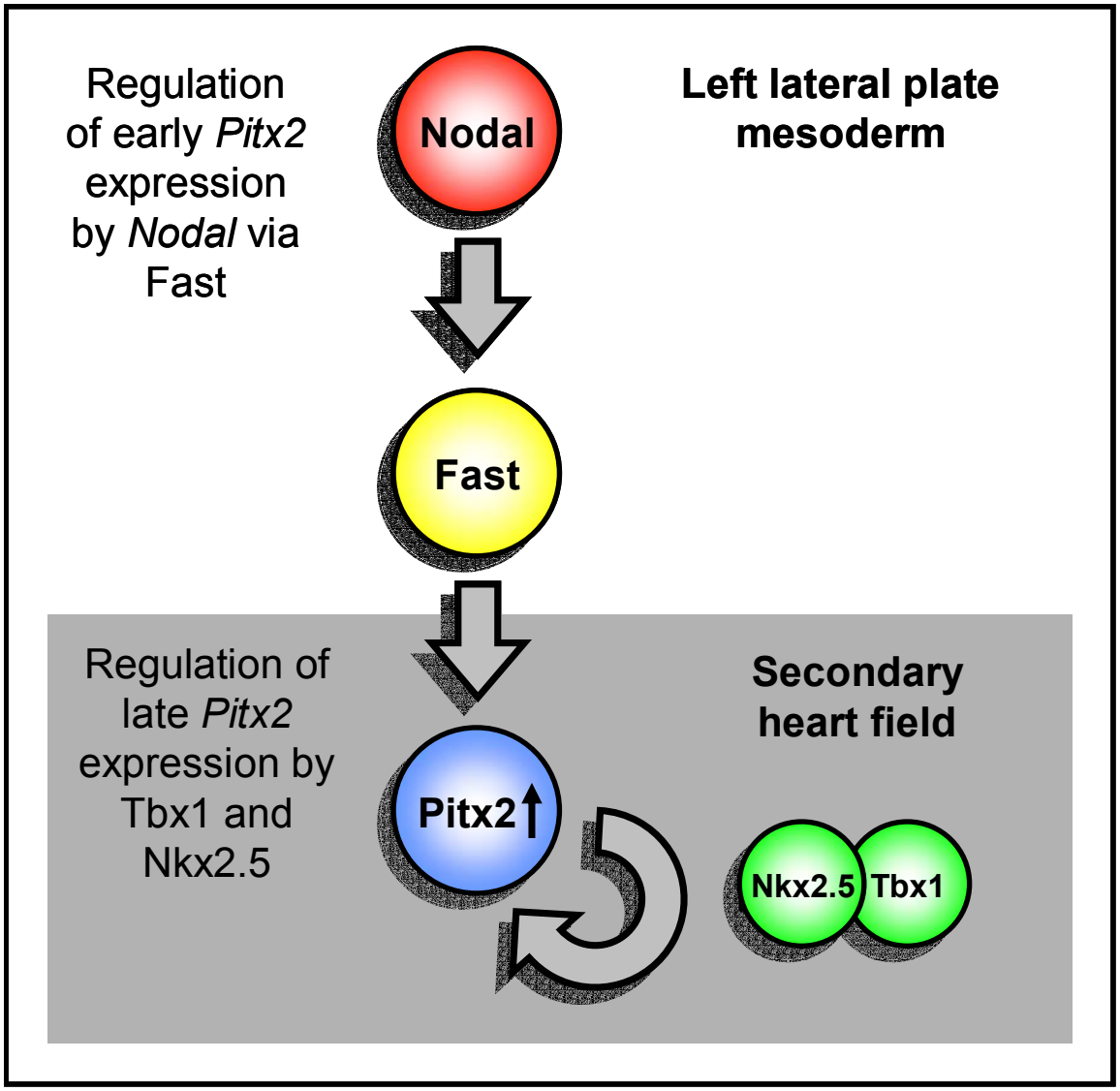

Fig. 4.2: *Pitx2* expression is regulated in two ways in the SHF

The *Pitx2* gene is initially activated by Nodal. *Nodal* is only transiently expressed in early embryogenesis. However, *Pitx2* expression in the left SHF stays on at later stages as well. Maintenance of *Pitx2* expression in later stages is provided by synergistic action of Tbx1 and Nkx2.5.

4.4 A novel Tbx1-Pitx2 pathway in the left secondary heart field

The heart originates from three different cell populations, the cardiac crescent or primary heart field located in the anterior lateral mesoderm, the cardiac neural crest and the AHF/SHF. The AHF has recently been discovered in studies in chick and mouse. It was shown that cells from the pharyngeal mesoderm contribute to the distal part of the OFT and give rise to cardiomyocytes. Hence, the region of the pharyngeal mesoderm has been called AHF/SHF (Waldo *et al*., 2001; Mjaatvedt *et al.*, 2001; Kelly *et al*., 2001). Further studies have elucidated that cells of the AHF not only contribute to the OFT but to several structures of the arterial pole as well as the venous pole of the heart (Meilhac *et al*., 2004). A current model to explain the origin of different cell populations that give rise to the heart was recently published by Kelly (2005). This model proposes that the entire embryonic heart derives from two cell lineages. The first lineage contributes to the left ventricle, atria, inflow region and partly to the right ventricle. The second lineage is thought to contribute mainly to the right ventricle and the outflow tract, but also to the atria and the inflow region. The AHF/SHF is thought to be a subpopulation of the second lineage. The model assumes that cells from the SHF can contribute to both poles through the continuity of the splanchnic mesoderm. Cells can migrate into the heart as long as the dorsal mesocardium, a structure which attaches the heart to the foregut is still intact (Kelly and Buckingham, 2002). Supporting evidence for this model comes from studies of the LIM-homeodomain protein *Islet-1*. The linear heart tube fails to extend in *Islet-1*-/- embryos. *Islet-1* is only expressed in the pharyngeal mesoderm. Lineage tracing of these *Islet-1* expressing cells showed that they contribute to the OFT, RV, atria and inflow region (Cai *et al*., 2003). In this thesis I have shown that *Tbx1* and *Pitx2* are co-expressed in *Islet-1* positive regions, i.e. in cells of the SHF and that

double heterozygous mice for Tbx1 and *Pitx2* exhibit defects in both the arterial and the venous pole. According to the current model the Tbx1-Pitx2 pathway must be a crucial part of the second lineage regulating or promoting migration of the SHF cells to the outflow and inflow region of the heart.

Tbx1 expression has previously been identified in the region of the AHF in the pharyngeal mesoderm and in the pharyngeal endoderm. Since *Tbx1* null mutants display OFT hypoplasia it is hypothesized that *Tbx1* regulates addition of cells to the OFT by controlling cell proliferation through the fibroblasts growth factors *Fgf10 /8* (Vitelli *et al*., 2000b; Hu *et al*., 2004; Xu *et al*., 2004).

Cardiac defects in the *Pitx2*+/-; *Tbx1*+/- mice suggest that *Tbx1* not only regulates cell proliferation via the *fibroblast growth factors* in the SHF but that there exists an additional pathway in the left SHF to ensure correct asymmetric cardiac morphogenesis (Fig.4.3). This pathway regulates cell proliferation or migration in a cell autonomous way through *Pitx2*, resulting in addition of cells to the right ventricle, atria and OFT. These are also sites of *Pitx2* expression. In addition this study shows that not only daughter cells of *Tbx1* are expressed in the heart (Vitelli *et al*., 2002b), but also *Tbx1* it self is transiently asymmetrically expressed at E9.0 in *Pitx2* positive regions, in the left atrium as well as in the caudal pharyngeal mesoderm which mainly contributes to the development of the OFT. This emphasizes the role of Tbx1 in correct asymmetric cardiac morphogenesis.

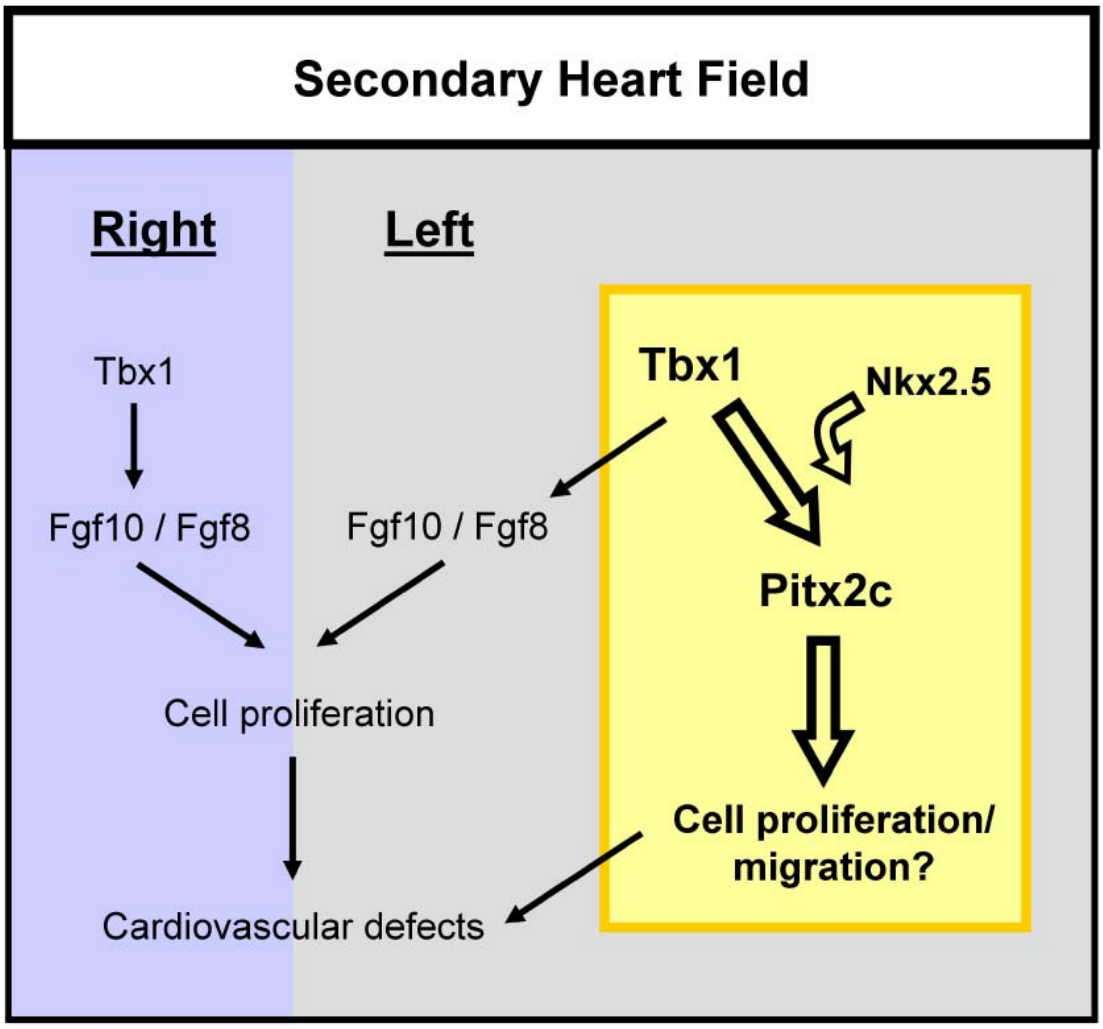

Fig 4.3: Model for the regulation of cardiac morphogenesis by Tbx1 in the secondary heart field

Tbx1 exerts a dual role on the left side of the SHF. Tbx1 acts through a novel second pathway in the left cardiac precursor cells of the SHF via *Pitx2c*. It regulates the activation of *Pitx2c* by interaction with Nkx2.5 to regulate cell proliferation or migration to ensure proper asymmetric cardiac morphogenesis. This pathway complements the previously described non cell autonomous Tbx1-Fgf8/10 pathway in the left SHF. The Tbx1-Fgf8/Fgf10 pathway is required for cell proliferation in the right and the left SHF.

4.5 Modifier genes for 22q11DS

22q11DS is caused by a heterozygous deletion in chromosome 22q11.2. The majority of the patients have a 3 Mb deletion; some carry a 1.5 Mb nested deletion (Lindsay *et al*., 1995a; Morrow *et al*., 1995). Patients suffer from congenital heart disease (aortic arch defects, OFT defects), thymic and parathyroid aplasia or hypoplasia, craniofacial anomalies and learning difficulties**.** The phenotype is characterized through 100% penetrance and variable expressivity (Lindsay *et al.,* 1995b; Morrow *et al*., 1995; Ryan *et al*., 1997; Scambler, 2000). There are no consistent differences in the phenotype between the 1.5 Mb and 3 Mb deletions (Carlson *et al.,* 1997) suggesting that the variability must be due to genetic modifiers in form of single nucleotide polymorphisms (SNPs) or other polymorphisms and/or environmental factors. Mouse models have been used to address the issue of genetic modifiers. Mice in mixed backgrounds which harbor a deletion of 1 Mb deleting 18 genes of the 22q11.2 region showed variable penetrance of cardiac defects (Taddei *et al.,* 2001) suggesting the presence of genetic modifiers. Nevertheless, variable severity of cardiac defects in *Tbx1*-/- mice in congenic FVB background (Liao *et al*., 2004) suggests that also stochastic factors might be a cause. Recently two genes, *Fgf8* and the *Vascular Endothelial Growth Factor* (*VEGF*) have been linked to 22q11DS and are thought to be genetic modifiers of this syndrome.

Mouse mutants that harbor hypomorphic alleles for *Fgf8* have been shown to phenocopy the cardiac defects of the 22q11DS. Moreover, *Fgf8* which is required for development of the pharyngeal arches acts in the same pathway as *Tbx1*. It is very likely that *Fgf8* is a genetic modifier of the syndrome and contributes to the phenotypic variability (Frank *et al*., 2002), though evidence in humans is still elusive.

VEGF is essential for vasculogenesis and angiogenesis. There exist three isoforms of 120, 164 and 188 aa ($VEGF^{120}$, $VEGF^{164}$ and $VEGF^{188}$). Mouse null

mutants for *VEGF* ^{164} display aortic arch defects, craniofacial, thymus and parathyroid anomalies as well as reduced density of the vasculature of the affected organs reminiscent of defects in 22q11DS patients (Stalmans *et al*., 2003). *Tbx1* expression was found to be reduced in these mice but it is not known whether this reduction is a direct down regulation or if it is a secondary effect. SNP analysis of 22q11DS patients showed a SNP variant in the 5' untranslated region of *VEGF* which was more frequent in patients with cardiac defects compared to WT. *VEGF* is a good candidate for a genetic modifier of the syndrome, though its interaction with Tbx1 still needs to be shown.

The fact, that *Tbx1* and *Pitx2* act in the same pathway regulating asymmetric cardiac morphogenesis and that *Pitx2*+/-; *Tbx1*+/- mice exhibit a subset of cardiac defects of 22q11DS patients makes it tempting to speculate that *PITX2* is a genetic modifier of this syndrome. It would be interesting to determine, if patients with cardiac defects have functional SNP variants in the *PITX2* gene. Changes in an amino acid or in conserved non-coding regulatory regions of *PITX2* could alter the expressivity of the syndrome. This still needs to be determined.

4.6 The T-half site in the Pitx2-ASE is only conserved in mammals

The vertebrate heart is specialized to pump blood through gills or lungs to get oxygen. This oxygenated blood is then pumped throughout the body to supply the tissues. This is established using a highly specialized vascular circulation system. With the advance of a separate pulmonary system and division of the cardiac chambers in vertebrate evolution, oxygenated and deoxygenated blood could be separated more and more efficiently. The blood enters the heart of gill breathing fish through the sinus venosus, and passes then through the atrium and the ventricle, which are not yet divided by septae. It leaves the heart via bulbus

cordis directly into the ventral aorta. All blood in the body is oxygenated and the oxygen exchange takes place in the gills. However, the lungfish which possess a pulmonary system have already an incomplete subdivision of their atrium and ventricle. Though, mixing of oxygenated and deoxygenated blood still occurs. The amphibian heart consists of a sinus venosus, two atria that are fully divided by an atrial septum, a non-septated ventricle and a conus arteriosus which possesses a spiral valve. This valve separates oxygenated and deoxygenated blood and leads it to the systemic and pulmocutaneous arches. Reptiles still have a small sinus venosus, a left and right atrium and an incompletely divided ventricle (except for crocodiles which have a fully developed ventricular septum). Birds and mammals are the only vertebrates which possess a four-chambered heart consisting of separate left and right atrium and ventricle, respectively. In addition, in contrast to other species, the outflow tract is fully subdivided into a pulmonary trunk and aorta which ensures complete separation of the oxygenated and the deoxygenated blood flow (Kardong, 2005).

Formation of the different septae in the heart are managed by different genetic pathways during development and evolution. To ensure the correct development and remodeling of the septae and valves in the mammalian heart, additional pathways were necessary to coordinate their formation. The Tbx1-Pitx2 pathway could be one of these pathways responsible for cell proliferation or migration of the cells necessary for septum formation in the outflow tract or in the ventricle and atria, respectively. Defects in these structures of *Pitx2*+/-; *Tbx1*+/- mice suggest that this pathway is indispensable for their proper development. Sequence analysis of the Pitx2-ASE in mouse, human, chimp, rat, frog and zebrafish has shown that the T-half site to which Tbx1 binds to activate the *Pitx2* gene in the left SHF is only conserved in mammals. This leads to my hypothesis that this T-half site represents an evolutionarily recent acquired regulator element in the enhancer. Asymmetric *Pitx2* expression is conserved throughout the vertebrates. In the Pitx2-ASE of *Xenopus* the FAST binding sites and the Nkx2.5

binding sites which are needed for initiation and maintenance of *Pitx2* expression in left-sided organs are conserved (Shiratori *et al*., 2001). However, a T-half site in the frog's *Pitx2c* enhancer could not be detected. Through the addition of the T-half site in the Pitx2-ASE of the mammalian species, the enhancer has gained an extra function. This function is likely used for regulating features like the complex cardiac remodeling especially the septum and valve formation which are distinct in the four-chambered heart of mammalian species.

Moreover, comparative studies in animals have shown how evolution in non-coding regulatory sequences can contribute to evolution of anatomy. It is assumed that one possibility how changes in regulation during development lead to gain, loss or modification of morphological traits are alterations in cis-regulatory elements. These changes in regulation of transcription factors can lead to changes in gene expression (Carroll, 2005). The addition of a cis-regulatory element, in this case a T-half site in the Pitx2-ASE leads to a more complex heart structure which provides advantages for mammals to survive in their specific environment.

4.7 Summary

In conclusion, this thesis unravels a novel Tbx1-Pitx2 genetic pathway. It shows that Tbx1 is able to bind directly to the *Pitx2* enhancer and transactivates *Pitx2c* expression through interaction with Nkx2.5 in cells. I hypothesize that activation of *Pitx2c* by Nkx2.5 and Tbx1 is needed to maintain *Pitx2c* expression in the left cardiac precursor cells of the SHF after its initial activation through Nodal. It has been shown that *Pitx2c* acts cell autonomously within these cells by promoting their proliferation and/or migration into the heart (Kioussi *et al*., 2002). Thus, the Tbx1-Pitx2 pathway represents a novel cell autonomous function of Tbx1 in the SHF. This pathway complements the previously shown non-cell autonomous function of Tbx1 via *Fgf10/Fgf8* regulating cell proliferation in the

SHF (Hu *et al*., 2004; Xu *et al.,* 2004; Kelly, 2005). The proven genetic interaction between the two genes and the reduced expression of *Pitx2c* in the *Tbx1*-/- mice must account for a discrete subset of the cardiac defects in these mice, which can, in the absence of asymmetric *Pitx2c* expression, be therefore classified as laterality defects.

4.8 Future directions

Targeted mutation of the T-half site in the endogenous *Pitx2c* enhancer which leads to abolishment of Tbx1 binding to the T-half site *in vivo* should help to verify the *in vitro* data obtained through the EMSA and the luciferase assays and will show if Tbx1 binding to the *Pitx2c* enhancer is crucial in cardiovascular development.

Furthermore, it will be interesting to understand which mechanisms underlie the Tbx1-Pitx2 pathway, whether it regulates cell proliferation or cell migration into the heart or both. Cell proliferation can be assessed by applying BrdU staining. Preliminary data showed no differences in cell proliferation at the stage E10.0 between *Pitx2*+/-; T*bx1*+/-, *Pitx2*+/-, *Tbx1*+/- and wt mice, respectively. Since co-expression of *Tbx1* and *Pitx2* starts much earlier in development, between E7.75 and E8.0 differences in proliferation might occur much earlier than E10.0. BrdU staining of E8.0 - E8.5 should help to clarify this aspect.

Lineage tracing experiments in *Pitx2*+/-; *Tbx1*+/- and wt mice which harbor a Cre-regulated lacZ gene could be crossed with *Islet1*-Cre mice (Srinivas *et al*., 2001). The resulting mice will express lacZ in SHF cells and their daughter cells only. LacZ staining of these embryos would help to understand if cell migration of SHF cells into heart plays a role in the defects of the *Pitx2*+/-; *Tbx1*+/- mice.

Moreover, it will be interesting to know which genes are immediately up- or downstream of the Tbx1-Pitx2 pathway. It is known that forkhead proteins Foxa2 and Foxc1 are upstream of *Tbx1* in the pharyngeal endoderm and in the head mesenchyme, respectively. Fox binding sites have been identified in the *Tbx1* promoter (Yamagishi *et al*., 2003; Hu *et al*., 2004). Fox proteins might also be upstream of Tbx1 in the Tbx1-Pitx2 pathway in the SHF. One possible candidate could be Foxh1. It is expressed in SHF and null mutants have defects in the outflow tract and the right ventricle (Von Both *et al*., 2004). Luciferase assays using a Foxh1 expression construct and *Tbx1* reporter as well as gel shift experiments to assess Foxh1 binding to the *Tbx1* promoter could provide information whether Foxh1 is involved in this pathway.

Only a limited number of Pitx2 downstream genes are known so far, two of them are *CyclinD2* and *Fgf8*. *Fgf8* is downstream of Pitx2 in craniofacial development (Liu *et al*., 2003). As mentioned before, *Fgf8* hypomorphs exhibit similar cardiac defects as *Pitx2*+/-; *Tbx1*+/- mice (Frank *et al*., 2002). However, my preliminary data from crosses between *Fgf8*+/- and *Pitx2*+/- mice do not suggest that *Fgf8* is a likely candidate. *Fgf8*+/-; *Pitx2*+/- double heterozygous mice survive in normal Mendelian ratios, which makes a genetic interaction between Fgf8 and Pitx2 in heart development unlikely. *CyclinD2*, another downstream target of Pitx2 has been shown to be involved in cell proliferation in the outflow tract, the pituitary and the muscle (Kioussi *et al*., 2002). It would be interesting to investigate if *CyclinD2* is also downstream of Pitx2 in the SHF.

5. References

Amendt, B. A., Semina, E. V. and Alward, W. L. M. (2000). Rieger syndrome: a clinical, molecular, and biochemical analysis. *Cell Mol Life Sci.* **57**:1652-1666.

Amendt, B. A., Sutherland, L. B., Semina, E. V. and Russo, A. F. (1998). The molecular basis of Rieger syndrome. Analysis of Pitx2 homeodomain protein activities. *J Biol Chem.* **273**:20066-20072.

Arakawa, H., Nakamura, T., Zhadanov, A. B., Fidanza, V., Yano, T., Bullrich, F., Shimizu, M., Blechman, J., Mazo, A., Canaani, E. and Croce, C. M. (1998). Identification and characterization of the ARP1 gene, a target for the human acute leukemia ALL1 gene. *Proc Natl Acad Sci U S A*. **95**:4573-4578.

Bamshad, M., Le, T., Watkins, W. S., Dixon, M. E., Kramer, B. E., Roeder, A. D., Carey, J. C., Root, S., Schinzel, A., Van Maldergem, L., Gardner, R. J. *et al.* (1999). The spectrum of mutations in TBX3: Genotype/Phenotype relationship in ulnar-mammary syndrome. *Am J Hum Genet.* **64**:1550-1562.

Bamshad, M., Lin, R. C., Law, D. J., Watkins, W. C., Krakowiak, P. A., Moore, M. E., Franceschini, P., Lala, R., Holmes, L. B., Gebuhr, T. C. *et al.* (1997). Mutations in human TBX3 alter limb, apocrine and genital development in ulnar-mammary syndrome. *Nat Genet*. **16**:311-315. Erratum in: *Nat Genet* 1998 **19**:102.

Beddington, R. S., Rashbass, P. and Wilson, V. (1992). Brachyury--a gene affecting mouse gastrulation and early organogenesis. *Dev Suppl*. 157-165.

Belo, J. A., Bouwmeester, T., Leyns, L., Kertesz, N. Gallo, M., Folletie, M. and De Robertis, E. M. (1997**).** Cerberus-like is a secreted factor with neutralizing activity expressed in the anterior primitive endoderm of the mouse gastrula. *Mech. Dev.* **68**:45-57.

Bongers, E. M., Duijf, P. H., van Beersum, S. E., Schoots, J., Van Kampen, A., Burckhardt, A., Hamel, B. C., Losan, F., Hoefsloot, L. H., Yntema, H. G. *et al.* (2004). Mutations in the human TBX4 gene cause small patella syndrome. *Am J Hum Genet.* **74**:1239-1248.

Brown, C. B., Wenning, J. M., Lu, M. M., Epstein, D. J. Meyers, E. N. and Epstein, J. A. (2004). Cre-mediated excision of Fgf8 in the Tbx1 expression domain reveals a critical role for Fgf8 in cardiovascular development in the mouse. *Dev. Biol*. **267**:190-192.

Bruneau, B. G., Nemer, G., Schmitt, J. P., Charron, F., Robitaille, L., Caron, S., Conner, D. A., Gessler, M., Nemer, M., Seidman, C. E. and Seidman, J. G. (2001). A murine model of Holt-Oram syndrome defines roles of the T-box transcription factor Tbx5 in cardiogenesis and disease. *Cell* **106**:709-721.

Burn, J. and Goodship, J. (1996). Congenital heart disease. In *Emery and Rimoin's Principles and Practice of Medical Genetics (3rd Ed.)*. (ed. D. L. Rimoin, J. M. Connor, R. E. Pyeritz), Vol.1, pp. 767-828.

Cai, C. L., Liang, X., Shi, Y., Chu, P-H., Pfaff, S. L., Chen, J. and Evans, S. (2003). Isl1 identifies a cardiac progenitor population that proliferates prior to differentiation and contributes a majority of cells to the heart. *Dev. Cell* **5**:877-889.

Campione, M., Acosta, L., Martinez, S., Icardo, J. M., Aranega, A. and Franco, D. (2002). Pitx2 and cardiac development: a molecular link between left/right signaling and congenital heart disease. *Cold Spring Harb Symp Quant Biol*. **67**:89-95.

Campione, M., Ros, M. A., Icardo, J. M., Piedra, E., Christoffels, V. M., Schweickert, A., Blum, M., Franco, D. and Moorman, A. F. M. (2001). *Pitx2* expression defines a left cardiac lineage of cells: Evidence for atrial and ventricular molecular isomerism in the *iv/iv* mice. *Dev Biol.* **231**:252-264.

Campione, M., Steinbeisser, H., Schweickert, A., Deissler, K., van Bebber, F., Lowe, L. A., Nowotschin, S., Viebahn, C., Haffter, P., Kuehn, M. R. and Blum, M. (1999). The homeobox gene Pitx2: mediator of asymmetric left-right signaling in vertebrate heart and gut looping. *Development* **126**:1225-1234.

Carlson, C., Sirotkin, H., Pandita, R., Goldberg, R., McKie, J., Wadey, R., Patanjali, S. R., Weissman, S. M., Anyane-Yeboa, K., Warburton, D. *et al.* (1997). Molecular definition of 22q11 deletions in 151 velo-cardio-facial syndrome patients. *Am J Hum Genet*. **61**:620-629.

Carroll, S. B. (2005). Evolution at two levels: on genes and form. *PLoS Biol.* **3**:1159-1166.

Chapman, D. L., Garvey, N., Hancock, S., Alexiou, M., Agulnik, S. I., Gibson-Brown, J. J., Cebra-Thomas, J., Bollag, R. J., Silver, L. M. and Papaioannou, V. E. (1996). Expression of the T-box family genes, Tbx1-Tbx5, during early mouse development. *Dev Dyn.* **206**:379-90.

Collignon, J., Varlet, I. and Robertson, E. J. (1996). Relationship between asymmetric nodal expression and the direction of embryonic turning. *Nature* **381**:155-158.

Cox, C. J., Espinoza, H. M., McWilliams, B., Chappell, K., Morton, L., Hjalt, T. A., Semina, E. V. and Amendt, B. A. (2002). Differential regulation of gene expression by PITX2 isoforms. *J Biol Chem.* **277**:25001-25010.

DiGeorge, A. (1965). A new concept of the cellular basis of immunity. *J. Pediatr*. **67**:907.

Dobrovolskaia-Zavadskaia, N. (1927). Sur la mortification spontanée de la queue chez la souris nouveau-née et sur l'existence d'un caratère (facteur) héréditaire "non viable". C. *R. Acad. Sci. Biol.* **97**:114-116.

Dodou, E., Verzi, M. P., Anderson, J. P., Xu, S. M. and Black, B. L. (2004). Mef2c is a direct transcriptional target of ISL1 and GATA factors in the anterior heart field during mouse embryonic development. *Development.* **131**:3931-3942.

Edelmann, L., Pandita, R. K, Spiteri, E., Funke, B., Goldberg, R., Palanisamy, N., Chaganti, R. S., Magenis, E., Shprintzen, R. J. and Morrow, B. E. (1999b). A common molecular basis for rearrangement disorders on chromosome 22q11. *Hum Mol Genet*. **8**:1157-1167.

Edelmann, L., Pandita, R. K. and Morrow, B. E. (1999a). Low-copy repeats mediate the common 3-Mb deletion in patients with velo-cardio-facial syndrome. *Am J Hum Genet.* **64**:1076-1086.

Edelmann, L., Spiteri, E., Koren, K., Pulijaal, V., Bialer, M. G., Shanske, A., Goldberg, R. and Morrow, B. E. (2001). AT-rich palindromes mediate the constitutional t(11;22) translocation. *Am J Hum Genet.* **68**:1-13.

Emanuel, B. S., McDonald-McGinn, D., Saitta, S. C. and Zackai, E. H. (2001). The 22q11.2 deletion syndrome. *Adv Pediatr.* **48**:39-73. Review.

Espinoza, H. M., Cox, C. J., Semina, E. V. and Amendt, B. A. (2002). A molecular basis for differential developmental anomalies in Axenfeld-Rieger syndrome. ***Hum Mol Genet***. **11**:743-753.

Franco, D. and Campione, M. (2003). The role of *Pitx2* during cardiac development. Linking left-right signaling and congenital heart diseases. *Trends Cardiovasc Med* **13**:157-163.

Franco, D., de Boer, P. A., de Gier-de Vries, C., Lamers, W. H. and Moorman, A. F. (2001). Methods on in situ hybridization, immunohistochemistry and beta-galactosidase reporter gene detection. *Eur. J. Morphol.* **39**:169-191.

Frank, D. U., Fotheringham, L. K., Brewer, J. A., Muglia, L. J., Tristani-Firouzi, M., Capecchi, M. R. And Moon, A. M. (2002). An Fgf8 mouse mutant phenocopies human 22q11 deletion syndrome. *Development* **129**:4591-4603.

Funke, B., Edelmann, L., McCain, N., Pandita, R. K., Ferreira, J., Merscher, S., Zohouri, M., Cannizzaro, L., Shanske, A. and Morrow B. E. (1999). Der(22) syndrome and velo-cardio-facial syndrome/DiGeorge syndrome share a 1.5-Mb region of overlap on chromosome 22q11. *Am J Hum Genet.* **64**:747-758.

Gage, P. J. and Camper, S. A. (1997). Pituitary homeobox 2, a novel member of the bicoid-related family of homeobox genes, is a potential regulator of the anterior structure formation. *Hum Mol Genet.* **6**:457-464.

Gage, P. J., Suh, H. and Camper S. A. (1999a). Dosage requirement of *Pitx2* for development of multiple organs. *Development* **126**:4643-4651.

Gage, P. J., Suh, H. and Camper, S. A. (1999b). The *bicoid*-related Pitx gene family in development. *Mamm Genome*. **10**:197-200.

Garg, V., Kathiriya, I. S., Barnes, R., Schluterman, M. K., King, I. N., Butler, C. A., Rothrock, C. R., Eapen, R. S., Hirayama-Yamada, K., Joo, K. *et al*. (2003). GATA4 mutations cause human congential heart defects and reveal an interaction with TBX5. *Nature* **424**:443-447.

Gehring, W.J. Qiu Qian, Y., Billeter, M., Furukubu-Tokunaga, K., Schier, A.F., Resendez-Perez, D., Affolter, M., Otting, G. and Wüthrich, K. (1994). Homeodomain-DNA recognition. *Cell* **78**:211-223.

Ghosh, T. K., Packham, E. A., Bonser, A. J., Robinson, T. E., Cross, S. J., Brook, J. D. (2001). Characterization of the TBX5 binding site and analysis of mutations that cause Holt-Oram syndrome. *Hum Mol Genet.***10**:1983-1994.

Gilbert, S. F. (2003). Neural crest and axonal specificity. In: *Developmental Biology 7th edition*. pp. 427-463. Sinauer Associates Inc. Sunderland.

Habets, P. E., Moorman, A. F., Clout, D. E., van Roon, M. A., Lingbeek, M., van Lohuizen, M., Campione, M. and Christoffels V. M. (2002). Cooperative action of Tbx2 and Nkx2.5 inhibits ANF expression in the atrioventricular canal: implications for cardiac chamber formation. *Genes Dev.* **16**:1234-1246.

Hamada, H. (2001). Left-Right Asymmetry. In *Mouse Development.* (ed. J. Rossant and P. P. L. Tam), pp. 55-70. San Diego: Academic Press.

Hanes, S.D. and Brent, R. (1991). A genetic model for interaction of the homeodomain recognition helix with DNA. *Science* **251**:426-430.

Harvey, R. P. (2002). Patterning the vertebrate heart. *Nat. Rev. Genet.* **3:**544-556. Review.

Hiroi, Y., Kudoh, S., Monzen, K., Ikeda, Y., Yazaki, Y., Nagai, R. and Komuro, I. (2001). Tbx5 associates with Nkx2-5 and synergistically promotes cardiomyocyte differentiation. *Nat Genet.* **28**:276-280.

Hjalt, T. A., Semina, E. V., Amendt, B. A. and Murray, J. C. (2000). The Pitx2 Protein in Mouse Development. *Dev. Dyn.* **218:**195-200.

Hoffman, J. I. and Kaplan, S. (2002). The incidence of congenital heart disease. *J Am Coll Cardiol.* **39:**1890-1900. Review.

Hu, T., Yamagishi, H., Maeda, J., McAnally, J., Yamagishi, C. and Srivastava, D. (2004). Tbx1 regulates fibroblast growth factors in the anterior heart field through a reinforcing autoregulatory loop involving forkhead transcription factors. *Development* **131**:5491-5502.

Jerome, L. A. and Papaioannou, V. E. (2001). DiGeorge syndrome phenotype in mice mutant for the T-box gene, *Tbx1*. *Nat. Genet.* **27**:286-291.

Karayiorgou, M., Morris, M. A., Morrow, B., Shprintzen, R. J., Goldberg, R., Borrow, J., Gos, A., Nestadt, G., Wolyniec, P. S., Lasseter, V. K., *et al.* (1995). Schizophrenia susceptibility associated with interstitial deletions of chromosome 22q11. *Proc Natl Acad Sci USA*. **92**:7612-7616.

Kardong, K. V. (2005). The Circulatory System. *In: Vertebrates: Comparative Anatomy, Function, Evolution 4th edition*. pp. 445-492. McGraw Hill. New York.

Kelly, R. G. (2005). Molecular inroads into the anterior heart field. *Trends Cardiovasc. Med.* **15**, 51-56.

Kelly, R. G. and Buckingham, M. E. (2002). The anterior heart-forming field: voyage to the arterial pole of the heart. *Trends Genet*. **18**:210-216. Review.

Kelly, R. G., Brown, N. A. and Buckingham, M. E. (2001). The arterial pole of the mouse heart forms from Fgf10-expressing cells in pharyngeal mesoderm. *Dev Cell.* **1**:435-440.

Kelly, R. G., Jerome-Majewska, L. A. and Papaioannou, V. E. (2004). The del22q11.2 candidate gene Tbx1 regulates branchiomeric myogenesis. *Hum Mol Genet.* **13**:2829-2840.

Kimber, W. L., Hsieh, P., Hirotsune, S., Yuva-Paylor, L., Sutherland, H. F., Chen, A., Ruiz-Lozano, P., Hoogstraten-Miller, S. L., Chien, K. R., Paylor, R. *et al.* (1999). Deletion of 150 kb in the minimal DiGeorge/velocardiofacial syndrome critical region in mouse. *Hum Mol Genet.* **8**:2229-2237.

Kioussi, C., Briata, P., Baek, S. H., Rose, D. W., Hamblet, N. S., Herman, T., Ohgi, K. A., Lin, C., Gleiberman, A., Wang, J. *et al.* (2002). Identification of a Wnt/Dvl/β-catenin → Pitx2 pathway mediating cell-type-specific proliferation during development. *Cell* **111**:673-685.

Kirby, M. L. (1989). Plasticity and predetermination of mesencephalic and trunk neural crest transplanted into the region of the cardiac neural crest. *Dev Biol.* **134**:402-412.

Kirby, M. L. and Waldo K. L. (1995). Neural crest and cardiovascular patterning. *Circ Res.* **77**:211-215. Review.

Kitamura, K., Miura, H., Miyagawa-Tomita, S., Yanazawa, M., Katoh-Fukui, Y., Suzuki, R., Ohuchi, H., Suehiro, A., Motegi, Y., Nakahara, Y. *et al.* (1999). Mouse Pitx2 deficiency leads to anomalies of the ventral body wall, heart, extra- and periocular mesoderm and right pulmonary isomerism. *Development* **126**:5749-5758.

Kitamura, K., Miura, H., Yanazawa, M., Miyashita, T. and Kato, K. (1997). Expression patterns of Brx1 (Rieg gene), Sonic hedgehog, Nkx2.2, Dlx1 and Arx during zona limitans intrathalamica and embryonic ventral lateral geniculate nuclear formation. *Mech. Dev.* **67**:83-96.

Krause, A., Zacharias, W., Carmata, T., Linkhart, B., Law, E., Lischke, A., Miljan, E. And Simon, H.-G. (2004). Tbx5 and Tbx4 transcription factors interact with a newchicken PDZ-LIM protein in limb and heart development. *Dev. Biol.* **273**:106-120.

Lee, K. H., Evans, S., Ruan, T. Y. and Lassar, A. B. (2004). SMAD-mediated modulation of YY1 activity regulates the BMP response and cardiac-specific expression of a GATA4/5/6-dependent chick Nkx2.5 enhancer. *Development* **131**:4709-4723.

Li, Q. Y., Newbury-Ecob, R. A., Terrett, J. A., Wilson, D. I., Curtis, A. R., Yi, C. H., Gebuhr, T., Bullen, P. J., Robson, S. C., Strachan, T. *et al.* (1997). Holt-Oram syndrome is caused by mutations in TBX5, a member of the Brachyury (T) gene family. *Nat Genet.* **15**:21-29.

Liao, J., Kochilas, L., Nowotschin, S., Arnold, J. S., Aggarwal, V. S., Epstein, J. A., Brown, M. C., Adams, J. and Morrow, B. E. (2004). Full spectrum of malformations in velo-cardio-facial syndrome/DiGeorge syndrome mouse models by altering Tbx1 dosage. *Hum. Mol. Genet.* **13**:1577-1585.

Lin, C. R., Kioussi, C., O'Connell, S., Briata, P., Szeto, D., Liu, F., Izpisua-Belmonte, J. C. and Rosenfeld, M. G. (1999). Pitx2 regulates lung asymmetry, cardiac positioning and pituitary and tooth morphogenesis. *Nature* **401**:279-282.

Lindsay, E. A., Goldberg, R., Jurecic, V., Morrow, B., Carlson, C., Kucherlapati, R. S., Shprintzen, R. J. and Baldini, A. (1995a). Velo-cardio-facial syndrome: frequency and extent of 22q11 deletions. *Am J Med Genet*. **57**:514-522.

Lindsay, E. A., Greenberg, F., Shaffer, L. G., Shapira, S. K., Scambler, P. J. and Baldini A. (1995b). Submicroscopic deletions at 22q11.2: variability of the clinical picture and delineation of a commonly deleted region. *Am J Med Genet*. **56**:191-197.

Lindsay, E. A., Vitelli, F., Su, H., Morishima, M., Huynh, T., Pramparo, T., Jurecic, V., Ogunrinu, G., Sutherland, H. F., Scambler, P. J. *et al.* (2001). *Tbx1* haploinsufficiency in the DiGeorge syndrome region causes aortic arch defects in mice. *Nature* **410**:97-101.

Liu, C., Liu, W, Palie, J., Lu, M. F., Brown, N. A. and Martin, J. F. (2002). Pitx2c patterns anterior myocardium and aortic arch vessels and is required for local cell movement into atrioventricular cushions. *Development* **129**:5081-5091.

Liu, C., Liu, W., Lu, M-F., Brown, N. A. and Martin, J. F. (2001) Regulation of left-right asymmetry by thresholds of Pitx2c activity. *Development* **128:**2039-2048.

Liu, W., Selever, J., Lu, M. F. and Martin, J. F. (2003). Genetic dissection of Pitx2 in craniofacial development uncovers new functions in branchial arch morphogenesis, late aspects of tooth morphogenesis and cell migration. *Development* **130**:6375-6385.

Logan, M., Pagan-Westphal, S. M., Smith, D. M., Paganessi, L. and Tabin, C. J. (1998). The transcription factor Pitx2 mediates situs-specific morphogenesis in response to left-right asymmetric signals. *Cell* **94**:307-317.

Lowe, L. A., Supp, D. M., Sampath, K., Yokoyama, T., Wright, C. V., Potter, S. S., Overbeek, P. and Kuehn, M. R. (1996). Conserved left-right asymmetry of nodal expression and alterations in murine situs inversus. *Nature* **381**:158-161.

Lu, M. F, Pressman, C., Dyer, R., Johnson, R. L. and Martin, J. F. (1999). Function of Rieger syndrome gene in left-right asymmetry and craniofacial development. *Nature* **401**:276-278.

Lyons, I., Parson, L. M., Harvey, L., Li, R., Andrews, J. E., Robb, L. and Harvey, R. P. (1995). Myogenic and morphogenesis defects in heart tubes of murine embryos lacking the homeobox gene Nkx2.5. *Genes Dev*. **9**:1654-1666.

Mammi, I., De Giorgio, P., Clementi, M. and Tenconi, R. (1998) Cardiovascular anomaly in Rieger Syndrome: heterogeneity or contiguity? *Acta Ophthalmol Scand*. **76**:509-512.

Meilhac, S. M., Esner, M., Kelly, R. G., Nicolas, J.-F. and Buckingham, M. E. (2004). The clonal origin of myocardial cells different regions of the embryonic mouse heart. *Dev. Cell* **6**:685-698.

Meno, C., Ito, Y., Saijoh, Y., Matsuda, Y., Tashiro, K., Kuhara, S. and Hamada, H. (1997). Two closely-related left-right asymmetrically expressed genes, lefty-1 and lefty-2: their distinct expression domains, chromosomal linkage and direct neuralizing activity in Xenopus embryos. *Genes Cells*. **2**:513-524.

Meno, C., Saijoh, Y., Fujii, H., Ikeda, M., Yokoyama, T., Yokoyama, M., Toyoda, Y. and Hamada H. (1996). Left-right asymmetric expression of the TGF beta-family member lefty in mouse embryos. *Nature* **381**:151-155.

Meno, C., Shimono, A., Saijoh, Y., Yashiro, K., Mochida, K., Ohishi, S., Noji, S., Kondoh, H. and Hamada, H. (1998). lefty-1 is required for left-right determination as a regulator of lefty-2 and nodal. *Cell* **94**:287-297.

Merscher, S., Funke, B., Epstein, J. A., Heyer, J., Puech, A., Lu, M. M., Xavier, R. J., Demay, M. B., Russell, R. G., Factor, S. *et al*. (2001). *TBX1* is responsible for cardiovascular defects in velo-cardio-facial/DiGeorge syndrome. *Cell* **104**:619-629.

Mjaatvedt, C. H., Nakaoka, T., Moreno-Rodriguez, R., Norris, R. A., Kern, M. J., Eisenberg, C. A., Turner, D. and Markwald, R. R. (2001). The outflow tract of the heart is recruited from a novel heart-forming field. *Dev Biol.* **238**:97-109.

Moraes, F., Novoa, A., Jerome-Majewska, L. A., Papaioannou, V. E. and Mallo, M. (2005). Tbx1 is required for proper neural crest migration and to stabilize spatial patterns during middle and inner ear development. *Mech Dev.* **122**:199-212.

Morrow, B., Goldberg, R., Carlson, C., Das Gupta, R., Sirotkin, H., Collins, J., Dunham, I., O'Donnell, H., Scambler, P., Shprintzen, R., *et al.* (1995). Molecular definition of the 22q11 deletions in velo-cardio-facial syndrome. *Am J Hum Genet.* **56**:1391-1403.

Mucchielli, M., Martinez, S., Pattyn, A., Goridis, C. and Brunet, J. (1996). Otlx2, an Otx-related homeobox gene expressed in the pituitary gland and in a restricted pattern in the forebrain. *Mol. Cell. Neurosci.* **8**:258-271.

Murray, J. C., Bennett, S. R., Kwitek, A. E., Small, K. W., Schinzel, A., Alward, W. L., Weber, J. L., Bell, G. I. and Buetow, K. H. (1992). Linkage of Rieger syndrome to the region of the epidermal growth factor gene on chromosome 4. *Nat Genet*. **2**:46-49.

Naiche, L. A., Harrelson, Z., Kelly, R. G., Papaioannou, V. E. (2005). T-Box Genes in Vertebrate Development. *Annu Rev Genet.* **39**:219-239.

Nowotschin, S. (1997). Expression des Homeoboxgens *Ptx-2* waehrend der Embryonalentwicklung der Maus. Diplomarbeit.

Oh, S. P. and Li, E. (1997). The signaling pathway mediated by the type IIB actvin receptor controls axial patterning and lateral asymmetry in the mouse. *Genes Dev.* **11**:1812-1826.

Papaioannou, V. E. (2001). T-box genes in development: from hydra to humans. *Int Rev Cytol.* **207**:1-70. Review.

Papaioannou, V. E. and Silver, L. M. (1998). The T-box gene family. *Bioessays* **20**:9-19. Review.

Piedra, M. E., Icardo, J. M., Albajar, M., Rodriguez-Rey, J. C. and Ros, M. A. (1998). Pitx2 participates in the late phase of the pathway controlling left-right asymmetry. *Cell* **94**:319-324.

Puech, A., Saint-Jore, B., Funke, B., Gilbert, D. J., Sirotkin, H., Copeland, N. G., Jenkins, N. A.., Kucherlapati, R., Morrow, B. and Skoultchi, A. I. (1997). Comparative mapping of the human 22q11 chromosomal region and the orthologous region in mice reveals complex changes in gene organization. *Proc Natl Acad Sci U S A.* **94**:14608-14613.

Raft, S., Nowotschin, S., Liao, J., Morrow, B. E. (2004). Suppression of neural fate and control of inner ear morphogenesis by Tbx1. *Development* **131**:1801-1812.

Rieger, H. (1935). Beiträge zur Kenntnis seltener Missbildungen der Iris. II. Ueber Hypoplasie des Irisvorderblattes mit Verlagerung und Entrundung der Pupille. *Graefe Arch Klin Exp Ophthalmol*. **133**:602-635.

Riise, R., Storhaug, K. and Brondum-Nielsen, K. (2001). Rieger syndrome is associated with PAX6 deletion. *Acta Ophthalmol. Scand*. **79**:201-203.

Ryan, A. K., Blumberg, B., Rodriguez-Esteban, C., Yonei-Tamura, S., Tamura, K., Tsukui, T., de la Pena, J., Sabbagh, W., Greenwald, J., Choe, S. *et al.* (1998). Pitx2 determines left-right asymmetry of internal organs in vertebrates. *Nature* **394**:545-551.

Ryan, A. K., Goodship, J. A., Wilson, D. I., Philip, N., Levy, A., Seidel, H., Schuffenhauer, S., Oechsler, H., Belohradsky, B., Prieur, M. *et al.* (1997). Spectrum of clinical features associated with interstitial chromosome 22q11 deletions: a European collaborative study. *J Med Genet.* **34**:798-804.

Sadler, T. W. (2000). The Cardiovascular System. In: *Langman's Medical Embryology (8th edition)*. pp. 208-259. Lippincott Williams and Wilkins, New York.

Scambler, P. J. (2000). The 22q11 deletion syndromes. *Hum Mol Genet.* **9**:2421-2426. Review.

Schweickert, A., Campione, M., Steinbeisser, H. and Blum, M. (2000). Pitx2 isoforms: involvement of Pitx2c but not Pitx2a or Pitx2b in vertebrate left-right asymmetry. *Mech. Dev*. **90**:41-51.

Semina, E. V., Reiter, R., Leysens, N. J., Alward, W. L., Small, K. W., Datson, N. A., Siegel-Bartelt, J., Bierke-Nelson, D., Bitoun, P., Zabel, B. U. *et al.* (1996). Cloning and characterization of a novel bicoid-related homeobox transcription factor gene, RIEG, involved in Rieger syndrome. *Nat Genet.* **14**:392-399.

Shaikh, T. H., Kurahashi, H. and Emanuel, B. S. (2001). Evolutionary conserved low copy repeats (LCRs) in 22q11 mediate deletions, duplications, translocations and genomic instability: An update and literature review. *Genet. Med*. **3**:6-13.

Shiratori, H., Sakuma, R., Watanabe, M., Hashiguchi, H., Mochida, K., Sakai, Y., Nishino, J., Saijoh, Y., Whitman, M. and Hamada, H. (2001). Two-step regulation of left-right asymmetric expression of Pitx2: initiation by nodal signaling and maintenance by Nkx2.5. *Mol. Cell.* **7**:137-149.

Shprintzen, R. J., Goldberg, R. B., Lewin, M. L., Sidoti, E. J., Berkman, M. D., Argamaso, R. V. and Young, D. (1978). A new syndrome involving cleft palate, cardiac anomalies, typical facies, and learning disabilities: velo-cardio-facial syndrome. *Cleft Palate J.* **15**:56-62.

Srinivas, S., Watanabe, T., Lin, C. S., William, C. M., Tanabe, Y., Jessell, T. M. and Costantini, F. (2001). Cre reporter strains produced by targeted insertion of EYFP and ECFP into the ROSA26 locus. *BMC Dev Biol.* **1**:4.

Srivastava, D. and Olson, E. N. (2000). A genetic blueprint for cardiac development. *Nature* **407**:221-226. Review.

Stennard, F. A., Costa, M. W., Elliott, D. A., Rankin, S., Haast, S. J., Lai, D., McDonald, L. P., Niederreither, K., Dolle, P., Bruneau, B. G. *et al.* (2003). Cardiac T-box factor Tbx20 directly interacts with Nkx2-5, GATA4, and GATA5 in regulation of gene expression in the developing heart. *Dev Biol*. **262**:206-24.

Stoller, J. Z. and Epstein, J. A. (2005). Identification of a novel nuclear localization signal in Tbx1 that is deleted in DiGeorge syndrome patients harboring the 1223delC mutation. *Hum Mol Genet.* **14**:885-892.

Takeuchi, J. K., Mileikovskaia, M., Koshiba-Takeuchi, K., Heidt, A. B., Mori, A. D., Arruda, E. P., Gertsenstein, M., Georges, R., Davidson, L., Mo, R. *et al.* (2005). Tbx20 dose-dependently regulates transcription factor networks required for mouse heart and motoneuron development. *Development* **132**:2463-2474.

van den Hoff, M. J., Kruithof, B. P., Moorman, A. F., Markwald, R. R. and Wessels, A. (2001). Formation of myocardium after the initial development of the linear heart tube. *Dev Biol.* **240**:61-76.

Vitelli, F., Morishima, M., Taddei, I., Lindsay, E. A. and Baldini, A. (2002a). Tbx1 mutation causes multiple cardiovascular defects and disrupts neural crest and cranial nerve migratory pathways. *Hum Mol Genet*. **11**:915-922.

Vitelli, F., Taddei, I., Morishima, M., Meyers, E.N. and Baldini, A. (2002b). A genetic link between Tbx1 and fibroblast growth factor signaling. *Development* **129**:4605-4611.

von Both, I., Silvestri, C., Erdemir, T., Lickert, H., Walls, J. R., Henkelman, R. M., Rossant, J., Harvey, R. P., Attisano, L. and Wrana, J. L. (2004). Foxh1 is essential for development of the anterior heart field. *Dev Cell.* **7**:331-345.

Waldo, K. L, Kumiski, D. H., Wallis, K. T., Stadt, H. A., Hutson, M. R., Platt, D. H. and Kirby, M. L. (2001). Conotruncal myocardium arises from a secondary heart field. *Development* **128**:3179-3188.

Waldo, K., Miyagawa-Tomita, S., Kumiski, D. and Kirby, M. L. (1998). Cardiac neural crest cells provide new insight into septation of the cardiac outflow tract: aortic sac to ventricular septal closure. *Dev Biol.* **196**:129-144.

Ward, C., Stadt, H., Hutson, M. and Kirby, M. L. (2005). Ablation of the secondary heart field leads to tetralogy of Fallot and pulmonary atresia. *Dev. Biol.* **284**:72-83.

Wilson V. and Conlon F. L. (2002). The T-box family. *Genome Biol.* **3**(6):reviews3008.1-3008.7.

Xu, H., Morishima, M., Wylie, J. N., Schwartz, R. J., Bruneau, B. G., Lindsay, E. A. and Baldini, A. (2004). *Tbx1* has a dual role in the morphogenesis of the cardiac outflow tract. *Development* **131**:3217-3227.

Yamagishi, H. (2002). The 22q11.2 deletion syndrome. Review. *Keio J. Med*. **51**: 77-88.

Yamagishi, H., Maeda, J., Hu, T., McAnally, J., Conway, S. J., Kume, T., Meyers, E. N., Yamagishi, C. and Srivastava, D. (2003). Tbx1 is regulated by tissue-specific forkhead proteins through a common Sonic hedgehog-responsive enhancer. *Genes Dev.* **17**:269-281.

Yi, C. H., Terrett, J. A., Li, Q. Y., Ellington, K., Packham, E. A., Armstrong-Buisseret, L., McClure, P., Slingsby, T. and Brook, J. D. (1999). Identification, mapping, and phylogenomic analysis of four new human members of the T-box gene family: EOMES, TBX6, TBX18, and TBX19. *Genomics* **55**:10-20.

Yoshioka, H., Meno, C., Koshiba, K., Sugihara, M., Itoh, H., Ishimaru, Y., Inoue, T., Ohuchi, H., Semina, E. V., Murray, J. C. *et al.* (1998). Pitx2, a bicoid-type homeobox gene, is involved in a lefty-signaling pathway in determination of left-right asymmetry. *Cell* **94**:299-305.

Yu, X., St Amand, T. R., Wang, S., Li, G., Zhang, Y., Hu, Y., Nguyen, L., Qiu, M. and Chen, Y. (2001). Differential expression and functional analysis of Pitx2 isoforms in regulation of heart looping in the chick. *Development* **128**:1005-1013.

Zaffran, S., Kelly, R. G., Meilhac, S. M., Buckingham, M. E. and Brown, N. A. (2004). Right ventricular myocardium derives from the anterior heart field. *Circ Res.* **95**:261-268.